AD_____

Award Number:
DAMD17-02-1-0677

TITLE:
Acceleration of Ligament Healing with Cellular Attractants

PRINCIPAL INVESTIGATOR:
Cahir A. McDevitt, Ph.D.

CONTRACTING ORGANIZATION:
The Cleveland Clinic Foundation

Cleveland, OH 44195

REPORT DATE:
July 2008

TYPE OF REPORT:

Final Addendum

PREPARED FOR:
U.S. Army Medical Research and Materiel Command
Fort Detrick, Maryland 21702-5012

DISTRIBUTION STATEMENT:

√ Approved for public release; distribution unlimited

REPORT DOCUMENTATION PAGE

Form Approved
OMB No. 0704-0188

1. REPORT DATE *(DD-MM-YYYY)*	2. REPORT TYPE	3. DATES COVERED *(From - To)*
01-07-2008	Final Addendum	1 JUL 2006 - 30 JUN 2008

4. TITLE AND SUBTITLE
Acceleration of Ligament Healing with Cellular Attractants

5a. CONTRACT NUMBER

5b. GRANT NUMBER
DAMD17-02-1-0677

5c. PROGRAM ELEMENT NUMBER

6. AUTHOR(S)
Cahir A. McDevitt, Ph.D.

5d. PROJECT NUMBER

5e. TASK NUMBER

5f. WORK UNIT NUMBER

7. PERFORMING ORGANIZATION NAME(S) AND ADDRESS(ES) AND ADDRESS(ES)
The Cleveland Clinic Foundation
Cleveland, OH 44195

8. PERFORMING ORGANIZATION REPORT NUMBER

9. SPONSORING / MONITORING AGENCY NAME(S) AND ADDRESS(ES)
U.S. Army Medical Research and Materiel Command
Fort Detrick, Maryland 21702-5012

10. SPONSOR/MONITOR'S ACRONYM(S)

11. SPONSOR/MONITOR'S REPORT NUMBER(S)

12. DISTRIBUTION / AVAILABILITY STATEMENT
Approved for Public Release; Distribution Unlimited

13. SUPPLEMENTARY NOTES

14. ABSTRACT

Rupture of the anterior cruciate ligament (ACL) with subsequent damage to the menisci and articular cartilage in the knee joint is a major cause of morbidity in the armed forces. type VI collagen is a haptotactic cell attractant. We have shown that type VI collagen with bound heparin/FGF-2 or hyaluronan or fibronectin promotes migration of canine ACL and DET cells. Insertion of type VI collagen into a wound in the canine meniscus increases that the cruciate ligaments results in the release of soluble factors that activate stern cells and stimulate proliferation and migration of these cells. The cells migrate toward the wound by moving along an interface of two collagen fibril systems. The appropriate scaffold combined with stem cells offers a powerful approach ot he the management of battlefields injuries to ligaments and menisci to minimize the sequelae in wounded warriors.

15. SUBJECT TERMS **aggrecan; anterior cruciate ligament/physiology; antigens, CD44/isolation & purification; cartilage/physiology; collagen; extracellular matrix proteins/biosynthesis; gene expression/physiology; hyaline; meniscus, tibial/physiology/ultrastrcuture; posterior cruciate ligament/physiology**

16. SECURITY CLASSIFICATION OF:			17. LIMITATION OF ABSTRACT	18. NUMBER OF PAGES	19a. NAME OF RESPONSIBLE PERSON
a. REPORT	b. ABSTRACT	c. THIS PAGE			19b. TELEPHONE NUMBER *(include area code)*
U	U	U	UU	67	USAMRMC

Table of Contents

INTRODUCTION

The anterior cruciate ligament (ACL) plays a pivotal role in the biomechanical stability of the knee joint. Rupture of the ACL is a common injury in training and sporting activities among armed forces personnel, particularly among females. ACL rupture and the consequent damage to the menisci and articular cartilage of the knee joint can lead to long-term disability. Factors promoting healing of tears in tissues such as the ACL would promote the well-being and readiness of armed forces personnel. In addition, such factors might be applicable to other tissues and improve healing in our wounded warriors.

Wound healing is a complex process. For the healing of any wound to occur, cells must migrate into the area of injury and synthesize new extracellular matrix; but for cells to migrate there must be a scaffold upon which to move and a stimulus, such as a chemotactic factor, for movement. The concentration of collagen, one of the scaffold proteins, is higher in fibrous cartilage, such as that found in the meniscus, ACL, and posterior cruciate ligament (PCL), than in articular cartilage (Nakano, 1997; Amiel, 1984). Type I collagen is known to be the predominant fibrillar collagen in the meniscus. Smaller amounts of type II collagen are also present. In hyaline cartilage, type II collagen is the dominant type and has no identifiable spatial organization (Eyre,1975). In striking contrast, type II collagen in the fibrocartilage of the meniscus is highly organized (Kambic, 2005). Defining the structure of the fibrillar meshwork in the normal ACL and meniscus is critical in understanding the role of fibril reorganizations in the healing process.

The reparative process after injury begins with cells moving towards the wound. Cellular attractants, such as chemotactic attractants, are proteins capable of attracting cells to a specific site such as a wound. Type VI collagen is a cell adhesion and haptotactic attractant protein, i.e., it can attract cells in an insoluble state (Marcelino and MeDevitt, 1995). (Note: Haptotaxis is the migration of cells along a concentration gradient of an insoluble substance.) Type VI collagens has an affinity for a range of extracellular matrix macromolecules, including heparin, fibronectin, and hyaluronan (McDevitt, 1991; McDevitt, 1994; Marcelino, 1995; Ricard-Blum, 2000). Type VI collagen, however, can also bind growth factors such as FGF-2. Thus, it has the potential not only to attract cell to wounds *in vivo*, but with an attached growth factor, to stimulate the cells to divide. However, it was not known whether FGF-2 bound to type VI collagen through a heparin bridge would influence the cell attractant properties of the protein. Thus, we planned to test the capacity of selected matrix macromolecules, with and without added growth factor bound to them, to attract ligament cells *in vitro* and *in vivo* and thereby accelerate the process of wound healing in knee joint tissues. The overall goal is to promote wound healing in knee joint tissues. We are testing the ability of type VI collagen, alone or in combination with other molecules, to promote wound healing in knee joint tissues, particularly tendons and ligaments and the meniscus.

The reviewers of the original grant application recommended that we invest effort in exploring the mechanisms involved in wound healing in knee joint tissues. Therefore, we expanded the *in vitro* phase of the program to:

a. Explore the spatial organization, at the level of both the light and electron microscope, of the fibrillar meshwork in knee joint tissues that might facilitate or promote migration of cells in

wound healing processes. We show that the cells moving towards a wound in the knee joint meniscus migrate at the interface of two collagen fibril systems.

b. Explore the influence of inserting type VI collagen into wound in knee joint menisci in an *in vitro* model of wound healing. This study has shown that type VI collagen does appear to signal to the cells invading the wounds, as it does in cell migration assays.

c. Explore the possibility that stem or progenitor cells might contribute to these wound healing processes.

Since the award of the grant, we developed an organ culture assay for wound healing in the canine knee joint meniscus. This involves generating a wound in a freshly harvested canine meniscus and culturing the meniscus in organ culture. This permits us to test type VI collagen constructs for their capacity to influence healing processes in a system that is much more "physiological" than the simple cell attraction assays that we originally proposed. Our model also permits us to explore the identity of the cells in the wound healing process with emphasis on the possible role of stem or progenitor cells. The ACL is similar to the meniscus in being partly vascularized and being composed predominantly of parallel fibril bundles of type I collagen. Thus, we can evaluate healing *in vitro* in a tissue, the meniscus, that is identical to ligaments in its outer attachment zone and is very similar to these tissues in its inner zone. Moreover, the meniscus is a knee joint tissue that, as mentioned above, invariably becomes injured after ACL rupture. This model permits us to focus on the mechanism of healing of knee joint injuries that are common in Armed Forces personnel.

BODY

The matrix available for migration of cells in wound healing:

Certain tissues within the knee joint, such as the meniscus, have the capacity to heal wounds. Others, such as articular cartilage and the ACL, seldom (if ever) heal wounds. Why is it that connective tissues that bear certain similarities in composition should in some cases have the capacity to heal wounds and in other cases not? We explored the possibility that the local fibrillar organization contributes to the migration of cells toward a wound. We wondered if the meniscus had "cell highways" along which the cells would preferentially migrate.

We undertook light and electron microscopy studies of the normal ACL, posterior cruciate ligament (PCL), and meniscus and articular cartilage of the knee joint. Specifically, the spatial organization of types I and II collagen, the proteoglycan aggrecan, and tenascin-C was determined in these tissues. We then employed an *in vitro* organ culture model of wound healing in the meniscus to localize the migratory paths of the cells that move through this tissue towards a wound.

Light microscopic studies:

Study 1. Spatial distribution, concentration and gene expression of the proteoglycan aggrecan in the knee joint ACL, PCL, meniscus and articular cartilage.

Rationale: The proteoglycan, aggrecan, a model of which is shown in Fig. 1, is a constituent of all knee joint tissues and is enriched in the hyaline articular cartilage. Its role is to entrain water and contribute to the compressive stiffness of tissues or parts of tissues. It is a particularly valuable matrix constituent to study in scenarios where breakdown of tissue occurs, as in wounding and in the migration of cells through matrices to the wound. We have antibodies against neo-epitopes on aggrecan, that is, against the new amino group and adjacent sequence of amino acids on scission of a peptide bond. We undertook the first study of the concentration, gene expression and spatial distribution of aggrecan in the anterior cruciate ligament (ACL), the posterior cruciate ligament (PCL), the medial and lateral menisci and the femoral articular cartilage of the mature canine knee joint.

Methods:

Tissue dissection: The ACL and PCL and the lateral and medial meniscus and femoral articular cartilage were dissected from the knee joints from five skeletally normal adult mongrel dogs. Each meniscus was sectioned into the inner and outer meniscus, as defined by half the radial distance from the outer boundary to the inner tip.

FIG. 1A and 1B.

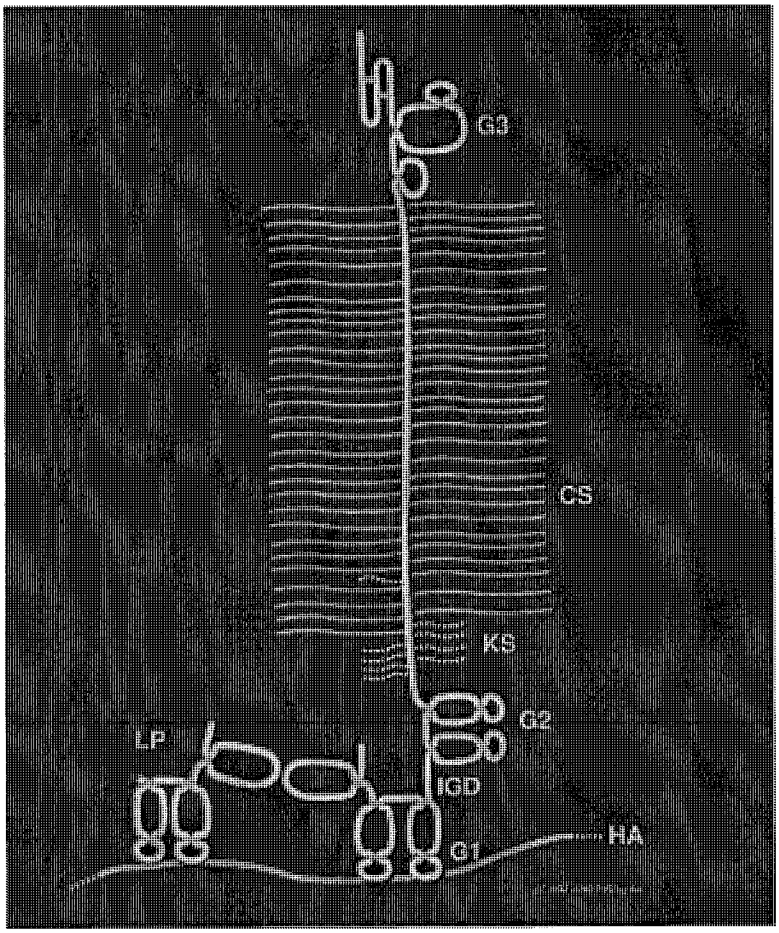

Fig. 1A. Model of aggrecan molecule. The anti-aggrecan anti-serum was generated against synthesized peptides specific to the G1 domain.

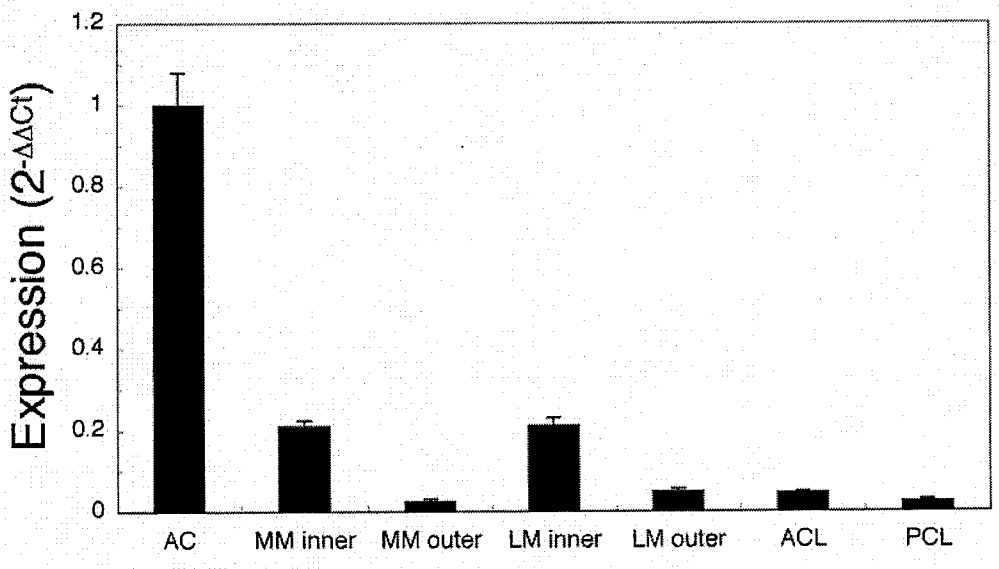

Fig. 1B. Gene expression of aggrecan as determined by real time TaqMan PCR. AC: Articular cartilage, MM: Medial meniscus, LM: Lateral meniscus, ACL: anterior cruciate ligament, PCL: posterior cruciate ligament.

The concentration of aggrecan in guanidine extracts of powdered tissues and its spatial distribution in these tissues was determined with a polyclonal antibody against the G1 domain of aggrecan core protein developed by our collaborator, John Mort, Ph.D., Shriners Research Institute, Montreal, Canada. Rabbits were immunized with a mixture of peptide-ovalbumin conjugates of the sequences **HDNSLSVSIPQPS***GGC*, **RVLLGTSLTIPCYFIDPMHPVTTAPS**, **TEGRVRVNSAYQDK**-*GGC* and **SSRYDAICYTG**. These sequences are specific (sequences in bold font) to the G1 domain of aggrecan.

Measurement of Gene Expression of aggrecan by TaqMan Real-Time PCR

Total RNA (500 ng) was reverse transcribed into first-strand cDNA with MuLV reverse transcriptase with the Taqan reverse-transcriptase kit (Applied Biosystems, Foster City, CA, U.S.A.). PCR amplification of cDNA was performed using the following oligonucleotide primers and probe in an ABI Prism 7700 sequence detection system (Applied Biosystems, Foster City, CA, U.S.A.): forward primer, GACGCCATCGACTCTTTCAC; reverse primer, ACACAGCTCCTGGTCGATCT; and probe, FAM-TGCCTTCCCAGCTACCGAGGG-MGB. Human 18s rRNA (Applied Biosystems, Foster City, CA, U.S.A.) was included in each sample as the internal control. Using the comparative Ct method and calculating the relative gene expression as the $2^{-\Delta\Delta Ct}$ value [33], the data were calculated as the fold change in gene expression normalized to the endogenous reference gene 18s rRNA and relative to the control.

Immunofluorescence Microscopy

The ACL and PCL and the lateral and medial meniscus and femoral articular cartilage were dissected from the knee joints from skeletally normal adult mongrel dogs. Each meniscus was sectioned into the inner and outer meniscus, as defined by half the radial distance from the outer boundary to the inner tip. Tissues were embedded in tissue freezing medium and 5 μm frozen sections cut on a motorized Leica CM 3050 cryostat (Leica Microsystems, Nussloch, Germany). The menisci were sectioned in both longitudinal and coronal planes. For aggrecan staining, the tissue sections were reduced by pipetting 250 μl of 10 mM dithiothreitol onto the slide and incubating uncovered for 2 h at 37 °C. The tissues were washed in TBS, then alkylated with 250 μl of 40 mM iodoacetamide at 37 °C for 1 h, and finally blocked with 1% BSA in TBS. Sections were incubated overnight with the appropriate monoclonal antibody or polyclonal anti-sera, or a mixture of both. Sections were washed and stained for 2 h with AlexaFluor® 594-conjugated $F(ab')_2$ fragment of rabbit anti-goat IgG (Molecular Probes, Inc., Eugene, OR) and/or the FITC-conjugated goat anti-mouse IgG secondary antibodies. After incubation, the slides were copiously rinsed in PBS for 6 hours and mounted in Vectashield with DAPI (Vector Laboratories, Burlingame, CA).

Incubation of tissues without the primary antibody served as the negative controls.

Microscopy was performed on an Olympus BX51 microscope (Tokyo, Japan) equipped with a QED Camera Plug-In™Package (QED Imaging Inc., Pittsburgh, PA, U.S.A.) that were purchased with this grant.

Results:

Concentration of aggrecan in knee joint tissues: Table 1 shows the molar concentration of aggrecan in knee joint tissues as determined by competitive inhibition ELISA. The ligaments contained much less aggrecan G1 domain than articular cartilage or meniscus. The concentration of aggrecan G1 domain in hyaline articular cartilage was 7.2 times higher than that of meniscus fibrocartilage (**Table 1**), while in the lateral meniscus it was half that of the medial meniscus. The aggrecan G1 was not evenly distributed in the meniscus: the concentration of G1 of the inner portion of both lateral and medial menisci was higher than the outer portion (Table 1).

TABLE 1

Concentration of aggrecan G1 domain in the articular cartilage, meniscus, and anterior and posterior cruciate ligaments of canine knee joint

Samples	Concentration of G1 domain (nMol/g dry weight)
Articular Cartilage	240.1 ± 32.5
Meniscus	
Medial	33.4 ± 4.3
Lateral	16.9 ± 2.1
Medial, inner	69.9 ± 4.7
Medial, outer	19.9 ± 4.6
Lateral, inner	25.1 ± 4.4
Lateral, outer	14.5 ± 2.8
Ligaments	
Anterior Cruciate Ligament	6.8 ± 0.9
Posterior Cruciate Ligament	0.9 ± 0.09

Gene Expression of Aggrecan: The relative differences in aggrecan gene expression (Fig. 1B), as assessed by TaqMan real-time PCR, for the most part reflected the differences in protein concentration as determined by ELISA. Very low gene expression was demonstrable in the ligaments. Gene expression of aggrecan in articular cartilage was much higher than that in the meniscus and ligaments. As with the

relative concentration of the G1 protein, the gene expression in the inner medial and lateral menisci was higher than that of the outer meniscus.

Spatial distribution of aggrecan in ACL, PCL, meniscus and articular cartilage as determined by immunofluorescence microscopy: Figure 2 shows the spatial distribution of aggrecan in articular cartilage, meniscus, ACL and PCL. Both ACL (Fig. 2A) and PCL (Fig. 2B) showed aggrecan as linear streaks parallel with the linear cellular arrays and therefore parallel with the collagen fibrils. A coronal section of the meniscus (Fig. 2C) showed the aggrecan staining as an interconnecting network, with fairly intense staining in the radial "tie fiber" across the bottom of the figure. Interestingly, the cells were located at the bifurcation of the strands in the network, but seemed more randomly distributed in the radial "tie fiber". No organization was evident in the distribution of aggrecan in the articular cartilage (Fig. 2D). The negative controls, in which the primary antibody was omitted, showed no fluorescence (not shown).

FIG. 2.

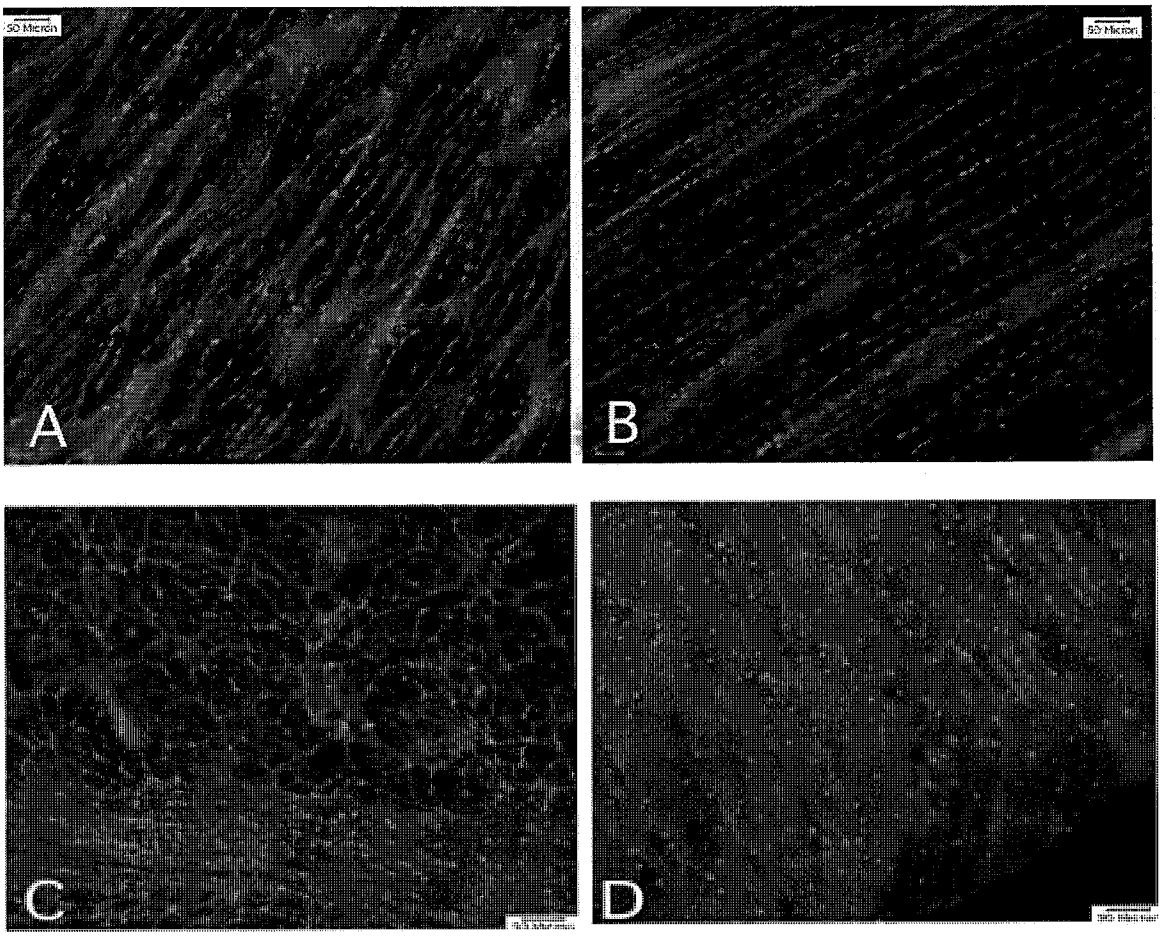

Fig. 2. Immunolocalization of aggrecan in canine anterior cruciate ligament (A), posterior cruciate ligament (B), coronal section of medial meniscus(C), and articular cartilage (D). Bar=50μm.

In summary, these studies show that fibrous tissue (such as the ACL and the meniscus fibrocartilage) have lower concentrations and gene expression levels of aggrecan than the articular cartilage and meniscus of the knee joint. In the ACL and meniscus, aggrecan is confined to the spaces between the collagen fibrillar bundles. In contrast, aggrecan is diffusely distributed in articular cartilage. This study was published in full (Valiyaveettil, Mort and McDevitt, 2005) and is in the Appendix.

Study 2. Spatial distribution of the adhesion protein tenascin-C.

Rationale: The outer 12% of the radial distance of the meniscus is vascular. The remainder is non-vascular. Interestingly, our study of the collagen distribution in the meniscus showed that while a type I collagen meshwork was present throughout the entire meniscus in coronal sections, type II collagen, in contrast, was confined to the avascular portion of the tissue and was absent in the vascular zone. These observations raise the interesting possibility of an extracellular matrix that favors angiogenesis in the outer zone of the meniscus, and a matrix in the inner zone that resists blood vessel invasion.

Tenascin-C is a large extracellular matrix glycoprotein found predominantly around blood vessels in connective tissues. We explored the spatial relationship of tenascin-C with the blood vessels in the ACL and meniscus of the canine knee joint.

Methods: Canine ACL and menisci were harvested, sectioned, stained with antibodies and imaged as described above. The monoclonal antibody B28 to human tenascin-C (generously provided by Dr. Chiquet-Ehrissman) and a rabbit polyclonal antibody to human von Willebrand factor (Novocastra Lab, Newcastle, UK) to detect blood vessels were employed.

To obtain images of the whole meniscus, gray-scale images of the stained sections were obtained using a Quantix 1602E 12-bit digital camera (Roper Scientific, Tucson, AZ) attached to Leica DMXRA motorized microscope (Leica Microsystems, Wetzlar, Germany). The entire imaging system is controlled by Metamorph (v6.0) imaging software(Universal Imaging Inc, Downington, PA) running on a 2.6 GHz Windows XP workstation with 2.048 GB RAM. The microscope is equipped with a Prior Proscan 8-slide motorized X-Y stage (Prior Inc., Rockland MA) for scanning multiple slides and sequential images automatically. A 20 x 24 matrix of images was acquired over the entire section field-of-view (25 mm x 25 mm). Individual images were collected at 461 x 344, 8-bit gray level, using a 10x objective (magnification = 100x). The FITC and AlexaFluor 594 images were collected for the same field-of-view, so that the positive-stained areas would be co-localized.

Results: The spatial relationship between tenascin-C and blood vessels, as revealed by staining with von Willebrand factor, is shown in Fig. 3A. Tenascin-C (green) was present in discrete tracts of the ACL. with a sharp transition to sites where no or minimal staining was evident. The von Willebrand factor (red) staining was only present in those areas where tenascin-C stained intensely (Fig. 3A). Fig. 3B shows the spatial relationship of tenascin-C to the blood vessels in the outer region of the meniscus. Blood vessels, as revealed by von Willebrand factor staining (red), penetrated about 10 to 15% of the radial distance of the meniscus. The staining for tenascin-C (green) was distributed throughout the extracellular matrix in the outer, vascular region, but, remarkably, terminated abruptly at the junction between the vascular and non-vascular zones of the tissue. In some sites, evident as yellow staining, co-localization of tenascin-C

FIG. 3A, 3B and FIG. 4.

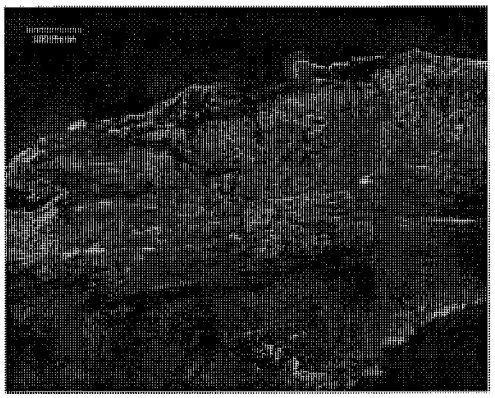

Fig. 3A. Longitudinal section of canine ACL stained for tenascin C (green) and for blood vessels with an anti-von Willebrand factor (vWF) anti serum (red). Note that tenascin C is confined to vascular area. Bar=200μm.

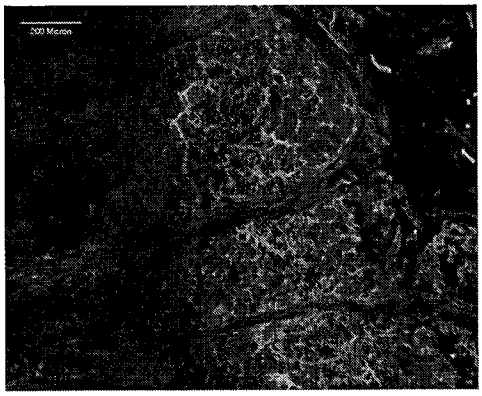

Fig. 3B. Coronal section of canine meniscus stained for tenascin C (green) and vWF (red) as in Fig. 3A. The inner avascular zone is on the left, and the outer, vascular zone in the right. As with the ACL, the tenascin stain is localized to the matrix surrounded the blood vessels. Bar=200μm.

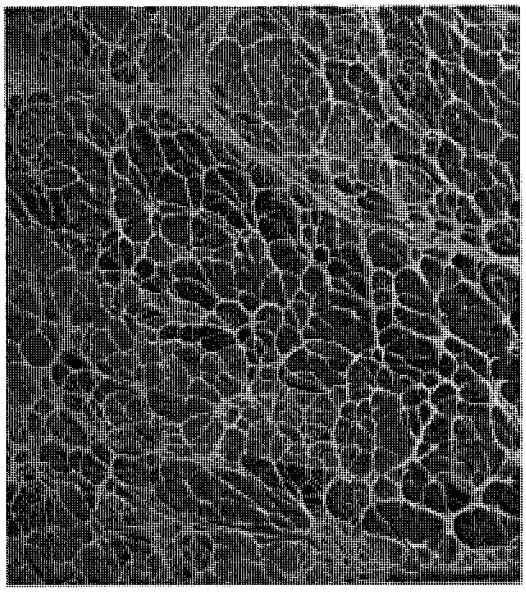

Fig. 4. Coronal section of canine medial meniscus stained for type I (green) and type II collagen (red). Overlay of both is yellow. Note fascicle-like organization in the meniscus.

and von Willebrand factor staining was seen. In some sections the blood vessels were located within "tie fibers" (Fig. 3B).

The distribution of tenascinC reported here in the meniscus is consistent with the function of the protein in angiogenesis (Tanaka et al., 2003). Tenascin-C is also expressed by vascular smooth muscle cells and regulates angiogenesis through the regulation of VEGF expression (Tanaka et al., 2003).

Study 3. Spatial distribution of type I and type II collagen in meniscus and articular cartilage.

Our immunohistochemistry study of the spatial organization of types I and II collagen revealed, for the first time, a fascicle-like structure composed of two distinct fibrillar systems in the meniscus. This study has been published (Kambic and McDevitt, 2005) and was described in last year's report. It is briefly restated here to put our electron microscopic studies in context.

Fig. 4 shows a confocal image of type I collagen (green), type II collagen (red) and cell nuclei (blue) in a coronal section of the dog meniscus. It shows, for the first time, an organized mesh-like structure for type II collagen. The overlay of types I and II collagen, shown here in yellow, envelops the circumferential fibrils shown here in cross-section. We refer to this newly discovered, extrafascicular system as the peri-system (see Appendix). We follow below with an electron microscopic study of the fibrillar networks in meniscus.

Study 4. Electron microscopic analysis of normal knee joint tissues.

Rationale: We have included electron microscopic studies to identify the routes by which cells migrate in knee joint tissues. In studies in the 1980s, Ghadially showed fibrils at right angles to one another in the meniscus. Unfortunately, it is impossible to interpret the significance of this observation, as the orientation of the specimen was not mentioned in those studies, a deficiency that Ghadially himself acknowledges. Our immunohistochemistry studies imply that the orientation of the collagen in the perisystem is different from that of the circumferential fibrils. Our immunohistochemistry studies revealed that the cells are located in the peri-system and never within the bundles of circumferential fibrils, a feature of the tissue that will greatly facilitate interpretation of the EM studies. We wish to confirm this observation with extra studies and extend them to define the micro-architecture of the fibrillar network with a quantitative assessment of the fibril diameter and identification of the fibrils by immuno-electron microscopy. Moreover, we wish to identify how the differently shaped fibrochondrocytes and fibroblast-like cells relate morphologically to their matrices.

Approach: We shall undertake transmission EM on cross-sections of the canine meniscus from the inner two thirds by radial distance (where fibrochondrocytes and type II collagen are located) and from the outer portion (where blood vessels are located and fibroblast-like cells reside but where type II collagen is absent). The key to interpretation of these studies is to know the orientation and locus of the site being viewed in the EM. The major hypothesis being addressed here is that the circumferential fibrils are surrounded by a compartment in which the fibrils are orthogonal to the circumferential ones. We shall also establish what the spatial relationship of the long processes of the fibroblast-like cells are to the fibrils in both systems.

Results:

Figures 5 A-C show the longitudinal fibrillar organization in the canine ACL, knee DET, and outer meniscus, respectively. The outer meniscus (that is, the portion that is vascular and through which the meniscus is attached to the synovial wall of the joint) is essentially a fibrous tissue similar to ligaments and tendons. The collagen fibrils in the ACL, DET, and outer meniscus were parallel and densely packed, although apparently less so in the case of the meniscus.

Fig 6 shows coronal sections of the ACL, DET and knee joint meniscus. A range of fibril diameters was evident in all tissues. We measured the distribution of fibril diameters by quantitative image analyis and this portion of the study is reported below.

Figure 7A shows a canine knee ACL with the tissue and longitudinal fibrils in cross-section and surrounded by a matrix system that houses the cells.

Figure 7B shows, for the first time, a similar fascicle system in the meniscus. The coronal section of the meniscus shows the circumferential fibrils, those that course around the meniscus parallel to the outer boundary, in cross-section. Bundles of these fibrils are surrounded by what we are calling a "peri-fibrillar matrix" system, characterized by an abundant non-fibrillar matrix and fibrils in a longitudinal plane and therefore orthogonal to the circumferential fibrils. As in the ACL, the cells in the meniscus are situated in this peri-system.

Figure 8 shows the cells of the ACL (Fig. 8A) and DET (Fig. 8B) with striking elongated processes that envelop the fascicles of longitudinal fibrils, here shown in cross-section. In the inner meniscus, the fibrocartilage portion of the tissue, the cells are round (Fig. 8C), and we have termed them fibrochondrocytes. In the outer meniscus, the fibrous portion of the tissues, we show for the first time that the cells have the stellate processes that surround the fascicles (Fig.8D), as in the ACL and DET.

Measurement of fibril diameters.

Method: Meniscus, ACL and DET images were processed by ImageJ, an image processing software developed by the NIH, and MATLAB® (MathWorks, Natick, MA). Images acquired from the EM were first converted to 8-bit gray-scale mode. A number of spatial domain operations such as contrast equalization, noise filtering and smoothing were then performed on the images. To achieve the fibril segmentation, a non-linear intensity transformation was carried out. The gray-scale images were then thresholded to yield binary images. Holes created within the borders of fibrils were filled, and finally fibrils were segmented using the built-in functions in MATLAB®. Manual segmentation was also used where needed. The particles (fibrils) were then analyzed both in ImageJ and MATLAB®. The equivalent diameter of a fibril was calculated considering a circle that has the same surface area.

The distribution of tissue diameters in the ACL, DET and meniscus are shown in Figure 9. Most of the fibril diameters recorded for the ACL (Fig. 9A) and the meniscus (Fig.9C) fell within a 25 nm to 225 nm range. The DET (Fig.9B) seemed to have small-diameter fibrils that were in a 25 nm to 150 nm range.

FIG. 5A, 5B and 5C.

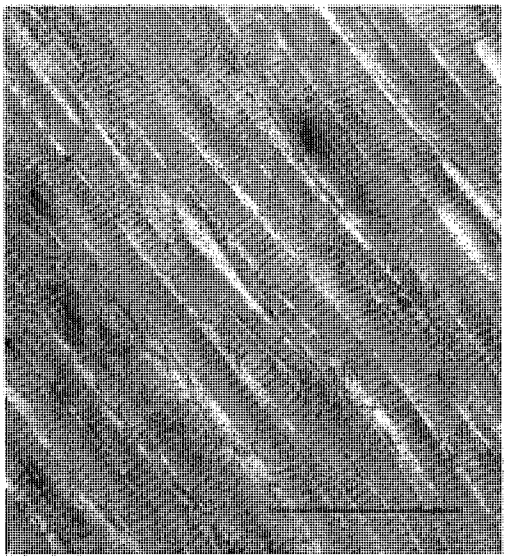

Fig. 5A. Longitudinal section of canine knee anterior cruciate ligament (ACL). Note closely packed fibrils. Bar=1μm.

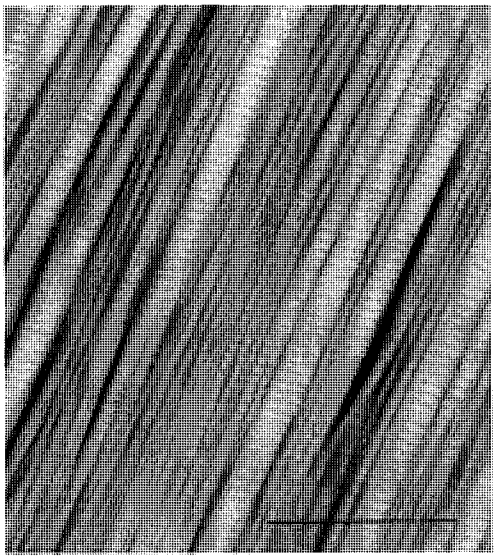

Fig. 5B. Longitudinal section of canine knee digital extensor tendon (DET). Note closely packed fibrils with characteristic collagen banding. Bar=1μm.

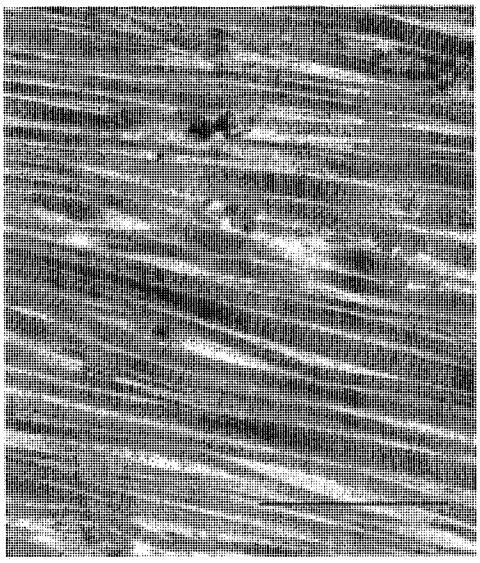

Fig. 5C. Longitudinal section of canine knee outer meniscus. The parallel collagen fibrils are loosely packed, in contrast to those in the ACL and DET. Bar=1μm.

FIG. 6A, 6B and 6C.

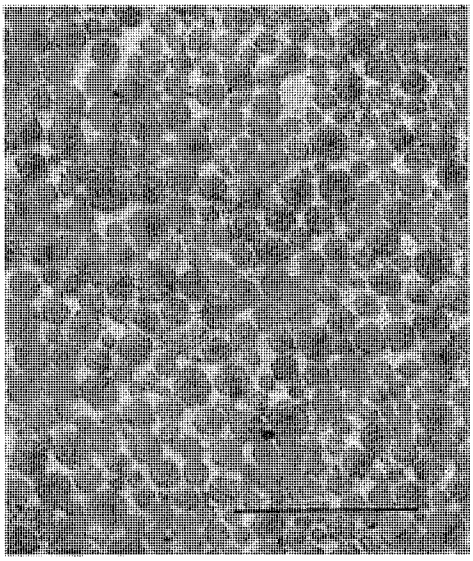

Fig. 6A. Cross-section of canine knee ACL showing collagen fibrils of different diameters. Bar=1μm.

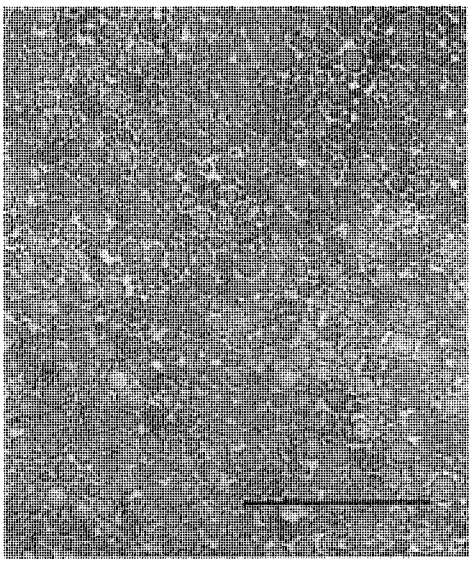

Fig. 6B. Cross-section of canine knee DET showing densely packed collagen fibrils of different diameters. Bar=1μm.

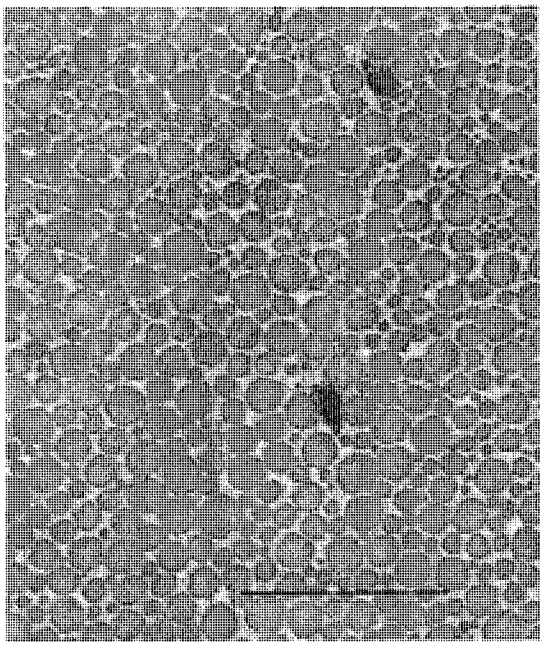

Fig. 6C. Cross-section of canine knee inner meniscus. Note collagen fibrils of different diameters and electron-dense clusters. Bar=1μm.

FIG. 7A and 7B.

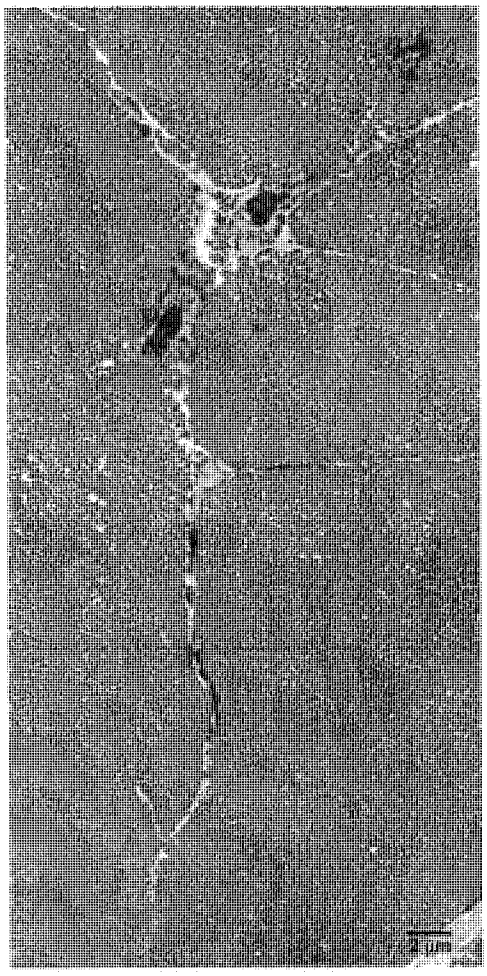

Fig. 7A. Canine knee anterior cruciate ligament (ACL) in cross-section. Longitudinal bundles of collagen fibrils in cross-section are shown here. Note cells and inter-fascicular matrix. Bar=2μm.

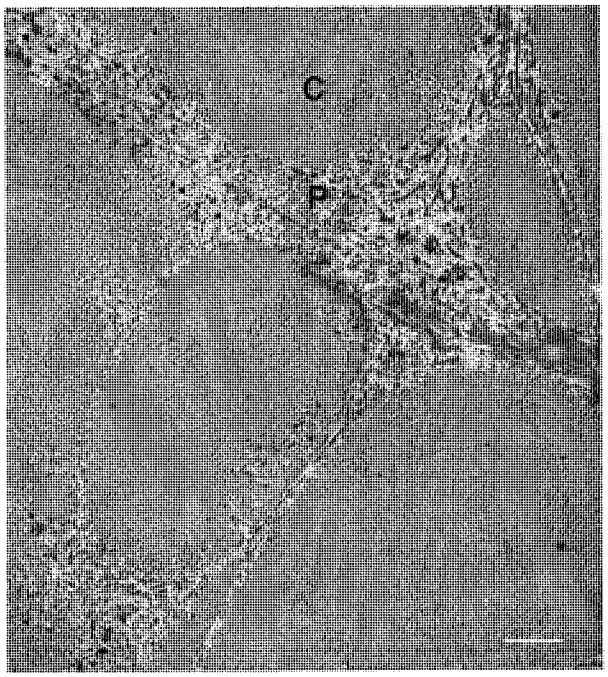

Fig. 7B. Coronal section of canine knee inner meniscus. A fascicle-like structure in the meniscus is shown here for the first time. The circumferential fibrils are shown in cross-section (C). Longitudinal fibrils (P) in a system we call the 'peri-fibrilar' system are shown surrounding the circumferential fibrils. Bar=1μm.

FIG. 8A, 8B, 8C, and 8D.

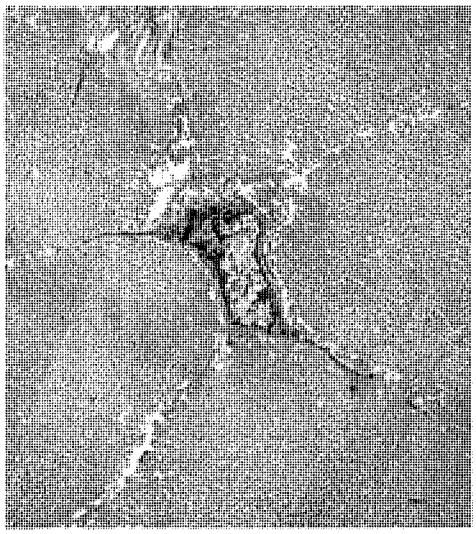

Fig. 8A. Cross-section of canine knee joint anterior cruciate ligament (ACL). Cell with extended processes that surround bundles of collagen bundles. Bar=1μm.

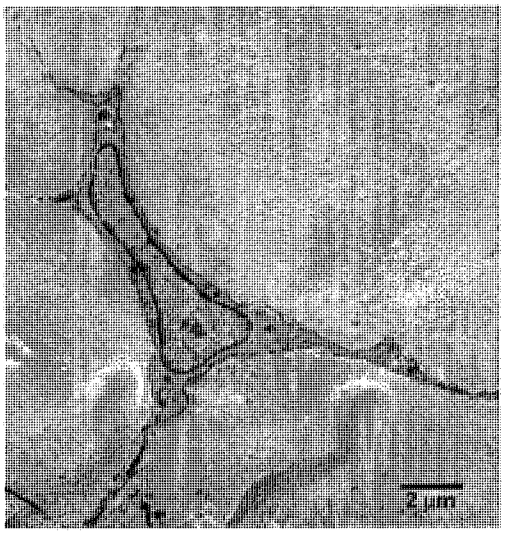

Fig. 8B. Cross-section of canine knee digital extensor tendon (DET). Cell with extended processes that wrap around fascicles of tightly packed collagen fibrils is seen. Bar=2μm.

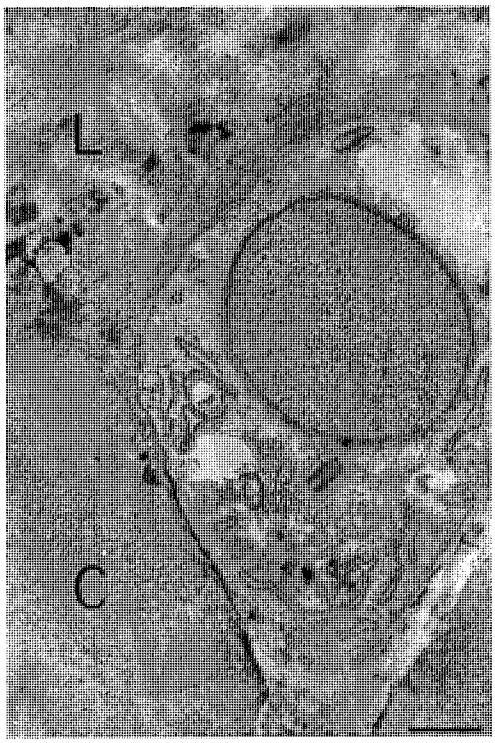

Fig. 8C. Coronal section of inner canine lateral meniscus showing oval fibrochondrocyte. Circumferential fibrils (C) in cross section and longitudinal fibrils (L) are seen. Bar=1μm.

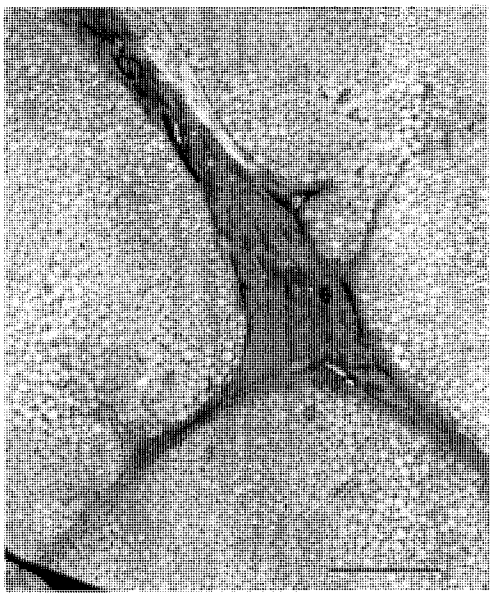

Fig. 8D. Coronal section of outer canine lateral meniscus. Fascicles of circumferential fibrils, seen in cross-section, surrounded by a cell and its elongated processes. Bar=1μm.

FIG. 9A, 9B, and 9C

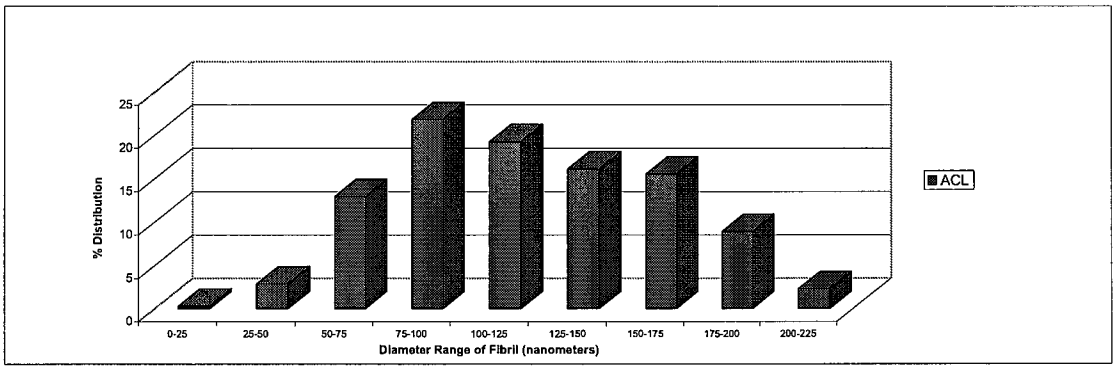

Fig. 9A. Histogram demonstrating the populations of collagen fibrils in canine anterior cruciate ligament (ACL). Note the distribution of the number of collagen fibrils with various diameters.

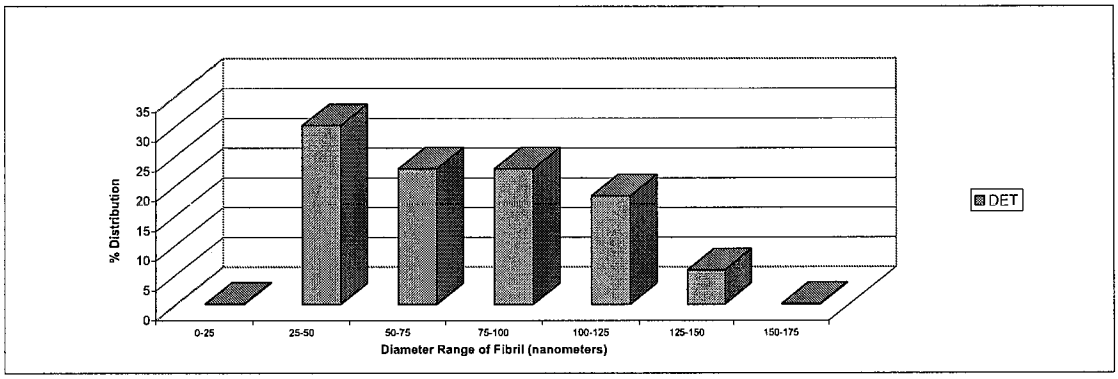

Fig. 9B. Histogram demonstrating the populations of collagen fibrils in canine digital exterior tendon (DET). Note the distribution of the number of collagen fibrils with various diameters.

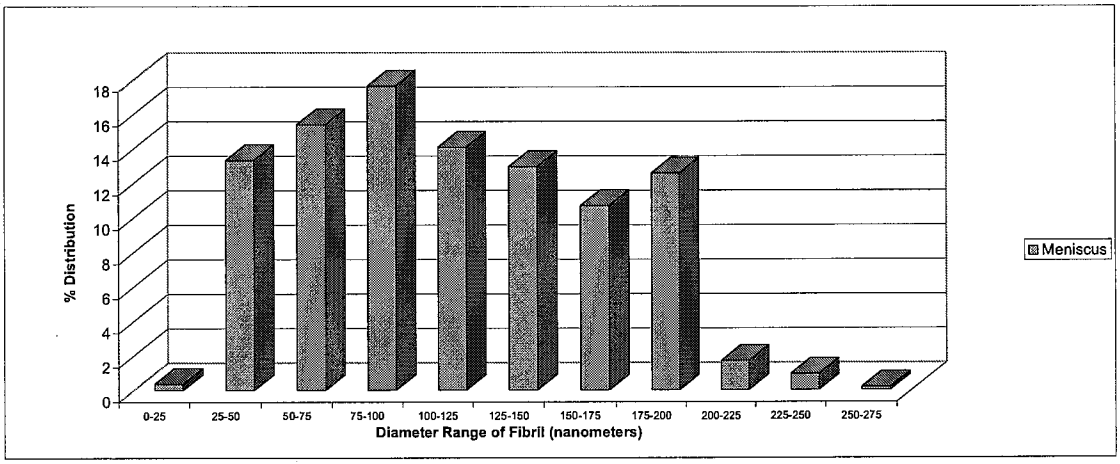

Fig. 9C. Histogram demonstrating the populations of collagen fibrils in canine meniscus. Note the distribution of the number of collagen fibrils with various diameters.

Study 5: Isolation of distinctive cell processes from ACL, DET, meniscus and articular cartilage with dispase-collagenase digestion.

The nature of the cells that participate in the wound healing process in knee joint tissues and the mechanisms by which they interact with their extracellular matrices as they navigate their way towards the wound are issues central to understanding wound healing in these tissues. The nature of the cells in these tissues and their relationship to their surrounding matrices was further explored with collagenase-dispase digestions. Type VI collagen is a key constituent of the pericellular matrices of chondrocytes. The combination of cell and pericellular matrix is called the chondron. Bacterial collagenase does not degrade type VI collagen as it does all other types of collagen. We have exploited the relative resistance of type VI collagen to collagenase to isolate cell-pericellular matrix complexes from the tissues of the knee joint. The tissues were digested with a combination of bacterial collagenase and dispase.

Results:
Two distinct cell populations were observed in the ACL and DET. Linear arrays of cells encased in a matrix of type VI collagen were isolated from the ACL (Fig. 10A) and DET (Fig. 10B) and also from the meniscus (Fig. 10C). This is the first time that these structures have been observed in cells isolated from in these tissues. The significance of these type VI collagen matrices surrounding the arrays remains to be established.

A second type of cell with stellate processes revealed by vimentin staining was evident in the ACL (Fig. 11A), DET (Fig. 11B), and meniscus (Fig. 11C). These striking cells were similar in shape to the cells demonstrable in the electron microscope in the extracellular matrix surrounding fascicles of collagen fibrils. No type VI collagen was demonstrable around these cells. Clearly, any effective healing process must result in a matrix with a fascicle structure and the presence of these two types of cells.

Study 6. Routes of cell migration in an *in vitro* wound healing model.

Rationale: The cells of the normal canine anterior and posterior cruciate ligament (ACL/PCL) and digital extensor tendon (DET) reside in the inter-fascicular matrix. Likewise, the cells in the meniscus reside in a similar extra-fascicular matrix, a matrix we call the "peri-fibrillar system." In the meniscus, this matrix appears to occupy a significant portion of the tissue. Is the meniscal wound-healing process, which can be quite effective, possible because the cells have this extensive peri-fibrillar matrix available to them for migration? As we noted above, the meniscus is similar to the ACL, and information on the cell migratory routes in the meniscus in wound healing should inform us about the processes operative in the ligament. We have developed an *in vitro,* organ culture, wound-healing model of the canine meniscus in serum-free medium.

Methods: The menisci are obtained fresh from dogs that have been killed after use by other investigators in protocols approved by the Institutional Animal Care and Use Committee of the Cleveland Clinic Foundation. Using a punch biopsy device, 2-mm plugs were removed, two from each meniscus, from the center, non-vascular portion of the tissue. Cells in each plug were killed by exposing the plugs to five cycles of repeated freezing in liquid nitrogen and thawing to room temperature. The plugs were then reinserted back into their holes in the meniscus. The menisci were cultured with gentle shaking in serum-free DMEM containing ITS (insulin, transferring, and selenium) for 2 weeks. Fig. 12A summarizes the

steps in creating the devitalized plug in the meniscus. Fig. 12B shows an actual meniscus with holes and the device we use for removing the plug with a plug of tissue protruding from it.

Results: Staining of tissue with DAPI (Fig. 12C) or evaluation under the electron microscope (Fig. 12D) confirmed that the cells in the plug were dead. Also, the act of cutting out the plug killed the cells in the live meniscus in a zone of tissue immediately adjacent to the crevice surrounding the plug. Thus, to begin with, the plug was completely void of cells, as was a rim of tissue in the live meniscus adjacent to the plug.

After 2 weeks in culture, cells from the superficial zone of the adjacent meniscus had migrated (*in vitro*) into the devitalized plug (Fig. 13A). It is interesting that such a process should occur in organ culture in the absence of a vascular or immune system. The cells appear to emerge from the superficial zone of the adjacent meniscus. Figs. 13B and 13C show electron micrographs of a cell in each instance that has populated the devitalized plug. The cell appears to be migrating through the peri-fibrillar system, but at the interface between this system and circumferential system. The surface of the cells make contact with the outer fibrils of the circumferential fibrillar system. The presence of the migrating cells at the interface between the two fibrillar systems is consistent with them boring their way through the less dense peri-fibrillar system, but perhaps finding traction and directionality on the surface of the parallel-aligned, closely-packed, circumferential fibrillar system. We consider this observation a major finding.

Study 7: Influence of type VI collagen on wound repair *in vitro*.

The driving hypothesis in our program is that insertion of exogenous type VI collagen, a cellular attractant, in a wound will accelerate the movement of repair cells, perhaps stem or progenitor cells, to the wound and thereby promote healing of wounds in ligaments or any other tissue in the knee joint *in vivo*. In the first and second year of the grant, we showed in an *in vitro* system that isolated ACL and DET cells were attracted to and moved over coated type VI collagen.

The protocol in our proposed program calls for insertion of type VI collagen, a cellular attractant, into the wounds in the ACL and PCL of canine knee joints *in vivo*. As noted above, we have developed an *in vitro* model for wound healing in the canine meniscus. The availability of an *in vitro* wound-healing model for the knee meniscus, a tissue very similar to the ACL in its outer zone, allowed us to test the consequences of inserting type VI collagen into wounds in the meniscus *in vitro*.

Method: Isolation of type VI collagen: Type VI collagen was isolated by polyethylene glycol precipitation of 6 M guanidinium chloride extracts from bovine menisci (Marcelino and McDevitt, 1995). In our experiments, we are using the intact form of type VI collagen extracted from tissues, which was shown to be superior to pepsin digested type VI collagen with respect to its adhesive properties. (Marcelino and McDevitt, 1995).

Testing of type VI collagen in wound healing model *in vitro*: Longitudinal, full-thickness slits were created in freshly harvested menisci. Sheets of purified type VI collagen were inserted into one crevice. The crevice on the meniscus from the contralateral joint was left empty and constituted the control. The menisci were cultured in serum-free DMEM containing ITS and then harvested fro sectioning and staining for cells with DAPI.

FIG. 10A, 10B, and 10C.

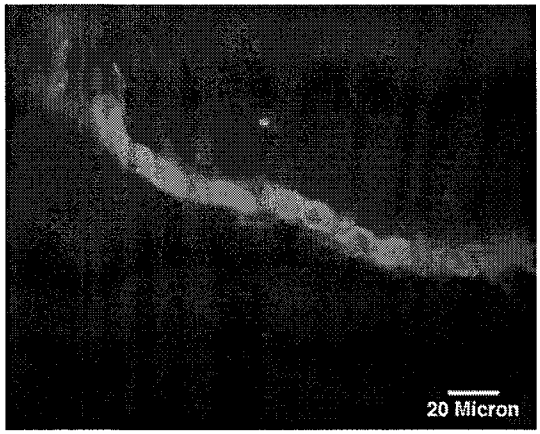

Fig. 10A. Linear array of cells (nuclei in blue) suspended by an enveloping matrix of type VI collagen (green). The complex was isolated from the canine ACL by dispase-collagenase digestion. Bar=20μm.

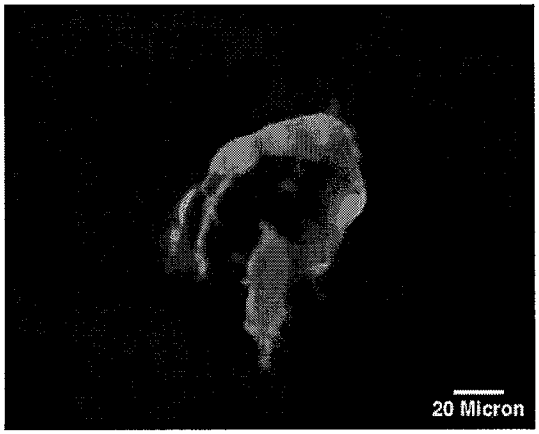

Fig. 10B. Linear array of cells isolated from canine DET. Type VI collagen (green) surrounds cells (nuclei in blue). Bar=20μm.

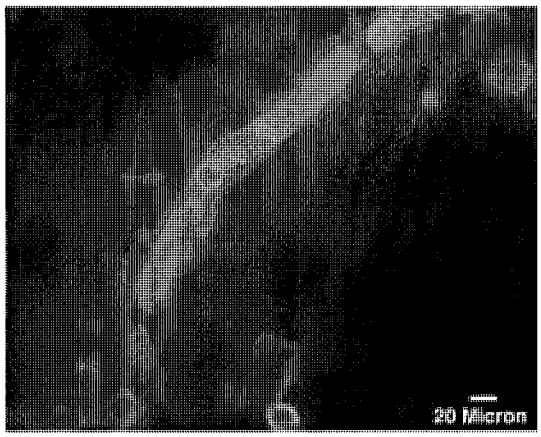

Fig. 10C. Linear array of cells (nuclei in blue) isolated by dispase-collagenase digestion from middle meniscus. Type VI collagen (green) surrounds cells. Bar=20μm.

FIG. 11A, 11B, and 11C.

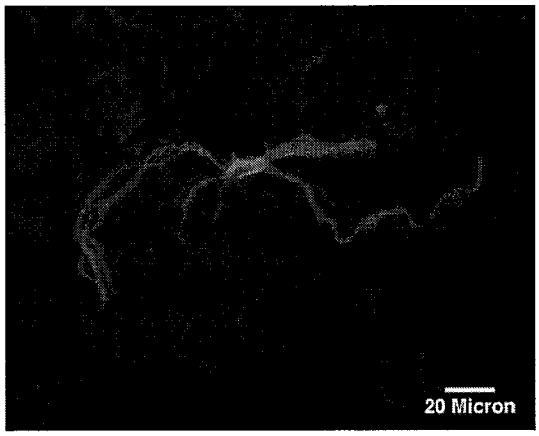

Fig. 11A. Cell isolated by dispase-collagenase digestion from canine ACL. Cell is stained for the intermediate filament vimentin (red), and cell nucleus (blue). Cell shows extended processes, some 123μm in length. Bar=20μm.

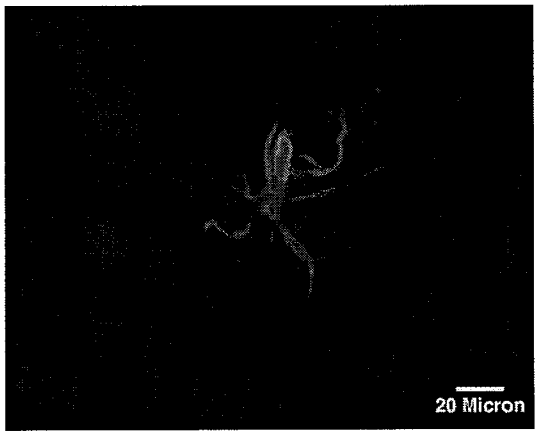

Fig. 11B. Cell isolated from canine DET similar to cell from ACL shown in Fig. 8A. Bar=20μm.

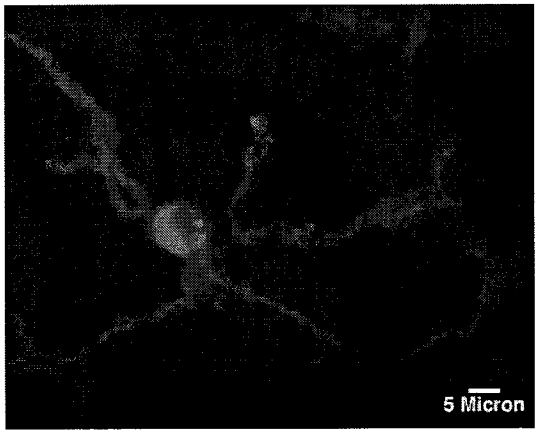

Fig. 11C. Cell with elongated processes isolated from canine outer meniscus. Bar=5μm.

FIG. 12A, 12B, 12C, and 12D.

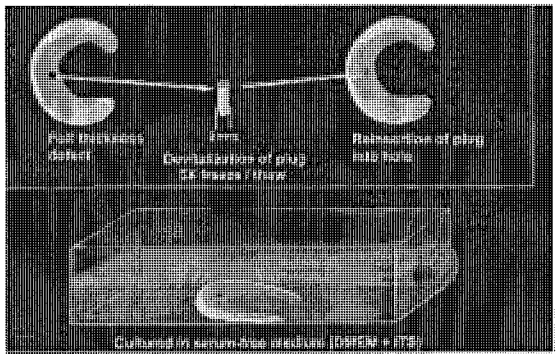

Fig. 12A. Wound healing model in canine meniscus *in vitro*. A 2mm plug of tissue was removed, rendered acellular by 5 cycles of freezing/thawing and then re-inserted into hole.

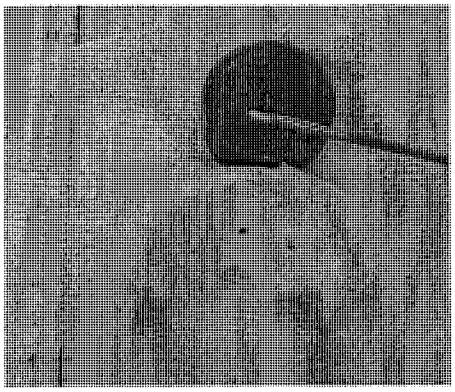

Fig. 12B. Hole in meniscus and hole-maker containing a plug of meniscus.

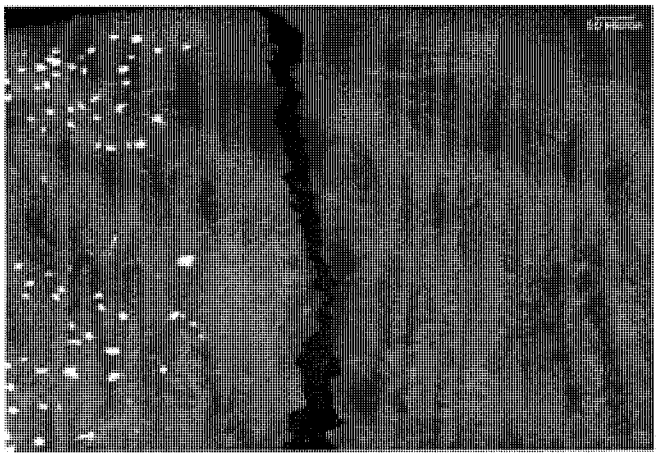

Fig. 12C. Coronal section of canine knee meniscus cultured for 3 days and stained for cell nuclei with DAPI. Note absence of cells in plug on right, and in zone of meniscus adjacent to crevice between live meniscus and plug. Bar=50μm.

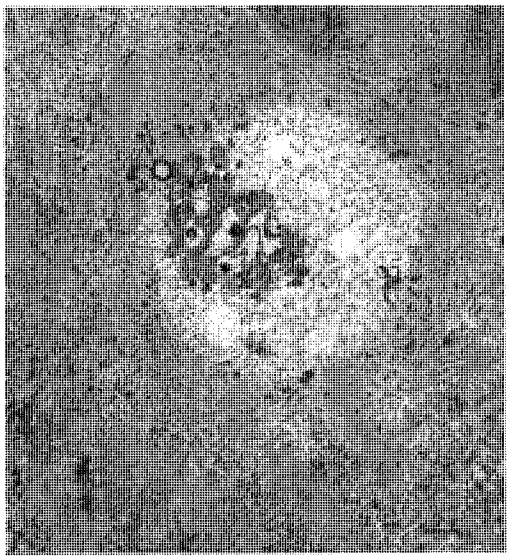

Fig. 12D. Necrotic fibrochondrocyte in devitalized plug. Bar=1μm.

FIG. 13A, 13B, and 13C.

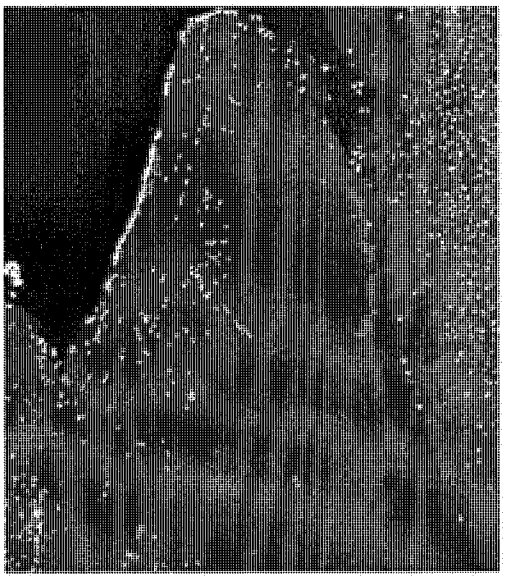

Fig. 13A. Coronal section of canine knee meniscus with plug after two weeks in culture. Cells nuclei stained with DAPI are seen migrating into devitalized plug.

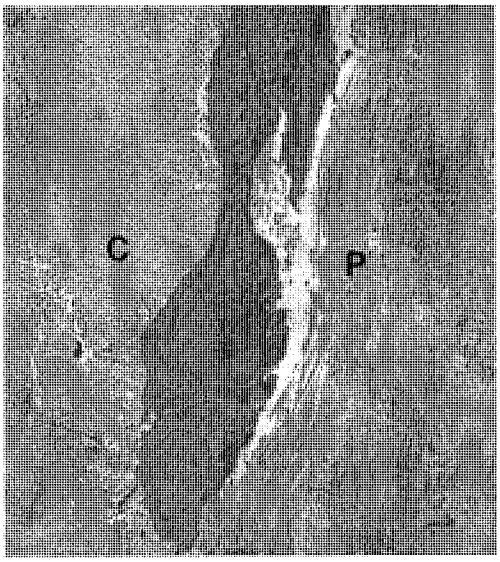

Fig. 13B. Cell migrating through devitalized plug after 2 weeks of culture. Cell appears to migrate along boundary between longitudinal fibrils of 'peri-fibrilar' system (P) and circumferential fibrils (C) seen in cross-section in coronal plug of canine meniscus. Bar=1μm.

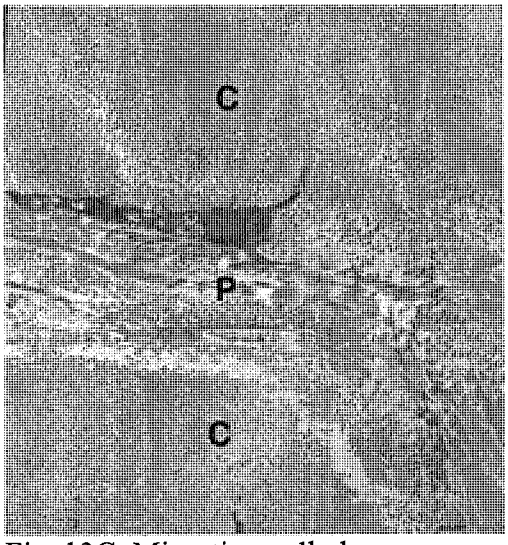

Fig. 13C. Migrating cell along boundary between longitudinal fibrils of 'peri-fibrilar' system (P) of devitalized plug and circumferential fibrils(C) seen in cross section in coronal plug of canine meniscus. Bar=1μm.

Results

Figure 14A shows a coronal section stained for cell nuclei with DAPI. The arrow points to the edge of the tissue at the crevice of the wound. Creation of a wound leads to cell death in the tissue adjacent to the wound. This relatively acellular zone is evident in Figure 14A. Figure 14B shows a corresponding tissue in which type VI collagen was inserted into the wound. We found no evidence that cells could penetrate the mass of type VI collagen. However, the zone of tissue adjacent to the crevice was much more cellular than the negative control (Fig. 14A). The presence of type VI collagen in the wound either protected the cells in the adjoining tissue from cell death or attracted cells into the tissue after cell death has occurred. We are exploring theses possibilities in further studies.

FIG. 14A and 14B.

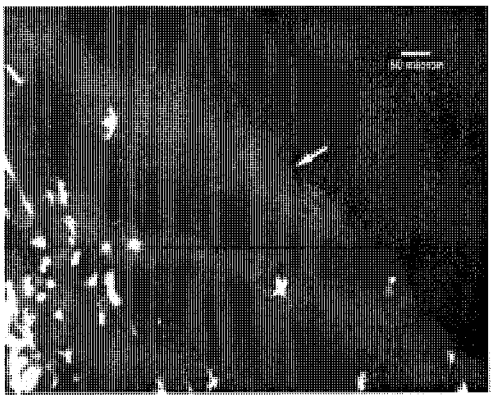

Fig. 14A. Coronal section of canine meniscus adjacent to wound. Arrow points to edge of tissue. No type VI collagen was inserted into wound. Meniscus was in culture for 4 weeks. Note acellular area adjacent to wound. Cell nuclei stained with DAPI. Bar=50μm.

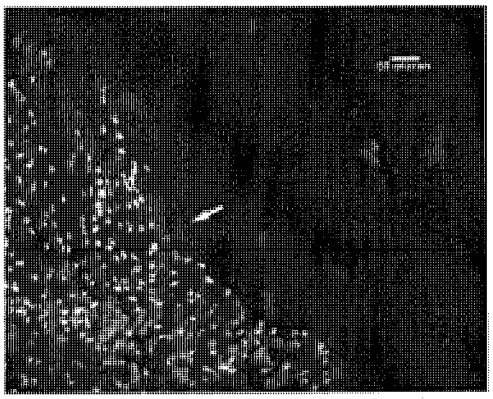

Fig. 14B. Coronal section of meniscus adjacent to wound. Type VI collagen was inserted into wound. Meniscus was in culture for 4 weeks. Cells are seen adjacent to wound (arrow). Cell nuclei stained with DAPI. Bar=50μm.

Study 8. Stem cells in wound repair of adult canine knee joint tissues

Rationale: Do the tissues of the skeletally mature knee joint harbor stem cells or progenitor cells that, under the appropriate stimulus, initiate a healing response? Given that the menisci seem to have the greatest capacity for repair in the knee joint, the possibility of progenitor cells was first explored in this tissue. As fat cells are absent in the inner nonvascular meniscus and are rare in the partially vascular outer tissue, the capacity to differentiate under appropriate stimuli into adipocytes was chosen as the indicator of the presence of progenitor cells in the meniscus.

Method: We generated our *in vitro* wound healing model with the devitalized plugs. These menisci, with controls in which no plug was removed, were cultured for 3 weeks. The cells were then released from the plugs, the outer meniscus and the inner meniscus and the cells cultured separately for 3 weeks until confluent.

Each cell population was then split in half and cultured in medium with or without adipogenic stimulators. Cells were then either stained for fat cells with Oil–Red O, or the RNA was extracted and assessed for gene expression of the adipogenic transcription factor peroxisome proliferator-activated receptor gamma-2 (PPAR-gamma2) by real-time TaqMan PCR.

Results: Fig. 15A shows the presence of adipocytes in medium containing the adipogenic factors, and Fig. 15B shows the absence of adipocytes in medium lacking such factors. Similarly, gene expression for PPAR-gamma2 was strikingly enhanced in the media containing the adipogenic factors (**Fig. 16**). In subsequent studies (not shown here) we observed that the culture of the the meniscus cells in an osteogenic medium led to the formation of colonies with a high expression of alkaline phosphatase levels. Both these observations are consistent with the presence of progenitor cells in the normal adult canine meniscus that can differentiate with the appropriate stimulus into adipocytes or osteoblasts. We would like to establish whether analogous progenitor cells are present in the ACL and DET of the adult canine knee joint. These observations are of major significance in designing strategies for repair of wounds in knee joint ligaments or menisci in a battlefield content.

FIG. 15A/ B and FIG. 16.

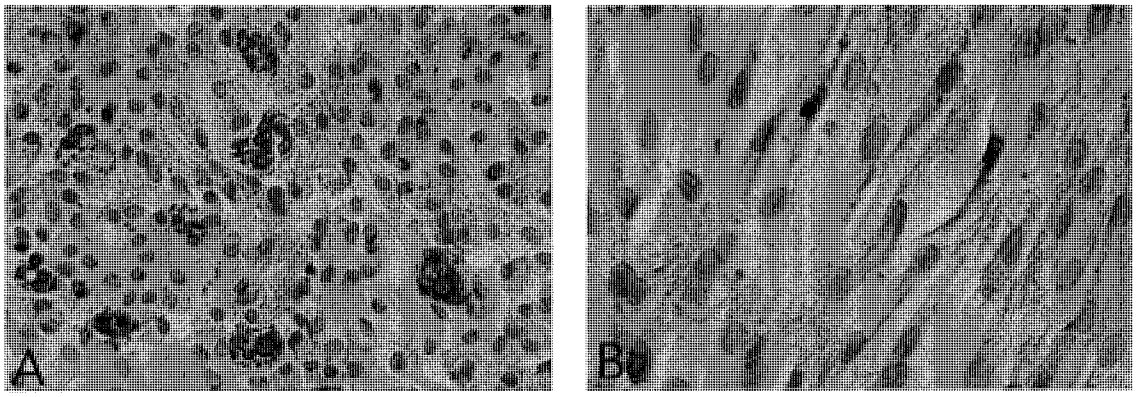

Fig. 15. Cells isolated from plug region of the *in vitro* canine meniscus wound-healing model. Cells were stimulated (A) in the adipogenic induction medium. Cells were stained for adipocytes using Oil red O (A). Control cells (B) were cultured on the same schedule as the experimental cells in the absence of adipogenic induction factors and stained for Oil red O. No staining observed (B). See figure 16 below.

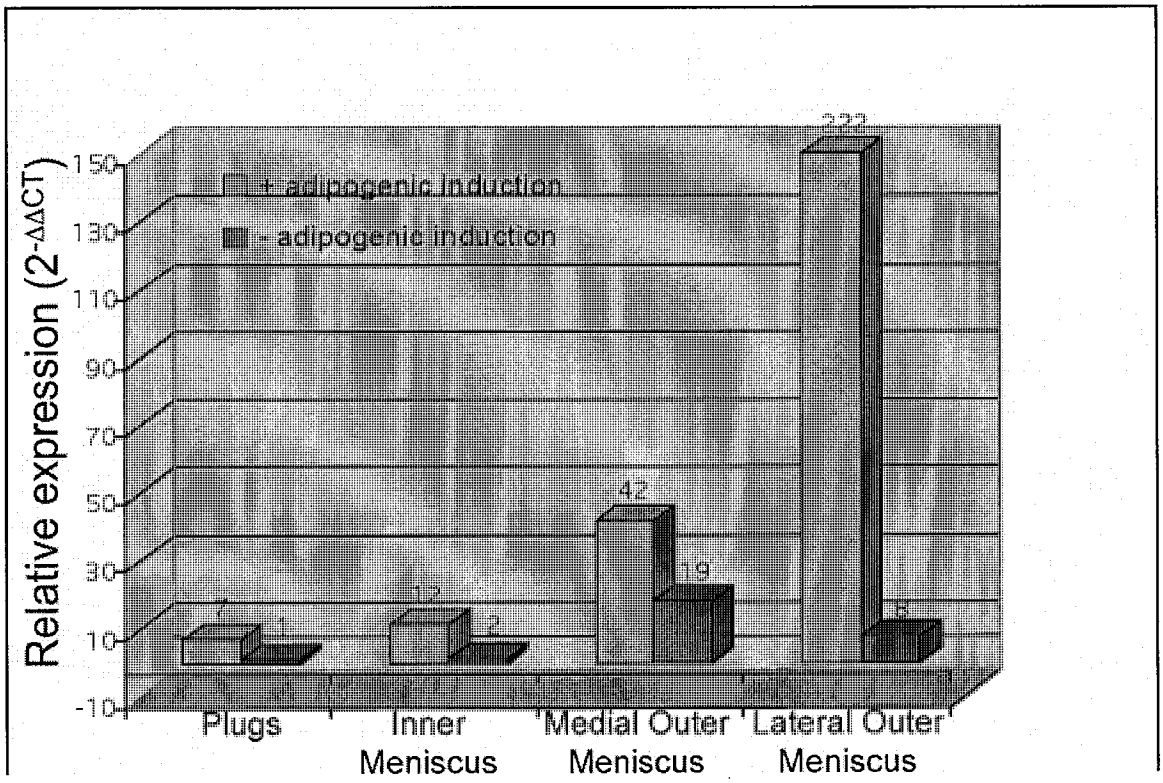

Fig 16. Cells isolated from different regions of the wound healing plug model *in vitro*, and cultured, as in Fig. 15, in the presence /absence of adipogenic induction medium. Gene expression for PPARgamma-2 was clearly demonstrable in cells that received the adipogenic induction, indicating, with the osteogenic data, not shown here, the presence of progenitor cells in the adult canine meniscus.

Our studies with type VI collagen demonstrate that this protein plays a critical role in wound healing in knee joint tissues. It is laid down early in the crevice of a wound, and is a cell attractant. Cells are stimulated to move across it, and it is an anti-apoptotic agent. The purified type VI collagen that was tested in the *in vitro* wound healing model formed a tight sheet that had excellent handling properties, but did not allow cell penetration. Type VI collagen mixed with other matrix components, particularly hyaluronan or type I collagen may provide a matrix through with cells can migrate and enhance wound healing.

Signaling factors in the conditioned media of wounded canine menisci can stimulate migration of cells *in vitro*. We created injuries in canine menisci, cultured the injured tissue, and harvested the conditioned medium. Conditioned medium or control medium was added to our *in vitro* wound healing model, and the tissues were compared after 4 weeks. The meniscus that was exposed to the conditioned medium had a much greater number of cells (261 in number in the slice image analysis) than the control tissue that was not exposed to the conditioned medium. Thus, there is a putative healing factor in the meniscus and perhaps the ligaments of the knee joint.

We have made the exciting discovery that the conditioned medium from a meniscus wounded *in vitro* will activate an adult human stem cell line to divide and migrate. Mesenchymal stem cells (Cambrex, Walkersville, MD) from adult human bone marrow were incubated for 24 hours first with 3-hour and then with 24-hour conditioned medium from injured menisci. Stem cells that were incubated in non-conditioned medium served as controls. The cells were then removed from the flasks and incubated for 48 hours in cell migration changers in fresh medium composed of DMEM and ITS. The wells in these migration chambers were coated with type VI collagen. The cells were applied as a focused spot at the center of the well. Cells that move on the well do so in a radial direction to form a colony with a larger diameter than cells that do not move or do so more slowly. Then number of cells in each chamber and the distance they had migrated were assessed by image analysis by the BME Imaging Core. Cells that had been exposed to the conditioned medium were greater in number and had migrated longer distances than the cells exposed to the control medium. Thus, the process of injury to the canine meniscus released one or more signaling factors that activated stem cells and stimulated them to divide and migrate. Conditioned medium from injured ACL can also induce human stem cells to divide and migrate and form three-dimensional colonies. In culture, these activated human stem cells will migrate onto and into a totally devitalized canine meniscus with a defect in it. The cells that migrate into devitalized plugs of tissue in the canine meniscus contain progenitor cells and poorly differentiated cells as assessed by shape and gene expression patterns. Taken together, these studies provide evidence of progenitor cells in the knee joint tissues of adult dogs that can be stimulated by injury to divide and migrate to repair the wound.

In summary, wound healing is a complex process. For healing of any wound to occur, cells must migrate into the area of injury and synthesize new extracellular matrix; but for cells to migrate there must be a scaffold upon which to move and a stimulus, such as a chemotactic factor, for movement. Our studies have begun to identify the cells and the chemotactic or haptotactic factors essential for normal wound healing.

KEY RESEARCH ACCOMPLISHMENTS

1. The relative gene expression, protein concentration, and spatial distribution of the proteoglycan aggrecan have been established in the canine knee joint ACL, PCL, meniscus, and articular cartilage (this has been published and a reprint is included in the Appendix).

2. The spatial relationship between tenascin-C and the vascularity of the canine ACL and meniscus has been established, with tenascin-C localized predominantly to the vascular zone.

3. The spatial distribution of types I and II collagen revealed a new fascicle-like structure in the meniscus similar to that of the ACL and DET. The spatial relationship of types I and II collagen in the knee joint meniscus and articular cartilage has been published, and a reprint is included in the Appendix.

4. An electron microscopic study of the ACL, DET, and meniscus in the canine knee joint revealed, for the first time, that the fibrillar orientation in the matrix (which we now call the peri-fibrillar matrix) is orthogonal to that of the main circumferential fibrillar system in the meniscus.

5. We have isolated different population of cells from the ACL, DET, and meniscus by dispase-collagenase dispersion and subsequent staining for vimentin and type VI collagen. This study revealed a stellate cell with distinctive long processes, revealed by vimentin staining, as well as round cells in linear arrays encased in a matrix of type VI collagen.

6. An *in vitro* model for wound healing of the canine meniscus was developed. This showed that migration of cells occurs, with the appropriate stimulus, within the interfascicular space, and along the outer surface of the longitudinally aligned circumferential fibrils. Type VI collagen is located along this peri-matrix in the meniscus.

7. The role of type VI collagen in ligamentous wound healing was identified. Insertion of purified type VI collagen into knee wounds in canine meniscus *in vitro* increased the cellularity along the tissue at the crevice of the wound.

8. We have demonstrated progenitor cells in the normal adult canine knee joint in the meniscus. Soluble factors in the milieu of an injury of the meniscus or ligament promote stem cell homing.

REPORTABLE OUTCOMES

1. Collagen organization in the meniscus and the cruciate ligaments.

   Kambic HE, McDevitt CA. Spatial organization of types I and II collagen in the canine meniscus. J Orthop Res 2005;23:142-9.

2. Aggrecan gene expression and organization in the meniscus and cruciate ligaments.

   Valiyaveettil M, Mort JS, McDevitt CA. The concentration, gene expression, and spatial distribution of aggrecan in canine articular cartilage, meniscus, and anterior and posterior cruciate ligaments: a new molecular distinction between hyaline cartilage and fibrocartilage in the knee joint. Connective Tissue Res 2005;46:83-91.

CONCLUSIONS

Using a combination of immunohistochemistry and electron microscopy, we have identified a new collagen fibril system which we call the peri-fibril system and which surrounds the parallel, circumferential bundles of collagen fibrils in the meniscus. We have shown that the proteoglycan, aggrecan, and type VI collagen are present in this peri-fibril system. We have developed a wound healing model *in vitro* by surgically creating wounds in freshly harvested canine menisci and culturing them in organ culture in serum-free medium. Using this organ culture system, we made the fascinating observation that cells migrating into acellular zones in the wound healing process do so within the peri-fibrillar system at the interface between this system and circumferential system. This major finding now allows us to construct type VI collagen scaffolds that mimic the composite matrix system that the cells employ for migration in the tissue.

We have found that type VI collagen promotes movement of ACL and DET cells. A complex of type VI collagen with heparin or hyaluronan, a macromolecule that binds to type VI collagen and has been implicated in cell movement, does not adversely affect the movement of cells on type VI collagen.

We have identified a range of cell types in the ACL and meniscus of the canine joint. These cell types include progenitor cells. Injury of the ACL or meniscus is accompanied by secretion of soluble factors that activate stem cells and stimulate their proliferation and migration into acellular tissue scaffolds.

Our findings, taken together suggest that it is possible to design a composite type VI collagen scaffold for insertion into wounds. Progenitor cells would move through these scaffolds to heal the wound. The combined scaffold/adult stem cell approach offers a powerful and realistic approach toward management of battlefield ligament and meniscus injuries to minimize sequelae in our wounded warriors.

Personnel on DoD grant/contract: Cahir A. McDevitt, Ph.D., Principal Investigator

Staff	Fellows	Techs	Students
McDevitt, C. -- PI	CHAKRABARTI, A – fellow	FEEBACK, KEVIN – tech	HAAS, JANE C - student
DOEHRING, TODD – Staff	MARULANDA, C- fellow	JOHNSON, CORY –tech	HENRY,MICHAEL - student
SHEKHAR, RAJ - Staff	OCHOA CHAAR, C - fellow	KLIKA, ALISON - tech	JONES, ELISA - student
	VALIYAVEETTIL, M –fellow	STACK, KAREN – tech	MUTHA, HEENA- student
		VARRECCHIA, M – tech	RUNDO, KRISTIN - student
			VIDMAR,ERICK - student

REFERENCES CITED

Amiel D, Frank C, Harwood F, Fronek J, Akeson W. Tendons and ligaments: a morphological and biochemical comparison. J. Orthop Res 1984;1:257-65.

Eyre D, Muir H. The distribution of different molecular species of collagens in fibrous, elastic and hyaline cartilages of the pig. Biochem J 1975;151:595-602.

Kambic HE, McDevitt CA. Spatial organization of types I and II collagen in the canine meniscus. J Orthop Res 2005;23:142-9.

Marcelino J, McDevitt CA. Attachment of articular cartilage chondrocytes to the tissue form of type VI collagen. Biochim Biophys Acta 1995;1249:180-188.

McDevitt CA, Marcelino J. Composition of articular cartilage. In Andrish J, ed. Sports Medicine Arthroscopy Reviews. 1994;2:1-12.

McDevitt CA, Marcelino J, Tucker L. Interaction of intact type VI collagen with hyaluronan. FEBS Lett 1991;294:167-170.

McDevitt CA, Mukherjee S, Kambic HE, Parker R. Emerging concepts of the cell biology of the meniscus. Curr Opin Orthop 2002;13:345-50.

Nakano T, Dodd CM, Scott PG. Glycosaminoglycans and proteoglycans from different zones of the porcine knee meniscus. J Orthop Res 1997;15:213-20.

Ricard-Blum S, Dublet B, Van der Rest M. Collagen VI: a beaded filament-forming collagen. In Ricard-Blum S, Dublet B, Van der Rest M (eds) Unconventional collagens: types VI, VII, VIII, IX, X, XII, XIV, XVI, AND XIX. Oxford and New York: Oxford University Press, 2000, pp. 4-24.

Tanaka K, Hiraiwa N, Hashimoto H, Yamazaki Y, Kaskabe M. Tenascin-C regulates angiogenesis in tumor through the regulation of vascular endothelial growth factor expression. Int J Cancer 2004;108:31-40.

Valiyaveettil M, Mort JS, McDevitt CA. The concentration, gene expression, and spatial distribution of aggrecan in canine articular cartilage, meniscus, and anterior and posterior cruciate ligaments: a new molecular distinction between hyaline cartilage and fibrocartilage in the knee joint. Connective Tissue Res 2005;46:83-91.

APPENDIX

Kambic HE, McDevitt CA. Spatial organization of types I and II collagen in the canine meniscus. J Orthop Res 2005;23:142-9.

Valiyaveettil M, Mort JS, McDevitt CA. The concentration, gene expression, and spatial distribution of aggrecan in canine articular cartilage, meniscus, and anterior and posterior cruciate ligaments: a new molecular distinction between hyaline cartilage and fibrocartilage in the knee joint. Connective Tissue Res 2005;46:83-91.

Functional Tissue Engineering Conference Group (including McDevitt CA). Evaluation criteria for musculoskeletal and craniofacial tissue engineering constructs: a conference report. Tiss Eng Part A 2008;14:2089-104.

ELSEVIER

Journal of Orthopaedic Research 23 (2005) 142–149

Journal of Orthopaedic Research

www.elsevier.com/locate/orthres

Spatial organization of types I and II collagen in the canine meniscus

Helen E. Kambic, Cahir A. McDevitt *

Department of Biomedical Engineering and Orthopaedic Research Center, Lerner Research Institute, The Cleveland Clinic Foundation, ND-20, 9500 Euclid Avenue, Cleveland, OH 44195-5254, USA

Received 26 February 2004; accepted 11 June 2004

Abstract

The meniscus of the knee joint is a fibrocartilage mainly composed of type I collagen and smaller amounts of type II collagen. The distribution of type II collagen in the canine meniscus and its spatial relationship to type I collagen was examined by immunohistochemistry and confocal microscopy.

Dorsal and coronal slices of the mid-section of medial and lateral menisci from the knee joints of skeletally mature dogs were predigested with *Streptomyces* hyaluronate lyase and bacterial Protease enzyme XXIV. Monoclonal antibodies against type I collagen (CP17L) and type II collagen (II-II6B3) and an anti-type II collagen polyclonal antibody (AB759) were employed.

The staining for type II collagen in the extracellular matrix of hyaline articular cartilage was diffuse without any identifiable spatial organization. In striking contrast, type II collagen in the fibrocartilage of the meniscus stained as an organized network. Type II collagen was distributed throughout the meniscus with the exception of the outer zone containing the blood vessels.

Coronal and dorsal staining of the meniscus showed bundles of circumferential fibrils of type I that colocalized with type II collagen in specific sites. These bundles were enwrapped in a second organizational fibrillar system of types I and II collagen that also colocalized. Bundles of circumferential fibrils appeared in cross-section in coronal sections as dots within the interstitial spaces framed by the network of types I and II collagen of the second system. Confocal overlays showed that types I and II collagens were superimposed, suggesting a close spatial proximity between the two collagens. The cells were confined to the types I and II collagen fibrils that enwrapped the bundles. A striking feature of the radial tie fibers was patches of type II collagen without colocalized type I collagen.

Our study reveals a unique network of type II collagen in fibrocartilage of the meniscus that serves as a morphological distinction between fibro- and hyaline cartilage.

Keywords: Knee meniscus; Type I collagen; Type II collagen; Fibrocartilage; Collagen fibrils

Introduction

The knee menisci are crescent-shaped structures that are thick at the outermost border and taper to a thin, free edge at their inner boundary in the joint (Fig. 1) [13]. Blood vessels penetrate 10–12% of the radial distance of the tissue in the skeletally mature human [15] and dog meniscus (this study).

The knee joint meniscus has been classified as a fibrocartilage [11,12]. Early polarized light microscopy [4] and X-ray diffraction [1] studies established that the fibrils in the superficial zones of human, pig, and dog meniscus were mainly radial in orientation, while those in the central body had bundles of fibrils with a predominantly circumferential orientation.

* Corresponding author. Tel.: +1 216 444 7692; fax: +1 216 444 9198.

E-mail address: mcdevic@ccf.org (C.A. McDevitt).

0736-0266/$ - see front matter © 2004 Orthopaedic Research Society. Published by Elsevier Ltd. All rights reserved.
doi:10.1016/j.orthres.2004.06.016

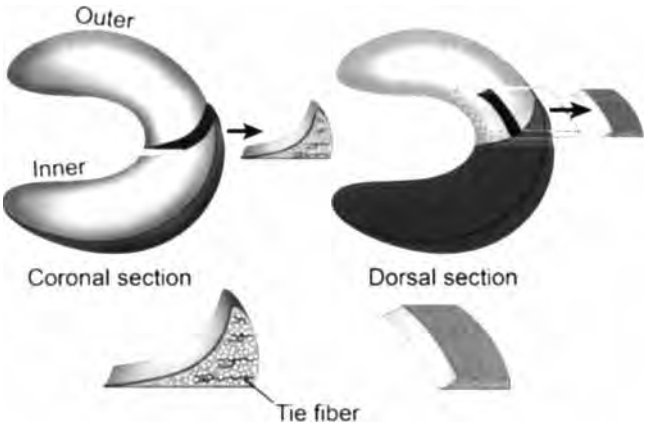

Fig. 1. Drawings depicting coronal and dorsal sections of the canine meniscus.

A scanning electron microscopy study [27] revealed three distinct layers in the organization of the fibrils in the meniscus: (A) a meshwork of thin fibrils of approximately 30 nm diameter that covers the surface of the tissue; (B) beneath the superficial network is a lamellar-like layer of collagen fibril bundles to a depth of 150–200 μm in the outer tissue that are either radial or at different angles; (C) the main body of the meniscus that is composed predominantly of circumferentially arranged bundles of collagen fibers [27] with occasional radial or "tie fibers" [30].

The meniscus has a composition similar to fibrous tissues like tendon or ligaments. The tissue is about 70% water, with collagen constituting about 60–70% of the dry weight of the tissue [22]. Proteoglycans, matrix glycoproteins and small amounts of elastin constitute the remainder of the dry weight [22].

Eyre and Muir [8], in a now classic study that provided molecular criteria for the distinction of hyaline and fibrocartilage, established that the predominant collagen in pig meniscus was type I collagen, while in hyaline articular cartilage the major collagen was type II. Bovine meniscus, however, does contain some type II collagen [6,9]. Supporting the biochemical studies, type II collagen gene expression has been demonstrated in rabbit menisci by in situ hybridization [3] and RT-PCR [17], in pig menisci by real time RT-PCR [31], and in isolated canine meniscus cells by RNase protection assay [34]. Gene expression for type I collagen is relatively dormant in the menisci of normal skeletally mature dogs, but is dramatically upregulated after wounding of the tissue [33].

It is not clear what the spatial relationship of type II collagen is to the type I collagen meshwork in the meniscus. Gao [10] demonstrated weak staining for type I and fairly intense staining for type II collagen in similar sites at the anterior attachment site of the rabbit medial meniscus to the tibial plateau. Gao's interesting study, however, was restricted to the collagens at the bony insertion site of the meniscus.

Naumann et al. [24] showed weak staining for type I collagen and diffuse patches of stain for type II collagen in relatively low magnification immunomicrographs of the rabbit meniscus. While this study clearly showed that type II collagen could be detected immunochemically in the meniscus, the finer organization of the type II collagen at the light microscopic level and its spatial relationship to type I collagen was not investigated.

The meniscus, unlike articular cartilage, has the capacity to heal wounds. We noted that integration of adjacent tissue across the crevice of a wound occurred in the meniscus of the dog [18]. Defining the structure of the collagen fibrillar meshwork in the normal meniscus is critical in understanding the role of fibril reorganization in the healing process. The purpose of our study was to identify the location and micro-anatomical organization of type II collagen and its spatial relationship to the type I collagen fibrils in the canine meniscus.

Materials and methods

Source and preparation of tissue

Whole knee joints were obtained from 10 skeletally mature dogs weighing approximately 25 kg. These studies received prior approval from the Animal Research Committee at our institution. Serial sections of the medial and lateral menisci were cut in either the dorsal plane or at 90° to the longitudinally oriented collagen fibers and were taken from the mid-body of the meniscus (Fig. 1). The dorsal plane in quadrupeds is the horizontal plane that separates the upper (dorsal) and lower (ventral) sections of the body [23]. Full thickness samples of femoral articular cartilage served as positive controls for the type II collagen staining.

Source and specificity of antibodies

Mouse anti-chick collagen type II mAb (II-II6B3) was obtained from the Developmental Studies Hybridoma Bank developed under the auspices of the NICHD and maintained by The University of Iowa, Department of Biological Sciences, Iowa City, IA 52242. This antibody was generated with pepsin-digested type II collagen from chick sternum and requires the intact collagenous triple helix for recognition [20]. This antibody has been used in a number studies and its specificity for type II collagen confirmed [5,25,29]. The goat anti-bovine type II collagen polyclonal antibody (AB759), was purchased from Chemicon International (Temecula, CA) as an affinity purified immunoglobulin. The antisera was adsorbed against collagen types I, III, IV, V and VI immobilized on Sepharose 4B. ELISA demonstrated that the anti-type II collagen antisera displayed low reactivity to other collagen types (information from Chemicon International). Mouse anti-type I collagen monoclonal antibody mAb (CP17L) was obtained from Oncogene Research Products (Boston, MA) and did not cross react with other collagen types according to the company literature. A variety of applications of this antibody have been reported [19,32].

Immunofluorescence

Dorsal and coronal slices of the mid-section of medial and lateral menisci from the knee joints of large, normal, skeletally mature dogs of both sexes were processed as frozen blocks. Sections (3–5 μm) were

cut on a motorized Leica CM 3050 cryostat (Leica Microsystems, Nussloch, Germany). Thawed sections were predigested with *Streptomyces* hyaluronate lyase and then bacterial Protease enzyme XXIV (EC 3.4.21.62; Sigma Chem. Co., St. Louis, MO) 0.05% in 10 mM sodium acetate and 5 mM-calcium acetate buffer (pH 7.52) for 10 min [28]. Sections were blocked overnight at 4 °C using 3% normal goat serum in PBS. Incubation overnight with monoclonal antibodies against type I collagen or type II collagen in 0.1% BSA, 0.5% Tween and PBS (antibody buffer) was followed by overnight incubation with fluorescein (FITC)-conjugated, affinity-purified purified goat anti-mouse IgG, F $(ab')_2$ secondary antibodies (Jackson ImmunoResearch Laboratories Inc., West Grove, PA.) in antibody buffer. In dual labeling experiments an affinity-purified, goat, anti-type II collagen polyclonal antibody (AB759) was mixed with the anti-type I collagen antibody and then incubated with an AlexaFluor® 594-conjugated F $(ab')_2$ fragment of rabbit anti-goat IgG secondary antibody (Molecular Probes, Inc., Eugene, OR) and the FITC-conjugated goat anti-mouse IgG. After incubation, the slides were copiously rinsed in PBS for 6 h and mounted in Vectashield with DAPI (Vector Laboratories, Burlingame, CA). Incubation of tissues without the primary antibody served as the negative controls.

Microscopy

Confocal images of the surface of the meniscus were collected using a Leica TCS-SP laser scanning confocal microscope (Mannheim, Germany). Conventional microscopy was performed on an Olympus BX microscope (Olympus, Tokyo, Japan) equipped with a QED Camera Plug-In™ Package (QED Imaging Inc., Pittsburgh, PA). This software permitted distance measurements on the images between selected points.

Results

Immunolocalization of type I collagen in coronal sections

The spatial distribution of type I collagen in the normal canine meniscus in the light microscope is shown in Fig. 2. Staining for type I collagen in coronal sections revealed a continuous, diffuse band about 100–125 μm in depth in the femoral and tibial superficial zones of the meniscus (Fig. 2(A)). In the main body of the meniscus, stretching from the peripheral attachment to the inner tip of the tissue, the type I collagen appeared as an intricate network of thick strands. Cell nuclei identified by DAPI were located along these strands. In the microscope, thinner strands and dots were evident within the interstices framed by the network, but were less evident in the electronic image (Fig. 2(A)). The network varied in shape and size with a mean diameter of the interstices of 49.3 ± 10.3 μm in the major axis and 30.0 ± 4.5 μm in the minor axis. Diffuse staining for type I collagen was demonstrable within the radial "tie fibers" (arrow, Fig. 2(A)) around blood vessels and within the joint capsule (not shown). The negative controls, in which incubation with the primary antibody was omitted, showed no staining (not shown).

Type II collagen in coronal sections of meniscus and articular cartilage

Staining of coronal sections of the medial meniscus with the monoclonal antibody against type II collagen showed staining that was both intense and diffuse in the superficial zone (Fig. 2(B)). Within the main body of the meniscus, type II collagen stained as a network of thick strands similar to that observed for type I collagen (Fig. 2(B)). The intensity of the staining for type II collagen, however, unlike that for type I collagen, was not uniform throughout the body of the meniscus. Intense staining was present throughout the middle region of the coronal section. Interestingly, the staining for type II collagen terminated fairly abruptly in a zone at the outer periphery (arrow, Fig. 2(B)), with little or no staining being evident in the region where the blood vessels are usually found. Staining with an anti-von Willebrand antibody demonstrated that the blood vessels in

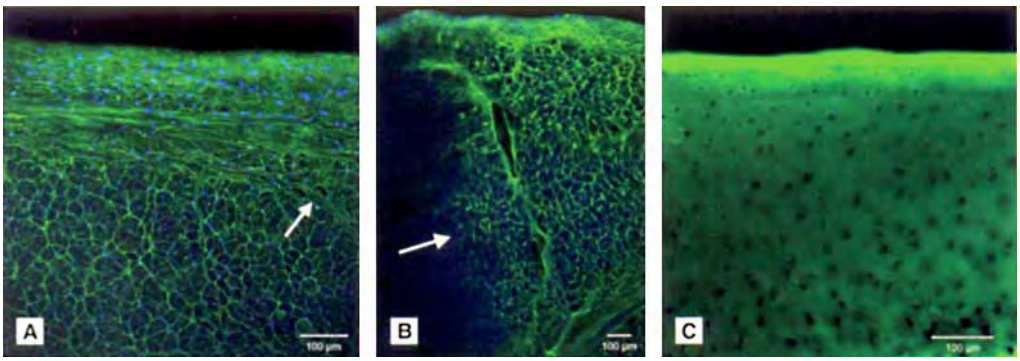

Fig. 2. Immunohistochemical staining of the medial meniscus (coronal sections) and articular cartilage in the light microscope. (A) Femoral surface of the meniscus stained with a monoclonal antibody against type I collagen. The arrow in (A) points to a "tie fiber". (B) Femoral surface of the meniscus stained with a monoclonal antibody against type II collagen. Note that the type II collagen staining abruptly diminishes in intensity towards the outer region of the meniscus (arrow in (B)). (C) Femoral condylar articular cartilage stained with a monoclonal antibody against type II collagen. The cell nuclei in blue in (A) and (B) were stained with DAPI. Note that the meshwork observed for type II collagen staining in the meniscus fibrocartilage is not evident in the articular cartilage.

the canine menisci employed in this study penetrated only 10–12% of the length of a coronal section (data not shown).

The organization of types I and II collagen in the superficial zone, approximately 125 μm in depth, lacked the meshwork of the underlying tissue, consistent with a different orientation for these collagens in this zone [27]. A thin layer at the surface of the superficial zone, apparently corresponding to the 10 μm layer observed by Petersen and Tillmann [27], did not stain for type II collagen.

Radial "tie fibers" in coronal sections, which extend from the outer periphery of the meniscus into the inner body where they branch out in several directions, stained heavily for type II collagen (Fig. 2(B)).

The lateral meniscus showed a similar pattern of staining for type II collagen as that found in the medial meniscus (not shown). More tie fibers were seen in the lateral meniscus than in the medial meniscus and these stained heavily for type II collagen.

Staining for type II collagen in articular cartilage is shown in Fig. 2(C). The monoclonal antibody against type II collagen revealed intense, diffuse staining in the interterritorial matrix outside the lacunae of the cells in the articular cartilage (Fig. 2(C)). This staining lacked any demonstrable, organized network, as was observed in the fibrocartilage of the meniscus, and was particularly intense in the superficial zone.

No staining was observed for the negative controls that lacked the primary antibodies.

Spatial relationship of type I to type II collagen in coronal sections

Fig. 3(C) shows a confocal micrograph of a coronal section of a medial meniscus in which the image obtained with an anti-type I collagen monoclonal antibody (green, Fig. 3(A)) was overlaid with that obtained with an anti-type II collagen polyclonal antibody (red, Fig. 3(B)). The main thick strands of the network as well as the finer strands within the interstices were mostly yellow, demonstrating a close spatial relationship of types I and II collagen in this structure. Patches of type II collagen without type I collagen were evident at some of the nodes of the network and were particularly pronounced along the radial "tie fibers" (arrow, Fig. 3(C)).

There was an interesting difference in the way the interstitial spaces between the interconnecting strands of the network stained, depending on their location within a tissue section. Image capture sensitivity and the selected magnification make the spaces framed by the network in Fig. 3 appear blank. Colocalized staining for types I and II collagen was evident, however, as a collection of dots and finer strands within the interstices of the network in discrete areas of the meniscus (e.g., above the "tie fiber" in Fig. 3(C)). The staining for type II collagen as dots within the interstitial spaces of the network is more evident at the higher magnification of the meniscus as shown in Fig. 4. In other areas only type I collagen staining was evident as green dots and patches within the interstices (for example, below the "tie fiber" and left of the arrow in Fig. 3(C)).

Collagen organization in the inner tip of the meniscus

The inner tip of the meniscus is the thinnest part of the tissue and is the zone most likely to experience compressive forces. We explored the possibility that the type II collagen organization in the inner tip might lack the organized appearance observed in the rest of the meniscus. The pattern of type II collagen staining with the monoclonal antibody in the innermost tip of the meniscus is shown in Fig. 4. The inner zone showed a network pattern in coronal sections of the inner meniscus similar to that observed in the main body of the tissue (Fig. 3(A) and (B)). The staining for type II collagen at the higher magnification in Fig. 4 was revealed as an array of dots within the interstitial spaces framed by the main fibrillar meshwork. As the innermost tip of the meniscus was approached, however, the network pattern was mostly lost, but the staining as dots was retained. Nowhere did the organization of type II collagen in the tip resemble the amorphous mass that we observed for this collagen in the hyaline articular cartilage.

Location of cells and types I and II collagen network

The location of the cells within the collagen network evident in the coronal sections was particularly notable. The cells were located on the strands of the network, often at the nodes, but never within the interstitial spaces (Figs. 3(C) and 4). Cells were also demonstrable within the "tie fibers".

Immunolocalization of types I and II collagen in dorsal sections

Two patterns of staining were evident for type I collagen in dorsal sections. Broad bands of type I collagen staining (thick arrow, Fig. 5(A)) were evident. Thin, slightly more intensely stained strands of type I collagen (thin arrow, Fig. 5(A)), were also evident between the broad bands in dorsal sections. Closer inspection revealed that these thin strands seem to be composed of linear arrays of dots, suggesting fibrils in cross-section. The cells in these dorsal sections were located in linear, longitudinal rows exclusively along the thin strands (Fig. 5(A)). Strands radiating out from the main longitudinal axis of the columns were also evident, giving the appearance of an interconnecting system (not shown).

Type II collagen in dorsal sections stained predominantly as thin longitudinal strands along which cells were

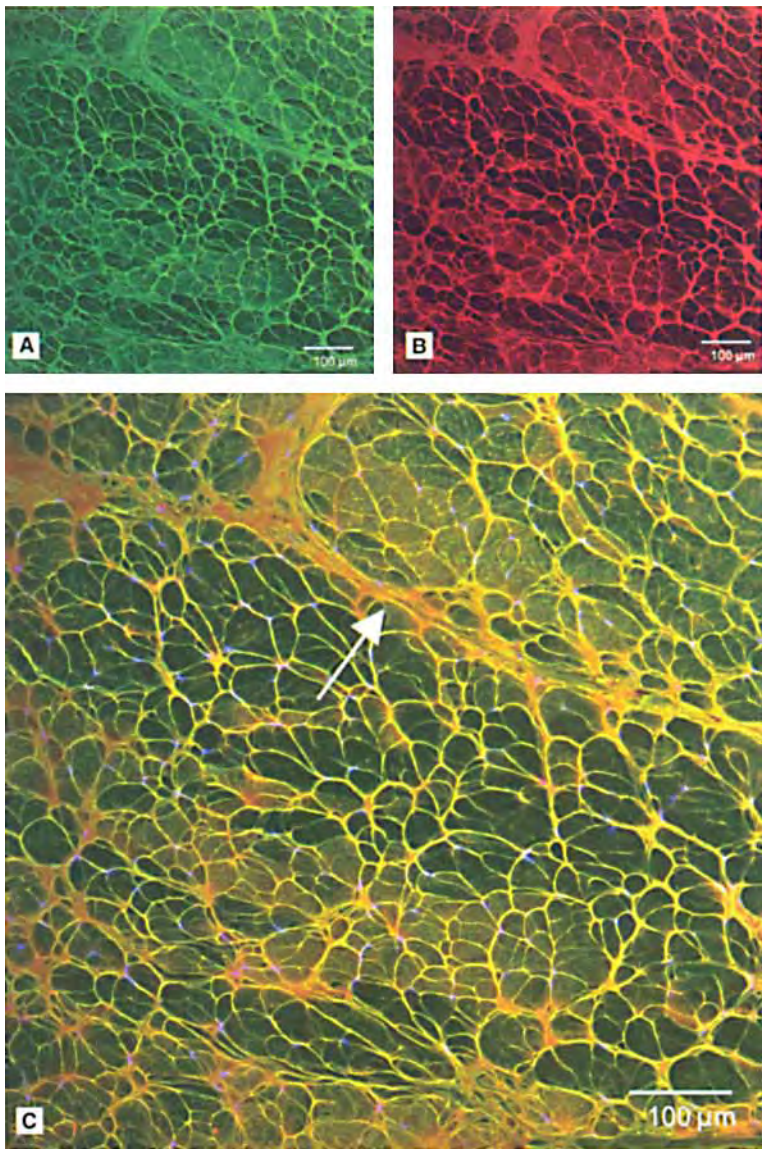

Fig. 3. Confocal micrographs of a coronal section of the medial meniscus stained for types I and II collagen. The bundles of circumferential fibrils are seen in cross-section. (A) Staining with a monoclonal antibody against type I collagen (green). (B) Staining with a polyclonal antibody against type II collagen (red). (C) Overlay of (A) and (B). Yellow fluorescence in (C) depicts the colocalization of types I and II collagen. Type II collagen is pronounced in the 'tie fiber' (arrow). Cell nuclei are stained blue with DAPI.

aligned (thin arrows, Fig. 5(B)). Many of the cells along these thin strands appeared encapsulated by a halo of type II collagen. The type II collagen also stained as broad longitudinal bands in which many cells were distributed (thick arrow, Fig. 5(B)). The width of the broad bands of type II collagen and the fact that they were much less numerous than the thin strands suggested that they were "tie fibers", seen here in the dorsal plane. In separate overlay studies (not shown) the thin strands of types I and II collagen were shown to colocalize.

The distinctive alignment of cells in coronal and dorsal sections and their spatial relationship to the collagen staining helps to define the nature of the three-dimensional fibrillar network. The thin strands of types I and II collagen along which the cells were arrayed in dorsal sections constitute the interconnecting strands of the network seen in coronal sections. The broad bands of type I collagen (thick arrow, Fig. 5(A)) evident between the linear array of cells in dorsal sections represent longitudinal staining of the fibrils stained in cross-section as dots within the interstitial spaces framed by the network in coronal sections (Fig. 3(C)).

Discussion

Our light and confocal microscopy study showed that type II collagen in the canine meniscus is organized into

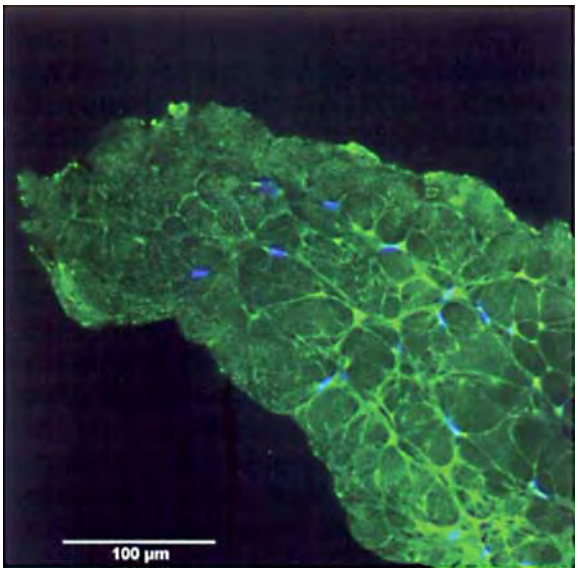

Fig. 4. Confocal micrograph of coronal section of inner meniscus stained with the monoclonal antibody against type II collagen. The higher magnification employed here reveals the type II collagen in the inner meniscus as a network of strands that frame an array of dots within the interstitial spaces. The meshwork of strands is progressively lost as the innermost tip of the meniscus is approached, but the array of dots is retained. Cell nuclei are stained blue with DAPI.

a network. In contrast, no such network was demonstrable in articular cartilage after staining for type II collagen. The capacity to form fibrillar networks of types I and II collagen is a distinctive property of the fibrochondrocyte cells in fibrocartilage.

To our knowledge, this is the first time a network has been reported for type II collagen in the meniscus. A similar network of type II collagen staining was observed by Beard et al. [2] in the annulus fibrosus of the porcine intervertebral disc, another fibrocartilage. The presence of the type II collagen network in the meniscus and the annulus fibrosus, and the absence of such a network in articular cartilage provide an extra, micro-anatomical distinction between fibrocartilage and hyaline cartilage. Clearly, the interpretation of the three-dimensional network organization of fibrocartilage is facilitated when tissues sections are cut perpendicular or parallel to the main fibrillar structures.

Our observation of intense staining for type II collagen in the inner body of the meniscus and the absence of staining in the outermost, attachment region, is consistent with Cheung's biochemical study of the distribution of type II collagen in the meniscus [6]. Cheung divided the bovine meniscus into the inner one third and outer two thirds according to radial distance. Both types I and II collagen were demonstrable in pepsin and cyanogen bromide digests of the inner meniscus. In contrast, only type I collagen with trace amounts of types III and V and no type II collagen was detected in the outer meniscus.

The staining patterns we observed imply that the bundles of circumferential fibrils observed in polarized light and electron microscopic studies [4,27] are composed of two distinct collagen fibrillar systems. The staining suggested that the broad, circumferential bundles of fibrils contained both types I and II collagen in some sites, and in other sites these bundles contained only or predominantly type I collagen and little or no type II collagen. A second, thinner fibrillar system composed of both types I and II collagen separated the

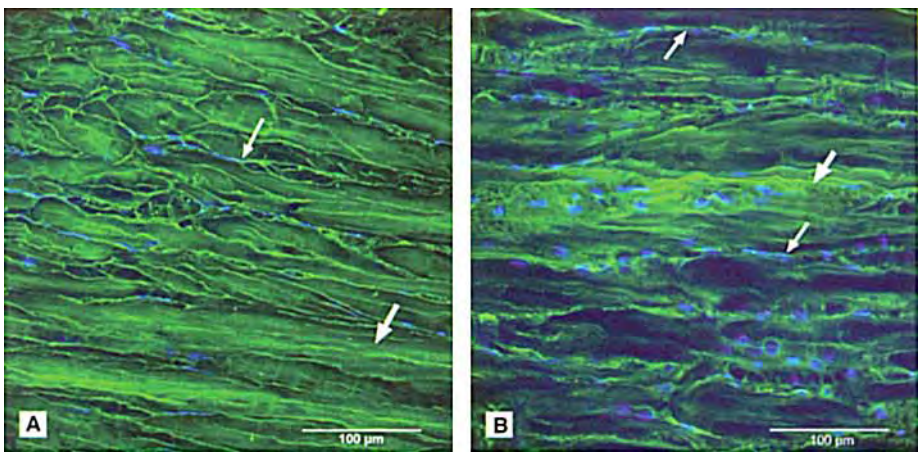

Fig. 5. Confocal micrographs of dorsal section of the medial meniscus stained for types I and II collagen and cell nuclei. (A) Confocal micrograph of a dorsal section of a medial meniscus stained with a monoclonal antibody against type I collagen and cell nuclei stained with DAPI. Two patterns of type I collagen staining were evident. Note the broad bands of type I collagen (thick arrow). A second pattern of thin, more intensely stained, strands of type I collagen was demonstrable (thin arrow). Longitudinal arrays of cells were aligned along these thin strands. (B) Confocal micrograph of another dorsal section of a medial meniscus stained with a monoclonal antibody against type II collagen and cell nuclei stained with DAPI. Type II collagen appeared mainly as thin longitudinal strands (thin arrow) along which the cells were aligned. Many of these cells appeared encapsulated by a halo of type II collagen. The occasional broad, longitudinal band of type II collagen (thick arrow) that has the appearance of a "tie fiber" with an abundance of cells was also seen.

broad bundles of fibrils. The staining for types I and II in this second system was generally super-imposable and appeared as a network in the coronal sections. Our light microscopy study does not allow us to make definitive conclusions on the orientation of the fibrils in this thin layer in relation to the bundles of circumferential fibrils. However, the punctate appearance of types I and II collagen staining in the dorsal sections suggests they represent bundles of fibrils observed in cross-section. The intense staining of the weave in the coronal sections is consistent with this interpretation and raises the possibility that the orientation of this collagen mix may be perpendicular or nearly perpendicular to the main circumferential fibrils. Such a model would be consistent with the electron microscopic studies of Ghadially et al. [12] that showed collagen fibrils at right angles to one another.

The colocalization of types I and II collagen in many sites in the meniscus raises the possibility that these two collagens could coexist within a single fibril or a bundle of fibrils. The cross-link between types I and II collagen in the bovine intervertebral disc identified by Eyre et al. [7] and the presence in the meniscus of contiguous fibrils with broad and small diameters in transmission electron micrographs [12] support these possibilities.

The major cell in the meniscus is the rounded fibrochondrocyte that is found in the inner and main body of the tissue [21] where the type II collagen is located. It would seem that the fibrochondrocytes synthesize both types I and II collagen, although not necessarily at the same time. In situ hybridization studies of fibrocartilaginous regions of the mature bovine deep flexor tendon imply that the same cells express mRNA for both types I and II collagen [26].

An interesting feature of the distribution of type II collagen in the meniscus was the absence of staining in the outermost zone of the tissue. Staining with antibodies specific for the G1 domain of aggrecan was also weakest in this zone of the meniscus (Valiyaveettil, Mort and McDevitt, unpublished data). This region of the meniscus is populated with fibroblast-like cells with extended processes [16], is vascularized [14], and has a fibrous character in contrast to the fibrocartilaginous nature of the remainder of the tissue. The absence of type II collagen in the vascular portion of the meniscus raises the interesting possibility that this collagen or some other matrix macromolecule associated with its presence can resist blood vessel penetration.

The radial "tie fibers" are a distinctive structural component of the meniscus. Skaggs et al. [30] reported that these so-called "tie fibers" were sheaths that penetrate deep into the meniscus. Our study (e.g., in Fig. 3(C)) showed that type II collagen was a prominent component of these tie fibers and stained as patches without any obvious network structure. The function of these interesting structures within the meniscus merits further investigation.

We have extended our observations on the distribution of type II collagen in the dog meniscus to that in the rabbit and the cow. Coronal sections of the rabbit and bovine meniscus stained with the anti-type II collagen monoclonal antibody and revealed networks similar to that of the dog meniscus reported here. Moreover, the loss of type II collagen staining in the outer attachment zone in the dog meniscus was also observed in the bovine and rabbit menisci.

Finally, we suggest that the presence of the distinct network of type II collagen in coronal sections of the meniscus may provide a ready substrate for testing the capacity of specific proteases to denature and degrade type II collagen fibrils.

Acknowledgement

This work was supported by NIH grants R01 AG 14342 and R21 AR 46991 and Department of Defense grant DAMD 17-02-1-0677. The authors wish to thank J. Drazba, Ph.D., for assistance with the confocal microscopy.

References

[1] Aspden R, Yarker Y, Hukins W. Collagen orientations in the meniscus of the knee joint. J Anat 1985;140:371–80.
[2] Beard H, Ryvar R, Brown R, Muir H. Immunochemical localization of collagen types and proteoglycan in pig intervertebral discs. Immunology 1980;41:491–501.
[3] Bland Y, Ashhurst D. Changes in the content of the fibrillar collagens and the expression of their mRNAs in the menisci of the rabbit knee joint during development and aging. Histochem J 1996;28:265–74.
[4] Bullough P, Munuera L, Murphy J, Weinstein A. The strength of the menisci of the knee as it relates to their fine structure. J Bone Joint Surg 1970;52B:564–70.
[5] Chen Q, Fitch J, Gibney E, Linsenmayer TF. Type II collagen during cartilage and corneal development: immunohistochemical analyses with an anti-telopeptide antibody. Develop Dyn 1993;196:47–53.
[6] Cheung H. Distribution of type I, II, III and V in the pepsin solubilized collagens in bovine menisci. Connect Tissue Res 1987;16:343–56.
[7] Eyre D, Matsui Y, Wu J. Collagen polymorphisms of the intervertebral disc. Biochem Soc Trans 2002;30(Part 6):844–8.
[8] Eyre D, Muir H. The distribution of different molecular species of collagens in fibrous, elastic and hyaline cartilages of the pig. Biochem J 1975;151:595–602.
[9] Eyre D, Wu J. Collagen of fibrocartilage: a distinctive molecular phenotype in bovine meniscus. FEBS Lett 1983;158:265–70.
[10] Gao J. Immunolocalization of types I, II, and X collagen in the tibial insertion sites of the medial meniscus. Knee Surg Sports Traumatol Arthrosc 2000;8:61–5.

[11] Ghadially FN. Fine structure of synovial joints: a text and atlas of the ultrastructure of normal and pathological articular tissues. London: Butterworths; 1983.
[12] Ghadially FN, Lalonde J, Wedge JH. Ultrastructure of normal and torn menisci of the human knee joint. J Anat 1983;136:773–91.
[13] Gray H. In: Goss CM, editor. Anatomy of the human body, 28th ed. Philadelphia: Lea and Febiger; 1966.
[14] Guisasola I, Vaquero J, Forriol F. Knee immobilization on meniscal healing after suture: an experimental study in sheep. Clin Orthop 2002;395:227-33.
[15] Hauger O, Frank LR, Boutin RD, et al. Characterization of the "red zone" of knee meniscus: MR imaging and histologic correlation. Radiology 2000;217:193–200.
[16] Hellio Le Graverand M, Ou Y, Schield-Yee T, et al. The cells of the rabbit meniscus: their arrangement, interrelationship morphological variations and cytoarchitecture. J Anat 2001;198:525–35.
[17] Hellio Le Graverand M, Reno C, Hart D. Gene expression in menisci from the knee of skeletally immature and mature female rabbits. J Orthop Res 1999;17:738–44.
[18] Kambic HE, Futani H, McDevitt CA. Cell, matrix changes and alpha-smooth muscle actin expression in repair of the canine meniscus. Wound Repair Regen 2000;8:554–61.
[19] Kreig T, Perlish JS, Mauch C, Fleischmajer R. Collagen synthesis by scleroderma fibroblasts. Ann NY Acad Sci 1985;460: 375–86.
[20] Linsenmayer TF, Hendrix MJ. Monoclonal antibodies to connective tissue macromolecules: type II collagen. Biochem Biophys Res Comm 1980;92:440–6.
[21] McDevitt C, Mukherjee S, Kambic H, Parker R. Emerging concepts of the cell biology of the meniscus. Current Opinion Orthop 2002;13:345–50.
[22] McDevitt C, Webber R. The ultrastructure and biochemistry of meniscal cartilage. Clin Orthop 1990;252:8–18.
[23] Miller M. In: Evans HE, editor. Anatomy of the dog. 3rd ed. Philadelphia: WB Saunders Co; 1993.
[24] Naumann A, Dennis JE, Awadallah A, et al. Immunochemical and mechanical characterization of cartilage subtypes in rabbit. J Histochem Cytochem 2002;50:1049-58.
[25] Nehrer S, Breinan H, Ramappa A, et al. Chondrocyte-seeded collagen matrices implanted in a chondral defect in a canine model. Biomaterials 1998;19:2313–28.
[26] Perez-Castro A, Vogel K. In situ expression of collagen and proteoglycan genes during development of fibrocartilage in bovine deep flexor tendon. J Orthop Res 1999;17:139–48.
[27] Peterson W, Tillmann B. Collagenous fibril texture of the human knee joint menisci. Anal Embryol 1998;197:317–24.
[28] Schaefer L, Hauser H, Altenburger M, et al. Decorin, biglycan and their endocytosis receptor in rat renal cortex. Kidney Int 1998;54:1529–41.
[29] Shortkoff S, Barone L, Hsu H-P, et al. Healing of chondral and osteochondral defects in a canine model: the role of cultured chondrocytes in regeneration of articular cartilage. Biomaterials 1996;17:147–54.
[30] Skaggs D, Warden W, Mow VC. Radial tie fibers influence the tensile properties of the bovine medial meniscus. J Orthop Res 1994;12:176–85.
[31] Upton ML, Chen J, Guilak F, Setton LA. Differential effects of static and dynamic compression on meniscal cell gene expression. J Orthop Res 2003;21:963–9.
[32] van der Loos CM, Marijianowski MH, Becker AE. Quantification in immunohistochemistry: the measurement of the ratios of collagen types I and III. Histochem J 1994;26:347–54.
[33] Wildey GM, Billetz A, Matyas JR, et al. Absolute concentrations of mRNA for type I and type VI collagen in the canine meniscus in normal and ACL-deficient knee joints obtained by RNase protection assay. J Orthop Res 2001;19:650–8.
[34] Wildey GM, McDevitt C. Matrix protein mRNA levels in canine meniscus in vitro. Arch Biochem Biophys 1998;353:10–5.

Connective Tissue Research, 46:83–91, 2005

ISSN: 0300-8207 print / 1521-0456 online
DOI: 10.1080/03008200590954113

Taylor & Francis
Taylor & Francis Group

The Concentration, Gene Expression, and Spatial Distribution of Aggrecan in Canine Articular Cartilage, Meniscus, and Anterior and Posterior Cruciate Ligaments: A New Molecular Distinction Between Hyaline Cartilage and Fibrocartilage in the Knee Joint

Manojkumar Valiyaveettil
Department of Biomedical Engineering, Lerner Research Institute and Orthopaedic Research Center, Cleveland Clinic Foundation, Cleveland, Ohio, USA

John S. Mort
Joint Diseases Laboratory, Shriners Hospital for Children and Department of Surgery, McGill University, Montreal, Quebec, Canada

Cahir A. McDevitt
Department of Biomedical Engineering, Lerner Research Institute and Orthopaedic Research Center, Cleveland Clinic Foundation, Cleveland, Ohio, USA

The concentration, spatial distribution, and gene expression of aggrecan in meniscus, articular cartilage, and the anterior and posterior cruciate ligaments (ACL and PCL) was determined in the knee joints of five mature dogs. An anti-serum against peptide sequences specific to the G1 domain of aggrecan was employed in competitive-inhibition ELISA of guanidine HCl extracts and immunofluorescence microscopy. Gene expression was determined by Taqman real-time PCR. The concentration of aggrecan in articular cartilage (240.1 ± 32 nMol/g dry weight) was higher than that in meniscus (medial meniscus: 33.4 ± 4.3 nMol/g) and ligaments (ACL: 6.8 ± 0.9 nMol/g). Aggrecan was more concentrated in the inner than the outer zone of the meniscus. Aggrecan in meniscus showed an organized, spatial network, in contrast to its diffuse distribution in articular cartilage. Thus, differences in the concentration, gene expression, and spatial distribution of aggrecan constitute another molecular distinction between hyaline cartilage and fibrocartilage of the knee.

Keywords Aggrecan, Articular Cartilage, Fibrocartilage, Hyaline, Ligaments, Meniscus

INTRODUCTION

Connective tissues vary from the fibrous ligaments and tendons with a predominantly tensile function to the different forms of cartilage that serve varying degrees of a compressive function. Cartilage tissue has been classified into three different forms: hyaline, fibrous, and elastic cartilage. Fibrocartilage is distinguishable from hyaline cartilage by differences in anatomical location, tissue composition, and fibrillar architecture as seen in gross and microanatomy [1].

The meniscus of the knee joint is a fibrocartilage in which the dominant cell is the fibrochondrocyte, with fibroblast-like cells populating the outer vascular portion of the tissue [2]. Type I collagen and smaller amouts of type II collagen are the major fibrillar collagens in the meniscus [3]. Type II collagen is the dominant fibrillar collagen in hyaline cartilage such as the articular cartilage of the knee joint [3].

Polarized light microscopy, x-ray diffraction, and scanning electron microscopic studies have established that the fibrils in the superficial zones of the meniscus from a variety of species are mainly radial in orientation, whereas the fibrils in the main body of the tissue have a predominantly circumferential orientation [see 4 for references]. The meniscus also has distinctive radial structures, referred in the literature as "tie fibers" or "tie sheaths," which emerge from the attachment region and branch toward the femoral and tibial surfaces [5]. Our recent studies, however, demonstrate the presence of a fibrillar system surrounding the circumferential fibrils. These immunohistochemical studies revealed that types I and II collagen have an organization in coronal sections of the meniscus that appears as an interconnecting fibrillar network in the light microscope, in contrast to hyaline cartilage

Received 22 October 2004; revised 9 February 2005; accepted 28 February 2005.

Address correspondence to Cahir A. McDevitt, Ph.D., Department of Biomedical Engineering/ND20, Cleveland Clinic Foundation, 9500 Euclid Avenue, Cleveland, OH 44195, USA. E-mail: mcdevic@ccf.org

where no such organization in type II collagen was evident [4].

Meniscus fibrocartilage has a much lower concentration of glycosaminoglycan (GAG) than hyaline cartilage [1]. Early studies demonstrated the presence of hyaluronan-binding proteoglycans in the meniscus [6–8]. Biosynthesis [9] and gene expression studies have demonstrated aggrecan RNA message in meniscus [10–13] and in cells isolated from the tissue [14].

Aggrecan is a large aggregating proteoglycan particularly enriched in hyaline cartilage but also present in a variety of other tissues including tendon, sclera, and cornea [15–17]. The core protein of aggrecan is composed of:

- Globular G1 domain at the N-terminus through which aggrecan can form aggregates by binding noncovalently to hyaluronan.
- Interglobular domain (IGD) sequence that spans about 150 amino acid residues.
- Second globular domain, G2.
- Long GAG attachment region composed of a keratan sulfate-rich domain and a long extended chondroitin sulfate attachment region.
- C-terminal globular domain G3 [18–20].

The link protein can bind to the G1 domain and hyaluronan, thus providing protection to the G1 domain and stability to the aggregate formed by association of many aggrecan molecules with a hyaluronan chain [21, 22]. In the older literature, the term "hyaluronic acid binding region" (HABR) has been used to describe the complex of G1 domain and link protein that survives digestion of aggrecan aggregates with trypsin [23].

Extensive degradation of aggrecan and loss of the degradation products from the tissue occur during normal cartilage metabolism [24–26]. In mature cartilage, up to half of the aggrecan molecules have lost their G3 domain [27]. The GAG-bearing domain also is subjected to cleavage, resulting in the release of degraded fragments into the matrix. These GAG-bearing degradation products evidently are removed fairly rapidly from cartilage, as the percentage of proteoglycans that do not bind to hyaluronan is very small. The G1 domain, however, is relatively protected from proteinase attack and accumulates with age in the tissue bound to hyaluronan [27]. Aggrecan therefore exists in cartilage as a heterogeneous population of molecules, essentially all with G1 domains and different lengths of core protein attached. Measuring the concentration of G1 domain yields the molar concentration of aggrecan in the tissue.

A substantive body of literature has addressed many aspects of the biology of aggrecan in hyaline cartilage. Whereas the concentration of GAG in meniscus has been documented [8], little is known about the concentration or distribution of the proteoglycan aggrecan in the meniscus fibrocartilage. Moreover, the absolute concentration of aggrecan in tissues is essentially unknown, largely due to the relative paucity of antibodies specific for this proteoglycan. Using competitive inhibition ELISA and an antiserum generated against peptides specific for the G1 domain of aggrecan, we report on the molar concentrations, spatial distribution as well as the relative gene expression as determined by Taqman real-time polymerase chain reaction (PCR) of aggrecan in fibrocartilage and hyaline cartilage, and in the fibrous tissue of the anterior cruciate and posterior cruciate ligaments (ACL, PCL) of the canine knee joint.

MATERIALS AND METHODS

Extraction and Purification of Aggrecan

Femoral articular cartilage from bovine knee joints was shaved off, diced, and extracted with 4 M guanidine HCl at 4°C overnight in the presence of protease inhibitors (Roche Diagnostics GmbH, Mannheim, Germany) [28]. The extract was clarified by centrifugation for 30 min at 10,000 rpm at 4°C, and the supernatant was collected. CsCl was added to the supernatant to yield a starting density of 1.5 g/ml and aggrecan isolated as the most dense bottom fraction (D1) by dissociative density gradient centrifugation at 100,000 *g* at 4°C for 72 hr. The D1 fraction was reduced with 0.08 M dithiothreitol (DTT, Sigma, St. Louis, MO, USA) at 37°C for 30 min, followed by alkylation with 0.16 M iodoacetamide (Sigma) at 37°C for 30 min [28]. The reduced and alkylated fraction was dialyzed and lyophilized. The lyophilized fraction was dissolved in 25 mM Tris-HCl buffer containing 30 mM sodium acetate, pH 8.0, and digested with 500 mU of protease-free chondroitinase ABC (Seikagaku America, East Falmouth, MA, USA) at 37°C for 2 hr [29]. The digest was dialyzed against distilled water and lyophilized.

Extraction of Proteoglycans

The lateral and medial meniscus, femoral articular cartilage, and ACL and PCL were dissected from the knee joints from 5 different mongrel dogs. Each meniscus was sectioned into the inner and outer meniscus as defined by half the radial distance from the outer boundary to the inner tip. Each tissue was diced and ground in liquid nitrogen to form a fine powder. An aliquot of the tissue was weighed and lyophilized to estimate the water content. The remaining tissue was weighed and extracted for 72 hr with 10 volumes of 4 M guanidine HCl in 50 mM Tris-HCl, 150 mM NaCl, 10 mM EDTA, pH 7.5 at 4°C overnight using a rotator [28]. The extracts were centrifuged at 10,000 rpm for 10 min at 4°C and the supernatants collected.

Reduction and Alkylation of Proteoglycan Extracts

An aliquot from the above extracts was reduced with 0.08 M DTT at 37°C for 30 min and alkylated with 0.16 M iodoacetamide at 37°C for 30 min [28]. The reduced and alkylated sample was recovered after extensive dialysis against Tris-buffered saline (TBS) at 4°C.

Preparation of Polyclonal Antiserum

A polyclonal antiserum to the G1 domain of human aggrecan core protein was prepared as described earlier [30]. Rabbits were immunized with a mixture of peptide-ovalbumin conjugates of the sequences (a) **HDNSLSVSIPQPS***GGC,* (b) **RVLLGTSLTIPCYFIDPMHPVTTAPS**, (c) **TEGRVRVNSAYQDK**-*GGC* and (d) **SSRYDAICYTG**, to avoid potential cross-reaction of the resulting antiserum with the aggrecan G2 region and the G1 domain of versican (residues in bold-face type are specific to the G1 domain of aggrecan, while the *GGC* regions were added to allow spacing of the Cys residue used for coupling of the peptide to the carrier protein). The resulting antiserum was shown to cross-react with bovine aggrecan G1 [30]. Comparison of the sequences of the G1 region of human and canine aggrecan indicates that region (d) is identical across both species. Regions (a) and (b) each contain a single conservative residue substitution (Q to E and T to S, respectively) between the human and dog sequences. These E and S residues are common to both dog and bovine sequences. Region (c) contains a nonconservative (R to Q) and a conservative (V to I) substitution. We concluded that three of four peptides used show sufficient identity to ensure cross-reactivity of the antiserum with canine G1.

SDS-PAGE Analysis of Hyaluronic Acid Binding Protein (HABP)

HABP (2 μg) (Seikagaku America) was dissolved in 60 mM Tris-HCl, pH 6.8, containing 2% sodium dodecyl sulfate (SDS), 10% glycerol, and 1% bromophenol blue and electrophoresed on a 4–15% gradient polyacrylamide minigel (Bio-Rad Laboratories, Hercules, CA, USA) under reducing condition [31]. The gel was stained with Coomassie blue.

Western Blotting

HABP (0.2–1.0 μg) was electrophoresed on 4–15% gradient polyacrylamide minigel as described above and the protein bands electroblotted onto a polyvinylidene difluoride (PVDF) membrane (Millipore Corporation, Bedford, MA, USA). The membrane was blocked with 1% BSA in 50 mM Tris-HCl, 150 mM NaCl, pH 8.0 for 2 hr, followed by incubation with polyclonal antiserum against the synthetic peptides corresponding to amino acid sequences specific to the G1 domain of human aggrecan (1:500 dilution), or the monoclonal antibody (8A4) against the link protein (1:10,000, Developmental Studies Hybridoma Bank, University of Iowa). The immunoreactivity was visualized using 1:5000 diluted alkaline-phosphatase-conjugated goat antirabbit or antimouse IgG (Sigma) as the secondary antibody and nitroblue tetrazolium/5-bromo-4-chloro-3-indolyl phosphate as the color-developing reagent (Bio-Rad Laboratories).

Mass Spectrometric Analysis of HABP

HABP (3–4 μg) was electrophoresed on a 4–15% gradient polyacrylamide minigel and stained with Coomassie blue as described above. The protein bands were cut from the gel, washed, and destained with 50% ethanol/5% acetic acid. The gel pieces were washed with 0.1 M ammonium bicarbonate and dehydrated in acetonitrile before reduction with DTT and alkylation with iodoacetamide. The gel pieces were dehydrated again in acetonitrile, washed with 0.1 M ammonium bicarbonate, and dried in a Speed-Vac. The gel pieces were treated with 30 μl of trypsin (20 μg/ml) in 50 mM ammonium bicarbonate on ice for 10 min. Any excess trypsin solution was removed, and 20 μl of 50 mM ammonium carbonate solution was added and incubated overnight at room temperature. The peptides formed were extracted from the polyacrylamide with 50% acetonitrile/5% formic acid, concentrated, and used for LC-MS analysis (ThermoFinnigan Corp., San Jose, CA, USA).

Immunofluorescence Microscopy

Frozen sections (5 μm) of tissue were cut on a motorized Leica CM 3050 cryostat (Leica Microsystems, Nussloch, Germany). The menisci were sectioned in both longitudinal and coronal planes. Tissue sections were reduced by pipetting 250 μl of 10 mM DTT onto the slide and incubating it uncovered for 2 hr at 37°C. The tissues were washed in TBS, then alkylated with 250 μl of 40 mM iodoacetamide at 37°C for 1 hr, and finally blocked with 1% BSA in TBS. Sections were incubated overnight with 1:50 diluted polyclonal antibody against the synthetic peptides specific to human aggrecan G1, washed thoroughly, and incubated with Alexafluor 594-conjugated antirabbit IgG (Molecular Probes, Eugene, OR, USA) as secondary antibody for 2 hr. Tissue sections were mounted on Vectashield containing DAPI stain. Microscopy was performed on an Olympus BX51 microscope (Tokyo, Japan) equipped with a QED Camera Plug-In^{TM} Package (QED Imaging, Pittsburgh, PA, USA).

Enzyme Linked Immunosorbent Assay (ELISA)

Falcon Probind 96-well plates (Becton Dickinson, Franklin Lakes, NJ, USA) were coated by incubation with 100 μl of purified aggrecan from bovine articular cartilage (2 μg/ml) in TBS, pH 7.2, overnight at 4°C. The plate was washed three times with TBS and the coated wells blocked with 1% BSA in TBS (200 μl) for 2 hr at room temperature. The reduced and alkylated aggrecan extracts at different dilutions and the HABP standards at different concentrations were incubated with 1:500 diluted primary antibody (rabbit polyclonal antibody raised against G1 domain of human aggrecan) in 1% BSA/TBS containing 0.05% Tween-20 (TTBS) at 4°C for overnight. The antigen-coated wells were incubated with these solutions at room temperature for 30 min. The unbound antibody was removed from the wells by washing five times with TTBS. The wells were incubated with alkaline phosphatase conjugated goat antirabbit IgG (Sigma, 1:5000 diluted in 1% BSA/TTBS) for 1 hr at room temperature followed by washing five times with TTBS. The plate was incubated with 100 μl of p-nitrophenyl phosphate

substrate solution (Bio-Rad Laboratories) and the amount of p-nitrophenol liberated was measured at 405 nm at different time intervals using a Spectra Max Plus (Molecular Devices Corporation, Sunnyvale, CA, USA) plate reader. Samples were assayed in triplicate. Each assay had an extra external reference standard of purified aggrecan; the day-to-day variation in concentration was 2.7%.

Extraction of RNA

Total RNA was extracted from different tissues of canine knee joint by using an RNeasy minikit (Qiagen, Valencia, CA, USA) as described earlier with slight modifications [32]. Briefly, tissue samples were ground in liquid nitrogen and 100 mg of each powdered frozen sample was extracted with 300 μl of lysis buffer (RLT buffer) for 15 min, followed by dilution with 590 μl of RNase-free water. The tissue homogenates were digested with 10 μl of Proteinase K (20 mg/ml, Qiagen) at 55°C for 15 min. The digests were centrifuged at 10,000 *g* for 5 min and the total RNA was precipitated from the supernatants by adding 0.5 volumes of absolute ethanol. The supernatant including the precipitate was transferred into an RNeasy minicolumn, centrifuged at 8,000 *g* for 15 sec, and washed with 350 μl of RW1 buffer. Genomic DNA contamination was removed by on-column RNase-free DNase treatment (Qiagen) and isolated RNA was quantified and analyzed for impurities by ultraviolet spectrophotometer.

TaqMan Real-Time PCR

Total RNA (500 ng) was reverse transcribed into first-strand cDNA with MuLV reverse transcriptase with the Taqman reverse-transcriptase kit (Applied Biosystems, Foster City, CA, USA). PCR amplification of cDNA was performed using the following oligonucleotide primers and probe in an ABI Prism 7700 sequence detection system (Applied Biosystems): forward primer, GACGCCATCGACTCTTTCAC; reverse primer, ACACAGCTCCTGGTCGATCT; and probe, FAM-TGCCTTCCCAGCTACCGAGGG-MGB. Human 18S rRNA (Applied Biosystems) was included in each sample as the internal control. Using the comparative Ct method and calculating the relative gene expression as the $2^{-\Delta\Delta Ct}$ value [33], the data are presented as the fold change in gene expression normalized to the endogenous reference gene 18S rRNA and relative to the control.

RESULTS

Standardization of ELISA

Bovine articular cartilage aggrecan was coated at different concentrations on a microtiter plate and the ELISA assay was performed using antiaggrecan G1 antibody as the primary antibody. Saturation was evident at a concentration of 2 μg/ml (not shown) and this concentration of bovine aggrecan was used in all the further studies.

Analysis of Constituents in HABP Preparation

SDS-PAGE of the HABP preparation under nonreducing conditions yielded a broad band at 60–80 kDa, a band at 40 kDa, and a doublet at 33–35 kDa (Figure 1, lane 1). Under reducing conditions, the HABP migrated as a broad band at 60–80 kDa, a band at 46 kDa, and a doublet at 40–43 kDa (Figure 1, lane 2). When probed with the antilink protein antiserum (8A4), both the 46 kDa and 40–43 kDa bands showed reactivity (Figure 1, lane 3). Immunoblot analysis with the antiaggrecan G1 antiserum yielded a 60–80 kDa band (Figure 1, lane 4).When extra loading of HABP was applied to the gel, an extra faint band at 46 kDa was evident with the antiaggrecan G1 antiserum indicating the presence of a small percentage of G1 domain in this region (not shown and see below).

Mass spectrometric Maldi-ToF of the 60–80 kDa band confirmed its identity as bovine aggrecan G1 domain. Similar analysis of the 46 kDa band revealed the presence of both link protein and the G1 domain of aggrecan. Further analysis of this band with liquid chromatography and mass spectrometry revealed that the ratio of link protein to G1 domain was 12.5 to 1.0. Thus, the aggrecan G1 domain constituted 7.5% of this band. The densitometry analysis of HABP after SDS-PAGE revealed that the 60- to 80-kDa, 46-kDa, and 40- to 43-kDa bands were present in percentages of 25%, 20%, and 55%, respectively. Combining these data and the mass spectrometric analysis led us to conclude that aggrecan G1 domain constituted

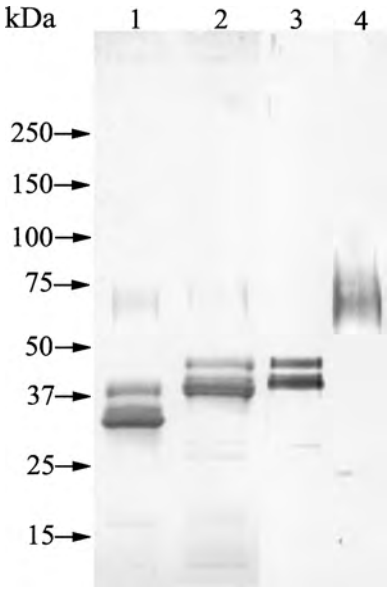

FIG. 1. SDS-PAGE and immunoblot analysis of aggrecan G1 domain in HABP. HABP (2 μg) was electrophoresed on 4–15% gradient gel, transferred onto PVDF membrane, and immunoblotted with antiaggrecan G1 antiserum as described in the Materials and Methods section. Lane 1, nonreduced HABP stained with Coomassie blue; lane 2, reduced HABP stained with Coomassie blue; lane 3, immunoblot developed with antilink protein antibody; and lane 4, immunoblot developed with antiaggrecan G1 antiserum. The positions of the molecular weight markers are indicated to the left.

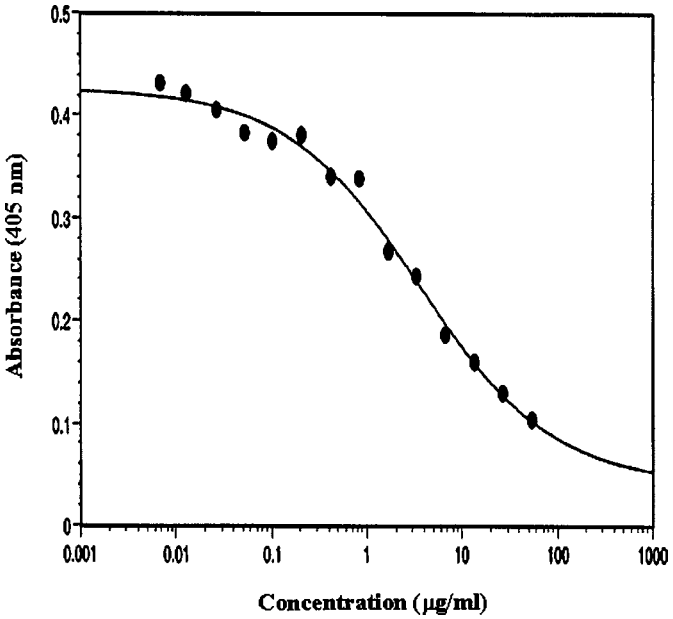

FIG. 2. Standard curve for competitive inhibition ELISA of HABP. Different concentrations of HABP (80 μg/ml to 8 ng/ml) were incubated with antiaggrecan G1 antiserum and used for competitive inhibition ELISA as described in the Materials and Methods section. The assay was done three times in duplicate. Concentration of aggrecan G1 domain in the tissue extracts was calculated using this standard graph and reading the optical density at 50% inhibition.

26.5% of the HABP preparation, with the remainder being link protein.

Concentration of Aggrecan G1 Domain

The standard curve obtained with HABP is shown in Figure 2. The concentration of aggrecan G1 domain was calculated in nanomoles (nMol) using 75 kDa as the molecular weight of G1 domain. The concentration of aggrecan G1 domain in hyaline articular cartilage (240.1 ± 32.5 nMol/g dry weight) was greater than seven times that of meniscus fibrocartilage (medial meniscus: 33.4 ± 4.3 nMol/g dry weight) (Table 1). In the lateral meniscus the concentration of aggrecan (16.9 ± 2.1 nMol/g dry weight) was half that of the medial meniscus. The aggrecan G1 was not evenly distributed in the meniscus. The concentration of aggrecan G1 in the inner medial meniscus was 69.9 ± 4.7 nMol/g dry weight, and in the outer meniscus was 19.9 ± 4.6 nMol/g dry weight. Similarly, the concentration of aggrecan in the inner lateral meniscus (25.1 ± 4.4 nMol/g dry weight) was higher than that in the outer lateral meniscus (14.5 ± 2.8 nMol/g dry weight). Both the ACL (6.8 ± 0.9 nMol/g) and the PCL (0.9 ± 0.09 nMol/g) contained much less aggrecan G1 domain than articular cartilage or meniscus.

Gene Expression of Aggrecan

The relative differences in aggrecan gene expression (Figure 3), as assessed by Taqman real-time PCR, for the most part reflected the differences in protein concentration as determined by ELISA. Gene expression of aggrecan in articular cartilage was much higher than that in the meniscus and ligaments. As with the relative concentration of the G1 protein, the gene expression in the inner medial and lateral menisci was higher than that of the outer meniscus. Very low gene expression was demonstrable in the ligaments.

TABLE 1
Concentration of aggrecan G1 domain in tissues of the canine knee joint

Samples	Concentration of G1 domain (nMol/g dry weight)
Articular cartilage	240.1 ± 32.5
Meniscus	
Medial	33.4 ± 4.3
Lateral	16.9 ± 2.1
Medial, inner	69.9 ± 4.7
Medial, outer	19.9 ± 4.6
Lateral, inner	25.1 ± 4.4
Lateral, outer	14.5 ± 2.8
Ligaments	
Anterior cruciate	6.8 ± 0.9
Posterior cruciate	0.9 ± 0.09

Immunofluorescence Microscopy

Figure 4 shows the spatial distribution of aggrecan in articular cartilage, meniscus, ACL, and PCL. Aggrecan was intensely stained at the surface of articular cartilage (not shown) and was diffusely distributed throughout the remainder of the tissue, with heavy concentrations around some cells and, interestingly, the occasional vertical streak (Figure 4A). A longitudinal section of the meniscus (Figure 4B) revealed the aggrecan staining as dots in a linear array and overlapping or parallel with the linear arrays of cells. The section also displayed a fairly broad band of aggrecan stain (across the middle of Figure 4B) that is probably a radial "tie fiber." A coronal section of the meniscus (Figure 4C) showed the aggrecan staining as an interconnecting network, with fairly intense staining in the radial tie fiber across the bottom of the figure. Interestingly, the cells were located at the bifurcation of the strands in the network, but they seemed more randomly distributed in the tie fiber. Both the ACL (Figure 4D) and PCL (Figure 4E) showed aggrecan as linear streaks parallel with the linear cellular arrays. The negative controls, in which the primary antiserum was omitted, showed no fluorescence (not shown).

DISCUSSION

The use of an antibody specific for the G1 domain of aggrecan in ELISA and immunohistochemical studies unequivocally

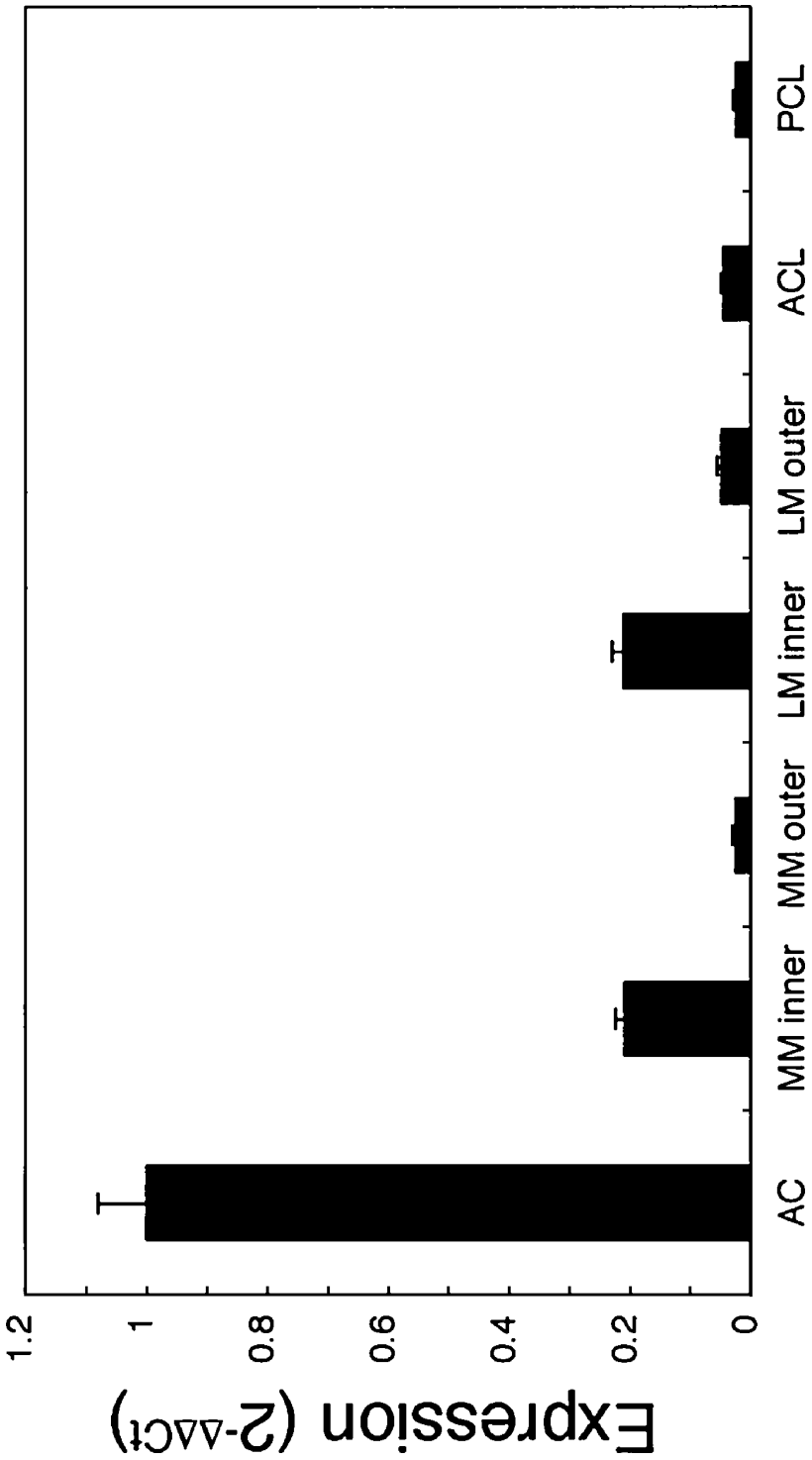

FIG. 3. TaqMan RT-PCR analysis of aggrecan gene expression. Total RNA from different tissues was reverse transcribed into cDNA, amplified, and the amplification plot was recorded by ABI prism sequence detection system as described in Materials and Methods. AC, femoral articular cartilage; MM, medial meniscus; LM, lateral meniscus.

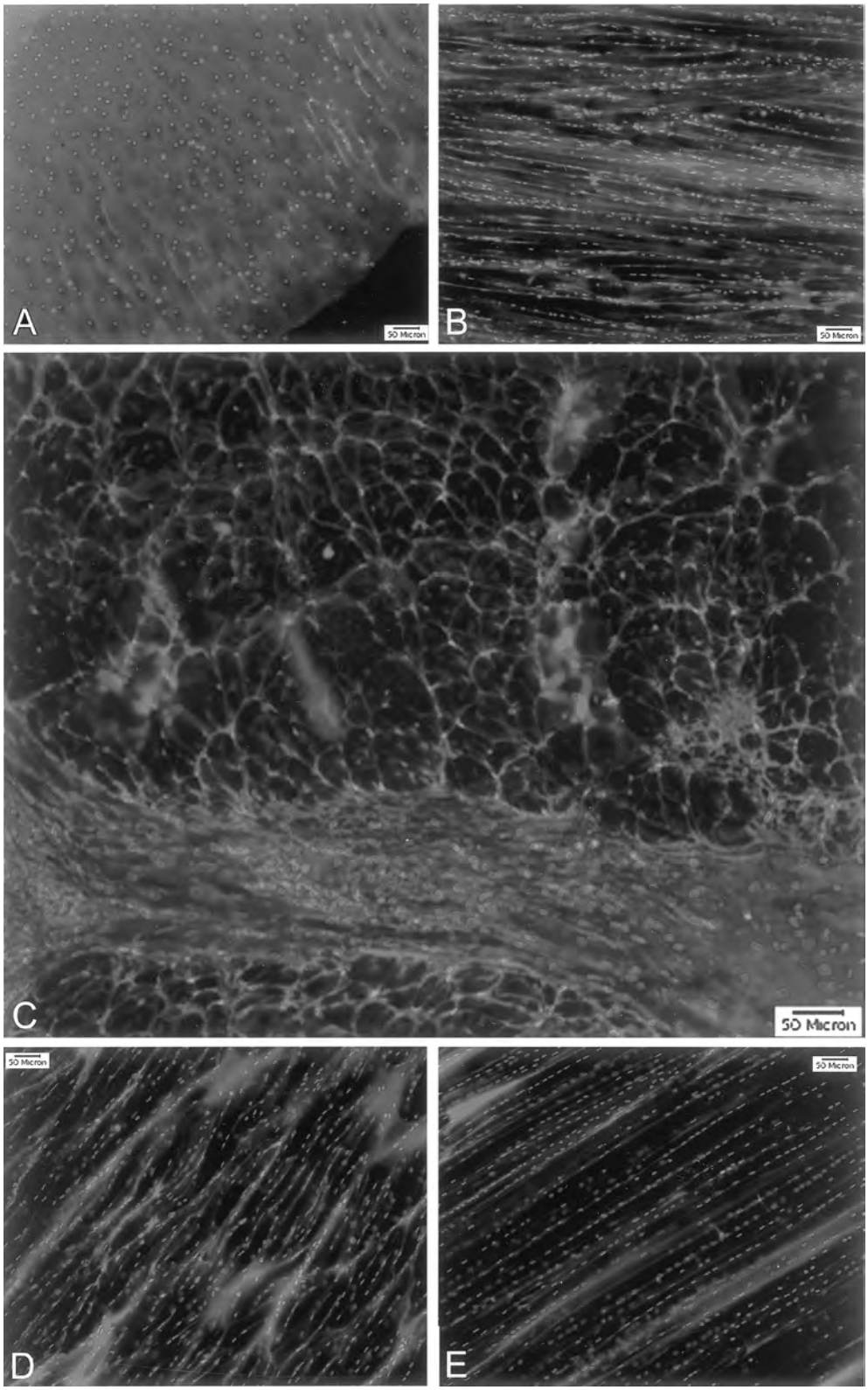

FIG. 4. Immunofluorescence microscopy of aggrecan G1 in articular cartilage, meniscus, and ligaments. Cryosections of articular cartilage, meniscus, and ligaments were reduced, alkylated, and stained with antiaggrecan G1 antibody (red) as described in Materials and Methods. Cells were visualized with DAPI (blue). (A) femoral articular cartilage, showing deeper zone, (B) longitudinal section of meniscus, (C) coronal section of meniscus, (D) ACL, and (E) PCL.

establishes the presence of this proteoglycan in meniscus, ACL, and PCL. Our studies are in agreement with previous demonstrations of gene expression for aggrecan in meniscal tissue [10–13] and in cells isolated from meniscus [14]. The large proteoglycan population that aggregated with hyaluronan reported in meniscus in earlier studies [6–8, 34] is clearly in part aggrecan. But it is very likely also composed of versican as we have detected this latter proteoglycan in meniscus by immunolocalization (Kambic, H. E., Sandy, J., and McDevitt, C. A., unpublished data).

Our study demonstrates that the concentration of aggrecan in hyaline articular cartilage is much higher than that in meniscus, ACL, and PCL. However, the concentration of collagen in meniscus [34], ACL, and PCL [35] is higher than in articular cartilage. Our immunohistochemical studies demonstrated that the aggrecan in fibrocartilage and ligament is not diffusely distributed, as it is in articular cartilage. But it is concentrated in linear strands in longitudinal section consistent with its occupying the space between the main, parallel bundles of collagen fibrils. Thus, given the volume occupied by the collagen fibrils, the possibility must be entertained that the local concentration of aggrecan in these specific sites is similar to that in articular cartilage.

The dominant fibrillar collagen in the meniscus is type I collagen, but meniscus does contain significant amounts of type II collagen as well [3]. A recent immunohistochemical study [4] showed that, when viewed in the light microscope, types I and type II collagen colocalize in an organized meshwork that surrounds the circumferential bundles of fibrils in a pattern similar to aggrecan in this study. In articular cartilage, in contrast, the type II collagen had a diffuse distribution in these studies [4]. The radial tie fibers in this study stained heavily in parts for type II collagen without any accompanying type I collagen [4]. It is notable that the tie fibers also stained heavily for aggrecan. Moreover, both type II collagen and aggrecan did not stain in the outer vascular portion of the meniscus, an observation that is consistent with the higher concentration of aggrecan in the inner meniscus compared with the outer zone.

The biomechanical properties of a connective tissue depend on the composite structure and organization of the extracellular matrix. Aggrecan can immobilize itself within a collagen meshwork by forming aggregates with hyaluronan [20, 21]. Aggrecan can draw large amounts of water into articular cartilage, thereby exerting a swelling pressure on the collagen meshwork and enabling the tissue to resist compressive load [21, 36]. The type II collagen and aggrecan in the tie fibers and in the fibrils that surround the bundles of tensile-bearing circumferential fibrils, although not a hyaline cartilage, may provide a compressive cushion when the tissue is under load and the circumferential fibrils are under tension.

The study by Kambic and McDevitt [4] and the results reported here provide new criteria for distinguishing hyaline cartilage from fibrocartilage in the knee joint. The much lower gene expression and tissue concentration and the organized spatial distribution of aggrecan in fibrocartilage provide a striking contrast with hyaline cartilage. Similarly, the type II collagen in fibrocartilage also has an organized, three-dimensional meshwork structure discernible under the light microscope that is absent in hyaline articular cartilage [4]. The fibrochondrocyte, although morphologically indistinguishable from the chondrocyte in terms of its shape and surrounding pericellular matrix of type VI collagen [2], apparently has the ability to organize the collagens and aggrecan into a structured network that is lacking in hyaline cartilage.

Aggrecan concentration in synovial fluid has been used as a marker for articular cartilage degeneration in osteoarthritis [37]. The menisci constitute a significant weight of the tissues that occupy the interior of the knee joint. The aggrecan in the menisci can clearly contribute to the pool in the synovial fluid, and that is a process that should be considered in evaluating the significance of any changes in synovial fluids.

Finally, our studies invite a reappraisal of the functional significance of the microanatomical architecture of the meniscus.

ACKNOWLEDGMENTS

The technical assistance of Kristin Rundo in the immunofluorescence studies is gratefully acknowledged. This work was supported by NIH grants R01 AG 14342 and R21 AR 46991 and Department of Defense grant DAMD 17-02-1-06677 to C.A. McDevitt and by a grant from the Shriners of North America to J.S. Mort.

REFERENCES

1. McDevitt, C., and Webber, R. (1990). The ultrastructure and biochemistry of meniscal cartilage. *Clin. Orthop.* 252:8–18.
2. McDevitt, C.A., Mukherjee, S., Kambic, H.E., and Parker, R. (2002). Emerging concepts of the cell biology of the meniscus. *Curr. Opin. Orthop.* 13:345–350.
3. Eyre, D., and Muir, H. (1975). The distribution of different species of collagen in fibrous, elastic and hyaline cartilages of the pig. *Biochem. J.* 151:595–602.
4. Kambic, H.E., and McDevitt, C.A. (2005). Spatial organization of type I and II collagen in the canine meniscus. *J. Orthop. Res.* 23:142–149.
5. Skaggs, D., Warden, W., and Mow, V.C. (1994). Radial tie fibers influence the tensile properties of the bovine medial meniscus *J. Orthop. Res.* 12:176–185.
6. Roughley, P.J., McNicol, D., Santer, V., and Buckwalter, J. (1981). The presence of a cartilage-like proteoglycan in the adult human meniscus. *Biochem. J.* 197:77–83.
7. McNicol, D., and Roughley, P.J. (1980). Extraction and characterization of proteoglycans from human meniscus. *Biochem. J.* 185:705–713.
8. Adams, M.E., Billingham, M.E.J., and Muir, H. (1983). The glycosaminoglycans in menisci in experimental and natural osteoarthritis. *Arthr. Rheumat.* 26:69–76.
9. Collier, S., and Ghosh, P. (1995). Effects of transforming growth factor beta on proteoglycan synthesis by cell and explant cultures derived from the knee joint meniscus. *Osteoarthr. Cartil.* 3:127–138.
10. Wildey, G.M., Billetz, A., Matyas, J.R., and McDevitt, C.A. (2001). Absolute concentrations of mRNA for type I and type VI collagen in the canine meniscus in normal and ACL-deficient knee joints obtained by RNase protection assay. *J. Orthop. Res.* 19:650–658.

11. Hellio Le Graverand, M., Reno, C., and Hart, D. (1999). Gene expression in menisci from the knee of skeletally immature and mature female rabbits. *J. Orthop. Res.* 17:738–744.
12. Djurasovic, M., Aldridge, J.W., Grumbles, R., Rosenwasser, M.P., Howell, D., and Ratcliffe, A. (1998). Knee joint immobilization decreases aggrecan gene expression in the meniscus. *Am. J. Sports Med.* 26:460–466.
13. McAlinden, A., Dudhia, J., Bolton, M.C., Lorenzo, P., Heinegard, D., Bayliss, M.T. (2001). Age-related changes in the synthesis and mRNA expression of decorin and aggrecan in human meniscus and articular cartilage. *Osteoarth. Cartil.* 9:33–41.
14. Wildey, G.M., and McDevitt, C.A. (1998). Matrix protein mRNA levels in canine meniscus cells *in virto*. *Arch. Biochem. Biophys.* 353:10–15.
15. Vogel, K.G., Sandy, J.D., Pogany, G., and Robbins, J.R. (1994). Aggrecan in bovine tendon. *Matrix Biol.* 14:171–179.
16. Rada, J.A., Thoft, R.A., and Hassell, J.R. (1991). Increased aggrecan (cartilage proteoglycan) production in the sclera of myopic chicks. *Dev. Biol.* 147:303–312.
17. Tsonis, P.A., and Goetinck, P.F. (1988). Expression of cartilage-matrix genes and localization of their translation products in the embryonic chick eye. *Exp. Eye Res.* 46:753–764.
18. Hardingham, T.E., and Fosang, A.J. (1995). The structure of aggrecan and its turnover in cartilage. *J. Rheumat.* 22:86–90.
19. Mercuri, F.A., Doege, K.J., Arner, E.C., Prataa, M.A., Last, K., and Fosang, A.J. (1990). Recombinant human aggrecan G1-G2 exhibits native binding properties and substrate specificity for matrix metallopeoteinases and aggrecanase. *J. Biol. Chem.* 274:32387–32395.
20. Kiani, C., Chen, L., Wu, Y.J., Yee, A.J., and Yang, B.B. (2002). Structure and function of aggrecan. *Cell Res.* 12:19–32.
21. Hardingham, T.E. (2001). Cartilage aggrecan-link protein-hyaluronan aggregates. *Glyco Forum/Sci. Hyaluronan* 5:1–17.
22. Hascall, V.C., and Heinegard, D. (1997). Aggregation of cartilage proteoglycans. I. The role of hyaluronic acid. *J. Biol. Chem.* 249:4232–4241.
23. Poole, A.R. (1986). Proteoglycans in health and disease: structures and functions. *Biochem. J.* 236:1–14.
24. Malfait, A.M., Liu, R.Q., Ijiri, K., Komiya, S., and Tortorella, M.D. (2002). Inhibition of ADAM-TS4 and ADAM-TS5 prevents aggrecan degradation in osteoarthritic cartilage. *J. Biol. Chem.* 277:22201–22208.
25. Fosang, A.J., Neame, P.J., Hardingham, T.E., Murphy, G., and Hamilton, J.A. (1991). Cleavage of cartilage proteoglycan between G1 and G2 domains by stromelysins. *J. Biol. Chem.* 266:15579–15582.
26. Ilic, M.Z., Handley, C.J., Robinson, H.C., and Mok, M.T. (1992). Mechanism of catabolism of aggrecan by articular cartilage. *Arch. Biochem. Biophys.* 294:115–122.
27. Lee, V., Chen, L., Paiwand, F., Cao, L., Wu, Y., Inman, R., Adams, M.E., and Yang, B.B. (2002). Cleavage of the carboxyl tail from the G3 domain of aggrecan but not vesican and identification of the amino acids involved in the degradation. *J. Biol. Chem.* 277:22279–22288.
28. Marcelino, J., and McDevitt, C.A. (1995). Attachment of articular cartilage chondrocytes to the tissue form of type VI collagen. *Biochem. Biophys. Acta* 1249:180–188.
29. Oike, Y., Kimata, K., Shinomura, T., Nakazawa, K., and Suzuki, S. (1980). Structural analysis of chick-embryo cartilage proteoglycan by selective degradation with chondroitin lyases (chondroitinases) and endo-beta-galactosidase (keratanase). *Biochem. J.* 191:193–207.
30. Sztrolovics, R., White, R.J., Roughley, P.J., and Mort, J.S. (2002). The mechanism of aggrecan release from cartilage differs with tissue origin and the agent used to stimulate catabolism. *Biochem. J.* 362:465–472.
31. Laemmli, U.K. (1970). Cleavage of structural proteins during the assembly of the head of bacteriophage T4. *Nature* 227:680–685.
32. Reno, C., Marchuk, L., Sciore, P., Frank, C.B., and Hart, D.A. (1997). Rapid isolation of total RNA from small samples of hypocellular, dense connective tissues. *Biotechniques* 22:1082–1086.
33. Livak, K.J., and Schmittgen, T.D. (2001). Analysis of relative gene expression data using real-time quantitative PCR and the $2^{-\Delta\Delta Ct}$ method. *Methods* 25:402–408.
34. Nakano, T., Dodd, C.M., and Scott, P.G. (1997). Glycosaminoglycans and proteoglycans from different zones of the porcine knee meniscus. *J. Orthop. Res.* 15:213–220.
35. Amiel, D., Frank, C., Harwood, F., Fronek, J., and Akeson, W. (1984). Tendons and ligaments: a morphological and biochemical comparison. *J. Orthop. Res.* 1: 257–265.
36. Hardingham, T.E., and Fosang, A.J. (1992). Proteoglycans: many forms and functions. *FASEB J.* 6:861–870.
37. Lohmander, S. (1988). Proteoglycans of joint cartilage. Structure, function, turnover and role as markers of joint disease. *Baillieres Clin. Rheumatol.* 2:37–62.

TISSUE ENGINEERING: Part A
Volume 14, Number 12, 2008

DOI: 10.1089/ten.tea.2007.0383

Evaluation Criteria for Musculoskeletal and Craniofacial Tissue Engineering Constructs: A Conference Report

Functional Tissue Engineering Conference Group†

Over the past 20 years, tissue engineering (TE) has evolved into a thriving research and commercial development field. However, applying TE strategies to musculoskeletal (MSK) and craniofacial tissues has been particularly challenging since these tissues must also transmit loads during activities of daily living. To address this need, organizers invited a small group of bioengineers, surgeons, biologists, and material scientists from academia, industry, and government to participate in a 2½-day conference to develop general and tissue-specific criteria for evaluating new concepts and tissue-engineered constructs, including threshold values of success. Participants were assigned to four breakout groups representing commonly injured tissues, including tendon and ligament, articular cartilage, meniscus and temporomandibular joint, and bone and intervertebral disc. Working in multidisciplinary teams, participants first carefully defined one or two important unmet clinical needs for each tissue type, including current standards of care and the potential impact of TE solutions. The groups then sought to identify important parameters for evaluating repair outcomes in preclinical studies and to specify minimally acceptable values for these parameters. The importance of *in vitro* TE studies was then discussed in the context of these preclinical studies. Where data were not currently available from clinical, preclinical, or culture studies, the groups sought to identify important areas of preclinical research needed to speed the development process. This report summarizes the findings of the conference.

Introduction

SINCE FIRST COINED ALMOST 20 YEARS ago by Y.C. Fung,[1] tissue engineering (TE) has evolved into a thriving research field, with active parallel commercial development. Academic and industry researchers have sought to repair a wide array of tissues using many approaches, with progress in some areas like skin graft substitutes, but more uneven progress in others. The early promise of success in TE has been tempered by the realism that tissue regeneration is complex, requiring innovative approaches to design individual tissue and organ repairs.

Applying TE strategies to musculoskeletal (MSK) and craniofacial tissues is particularly challenging, since these tissues must also transmit loads during activities of daily living (ADLs). Tissues like the anterior cruciate ligament (ACL), articular cartilage (AC), long bones, intervertebral disc (IVD), and temporomandibular joint (TMJ) can experience large and recurring *in vivo* forces in challenging environments during these ADLs. The tissue engineer thus faces mechanical and chemical demands in designing tissues that can carry load and remain functional during the entire healing and remodeling process after implantation.

Although TE has, thus far, led to few clinically successful products for patients with MSK and craniofacial disorders, the field has many potential bioengineered technologies currently under development. However, investigators seeking to evolve these technologies into clinical application are hindered by the lack of a coherent strategy to evaluate the relative merits of competing TE designs. While some areas like bone have a well-developed science base and preclinical models, experts still have not reached agreement on which preclinical models, parameters, and threshold values of success to use in their design strategy. This conference was intended to address these issues.

Rationale and Conference Design

To address this deficiency in TE evaluation criteria, two bioengineers (Butler and Lewis) and one surgeon (Frank) from academia organized a unique multidisciplinary meeting to begin to define and reach consensus on evaluation criteria for TE constructs. The small group invited to participate came from academia, industry, government, and so on (see Appendix). This group was asked to relate what they believe should be measured to evaluate success or failure for

The conference was held April 26–29, 2007, at the Hilton Oceanfront Resort in Hilton Head, South Carolina.
†The coauthors are the group of conference organizers and participants listed in the Appendix.

relevant MSK and craniofacial TE constructs. With current knowledge from the literature and input from other experts in the field, the group was charged to identify suitable controls and standards of comparison, parameters to measure in preclinical models, and values for these parameters that would constitute a successful outcome. The organizers initially assumed that practicing tissue engineers would follow a standard research and development process where *in vitro* studies are performed first to optimize the TE component, and then constructs are implanted and evaluated in suitable animals. This conference thus focused on the clinical problem, evaluation of the construct in the animal model, and the *in vitro* studies needed to support these animal studies.

Members split into four stakeholder groups with the following perspectives on TE goals and objectives.

Basic researchers (bioengineers, biologists, and material scientists): Researchers brought a spectrum of perspectives to the discussions. Many of the biologists and some of the engineers and material scientists emphasized the importance of understanding basic mechanisms and fundamental properties of the TE constructs and repairs like restoring normal cellularity and matrix composition as well as construct material quality. Several individuals stressed the value and challenges in designing constructs that could be translated in a more practical fashion into actual products to help patients. Nearly all members of this "stakeholder" group recognized the difficulties in bridging these large gaps between *in vitro*, preclinical, and clinical studies.

Clinicians: Surgeons brought clinical and translational perspectives to the discussions. They emphasized factors like ease of clinical use, including handling and *in vivo* fixation at surgery; reproducibility; safety; short- and long-term effectiveness; identifying risk/benefit ratio versus existing approaches (efficacy); and minimizing complications after surgical implantation. These stakeholders also recognized that researchers must perform *in vitro* and preclinical studies to identify the most promising treatments, but that translating these results to the clinic remains challenging.

Industry: Industry representatives contributed important practical perspectives to the discussions. They pointed out that TE must have a specific market size with limited competition to be economically viable. They cited other practical considerations for TE, including its complex regulatory and reimbursement pathways, its risk/benefit ratio (particularly for constructs involving cells), the relatively high costs of investigation, challenges in manufacturing and scale-up, and the complex analytical methods required to define its effectiveness. They also noted the need to judge clinical outcomes (efficacy and cost) against other current standard treatments and reminded the group of important intellectual property ownership and safety issues.

Funding agencies: Funding agency representatives brought key perspectives about the need for scientific excellence in the field of TE and the potential returns on investment to society associated with a successful design. It was noted that "NIH supports high quality basic, applied and clinical research that has the potential to improve the Nation's health" and "NIH feeds a pipeline for R&D work... and recognizes the translational nature of TE science." Representatives also shared the fact that NIH's "portfolio" differs from that of the private sector (Fig. 1) and that various funding options exist (through special emphasis panels and study sections) to pursue TE research. These include the Bioengineering Research Partnerships and Bioengineering Research Grants.

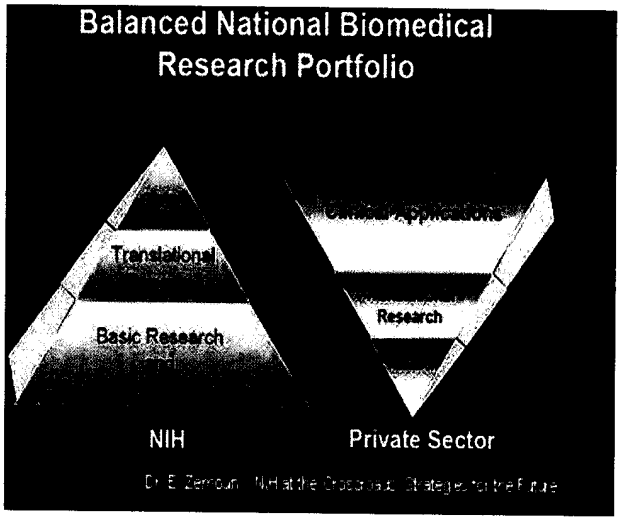

FIG. 1. Inverted pyramids showing opportunities and needs by the National Institutes of Health and the private sector. Slide originates from Dr. Zerhouni's presentation, "NIH at the crossroads: Strategies for the future."

One to three members from a stakeholder team joined a "tissue specific" breakout group. These groups included (1) tendon and ligament, (2) bone and IVD, (3) AC, and (4) meniscus and TMJ. We selected two breakout groups based on the similar structure, composition, and function of ligaments and tendons as well as meniscus and TMJ. We assigned AC to its own group because of its unique character. We grouped bone and IVD because they both sustain compression and because of their proximity in the spine. Less emphasis was placed on common technologies within groups. Each group focused on one or two clinical problems in order to complete the exercise during the conference (see "Defining the Clinical Problem" below). We intentionally mixed members of different groups (1) to provide complementary input and expertise, (2) to allow broader discussions about how to conduct basic research and product development, and (3) to highlight the needs of patient populations.

The Approach Used to Define Evaluation Criteria

Conference organizers (Butler, Lewis, and Frank) requested that participants work backward from the clinical problem to the preclinical models and then to *in vitro* development (Fig. 2). This strategy ensured that groups first clearly focused on the clinical goal and unmet medical need as the primary rationale for new development. Groups then identified evaluation criteria of success in preclinical studies that could be better controlled so as to provide clear benefits before starting expensive human clinical trials. *In vitro* studies were only addressed briefly on the last half day, since these would depend on the specific clinical and preclinical questions and evaluation criteria.

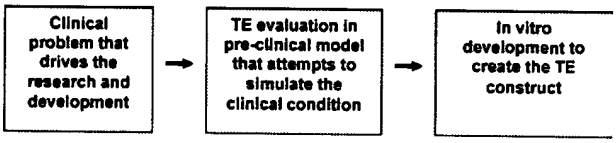

FIG. 2. Process followed in developing evaluation criteria recommendations.

Defining the clinical problem

Each breakout team, including surgeons, first identified one or two high-priority clinical problems for each tissue type. While any clinical problem could have been selected, team members rapidly reached consensus on their choices. Organizers reasoned that by successfully completing the clinical-to-preclinical-to-*in vitro* exercise for one or two problems, the paradigm could be repeated for other clinical problems in the future. Clinical problems were selected based on

- Clinical relevance (common clinical problems) in the MSK and craniofacial fields;
- Prevalence of the disease and its projected incidence in the future;
- Potential for TE to safely and effectively address unmet clinical needs, where current treatments (1) are not effective enough in the short or long term, (2) result in excessively slow recovery times, and/or (3) induce excessive morbidity;
- Existing evidence supporting strong potential for TE success over time (progressive improvements over existing standards).

Attendees generally agreed that successful TE constructs should be better than current standards of care by one or more of the following outcome measures. Patients should

- Demonstrate faster recovery time;
- Show better short-term and long-term functional outcomes (e.g., reduced pain or effusion; improved joint stability, range of motion, and overall function; return to preinjury activity; return to work, etc.);
- Exhibit more durable functional improvements in specific patient-related factors (e.g., by delaying disease progression and/or the need for later, more aggressive options);
- Show little or no morbidity (even when outcomes are no better, patients could dramatically benefit from decreasing morbidity and side effects associated with some existing treatments);
- Need less-expensive treatment in the longer term, resulting in fewer surgeries (for example, one surgical procedure rather than two required for Carticel).

Clinical evaluation issues

Although the conference was not primarily designed to discuss/debate current clinical evaluation problems, the group recognized that few validated clinical evaluation tools are currently available for the clinical problems to be addressed by TE. This problem was universally identified at the end of the conference as an important current and future research need. Specifically, the group noted the importance of establishing tools and methods for clinical evaluation of specific procedures, including better noninvasive diagnostics (imaging) as well as better joint-specific and condition-specific functional evaluation methods in patients.

Clinical target populations: tissue targets, intent of TE constructs, and their potential advantages and constraints

The groups then identified specific clinical needs for each tissue. For each clinical problem, pathological conditions were cited along with current standards of care, potential advantages of a TE approach over an existing standard, and any limitations and constraints that might result from a TE solution. Results of this process for specific clinical problems are shown in Table 1 for AC,[2–5] ACL,[6–8] rotator cuff,[9] bone,[10,11] IVD,[12,13] TMJ,[14–17] and meniscus.[18–20]

As an example, the AC group identified two clinical problems: late-stage osteoarthritis (OA) and focal cartilage defects.[2–5] Late-stage OA, and the attending diffuse, usually multicompartmental cartilage loss, was cited as an enormous clinical problem with few surgical treatment options before total joint replacement. Focal defects in AC, which the group defined as areas of acute partial or full-thickness chondral loss, usually restricted to an isolated area in one compartment of the knee, were judged to be less common. However, the group did recognize the important aspects of this clinical problem and its value as a "proving ground" for potential solutions for OA. The cartilage breakout team concluded that the acute focal defect may not be common enough to be commercially viable by itself, but its treatment could serve as an intermediate step toward the ultimate goal of treating larger, more diffuse, and opposing-surface OA lesions. The current clinical standard of care for focal defects is microfracture, a simple, fast, and fairly uncomplicated procedure. The team concluded that TE solutions after cartilage injury offer several potential advantages, including more natural-like tissue with improved short- and long-term function, delay of total joint replacement, and better compatibility with surrounding joint structures. However, the group also recognized the potentially high cost of TE repairs of focal defects as well as the increased technical demands at surgery and longer rehabilitation time needed to protect the early repairs. A similar process was followed for each tissue type by respective groups.

Conference participants then heard reports on all tissue types and identified common advantages and constraints. Potential advantages included normal or quasinormal tissue quality, reduced patient morbidity (e.g., compared to harvesting autografts), and increased durability of the treatment. The group also agreed that several constraints must be overcome for all of the tissue types examined. For example, the field has still not identified the clinical populations and "at-risk" subpopulations that should be treated. This limitation is, in part, due to the fact that not all clinical (or preclinical) standards of care have validated outcomes. In addition, many clinical and preclinical studies can be quite lengthy and costly, suggesting the need for short-term predictors of long-term outcome in animals and ultimately in patients.

Conference participants also heard about practical constraints facing companies seeking to bring products to market. These industry participants emphasized that the product

TABLE 1. TISSUES, TARGETS, CLINICAL TREATMENTS, AND POTENTIAL ADVANTAGES AND CONSTRAINTS OF TE

Tissue type	*Clinical target*	*Current standard clinical treatment(s) & any special considerations*	*Potential advantages of TE over existing standards*	*Potential constraints of TE for this application*	*References to clinical conditions and clinical demographics*
AC	OA	OA: treat symptoms, osteotomy, unicompartmental, or total joint replacement	Improved tissue quality, more natural tissue	Cost	Aroen *et al.*,[2] Arthritis Foundation,[3] American Academy of Orthopaedic Surgeons,[4] and American College of Rheumatology[5]
	Focal defects (partial and full thickness)	Focal defects: microfracture	Improved short- and long-term function Delayed TJR Better compatibility	Increased technical demands at surgery Rehabilitation time Identifying clinical population Morbidity	
ACL	Complete tear	Autograft or allograft tendon graft	No secondary morbidity site No disease transmission Improved knee mechanics Retention of proprioceptive function Normal insertion sites Less invasive Reduced OA	Ability to resist initial loads Synovial environment Reestablishment of bone–ligament insertion site Ability to restore complex ACL geometry Loss of neurologic function	Myer *et al.*,[6] Spindler *et al.*,[7] and Von Porat *et al.*[8]
Rotator cuff	Tendon tear	Suture repair	Faster healing Stronger repairs Lower failure rates Less invasive	Large tears may be hard to close Multidimensional loads Muscle atrophy Healing to bony insertion sites Synovial environment	Galatz *et al.*[9]
Bone	Large defects	Autograft	No secondary morbidity site	Cost	Kneser *et al.*[10] and Swiontkowski *et al.*[11]
	Spine fusion Fracture nonunions	Allograft BMPs	Faster, more consistent repair Engineering bone–soft tissue interfaces	High-functional loads Inflammatory/immune response Filling complex defect geometries	
IVD	Disc degeneration	Fusion	Less disruptive at surgery	Lack of knowledge of what is "normal"	Garfin[12] and Johannessen *et al.*[13]
		Disc replacement	Physiologically and structurally closer to normal	Unknown pain pathophysiology Ability to resist initial loads Retention of implant Cost	
TMJ	Pain, crepitus, clicking, opening deviation	Conservative treatment including diet modification; condyle replacement by prosthesis or autologous grafting (e.g., rib grafts)	Integration with host tissue; remodeling with host bone	Complexity of joint structures	Fricton,[14] Kapila,[15] Okeson,[16] and Sindelar and Herring[17]
Meniscus	Avascular zone tear	Direct surgical repair	Delay knee OA	High initial functional loads	Lozano *et al.*,[18] Matava,[19] and Ryzewicz *et al.*[20]
	Nonrepairable meniscus tears	Excision None	Restore a stable and functional meniscus	Complex geometry to prevent knee OA Synovial environment	

TJR, total joint replacement.

must be manufactured and delivered at a competitive price that generates profits for the company that must incur the development costs. Companies will not invest in technologies that pose too great a risk with too small a profit margin. Specific factors that enter into this position include the potential market size for each tissue-engineered clinical condition; specification of well-defined, necessary, and sufficient design requirements for these biologics and devices; and the ability of surgeons to implant these structures into their patients using common surgical technologies that do not introduce risk or safety issues. Industry experts also emphasized that although the biologic or device may be appealing on other grounds, ultimately it must be economically viable and worth the expenditure of additional research funds. This evaluation should be made as early as possible in the research and development process.

Identifying Evaluation Criteria in Preclinical Models: What Should Be Measured?

Given the previous considerations, then, what should be measured in a preclinical model and how should the experiment be designed? Critical elements of concern to this question are the aim of the experiment, model selection, appropriate controls and standard of care, and specific variables to measure.

To address these concerns and identify parameters, the entire group was given a common mission. They were challenged not to be "model-specific" in their comments, but rather to identify an idealized set of outcome measures that would capture important aspects of biology, integrity, structure, and/or function. They were also asked to identify differences between experimental arms and distinguish between competing TE approaches, including appropriate controls. The groups were also instructed to prioritize their overall results for individual tissues and models. These results are presented below.

Evaluation considerations in preclinical models—model selection

Animal models of relevance are required for each tissue application. Tissue engineers should consider models that actually simulate, as closely as possible, diseases, pathology, and age of interest. Investigators should also recognize the limitations of the various available models and that they often do not simulate the human clinical condition (e.g., in age, degenerative disease, avascularity, and pain). Researchers should clearly understand that when an acute injury is repaired in an otherwise normal young animal, it likely does not simulate the "real case." These models also introduce a series of "technical issues," including cost, size (bigger = better for some measures; worse for others), reproducibility, ease of surgical implantation, and similarity to clinical techniques regarding implantation and fixation. The group also concluded that less-invasive insertion methods would be best and that the model should ideally allow some type of realistic rehabilitation after surgery. The animal and tissue model selected should allow repairs to be examined over longer time intervals after surgery and provide adequate tissue for multiple, well-controlled analyses. Yet, the choice of animal and tissue models obviously depends on the question being asked and how the model relates to that question. For example, empty or "blank" defects might be useful to assess the natural healing (i.e., the absence of treatment; see next section).

Evaluation considerations in preclinical models—controls and standard of care

The question of "controls" and "standard of care" was a central issue debated in breakout groups and in plenary session. As with any experiment, appropriate controls are critical. Participants discussed the need for internal controls (two or more treatments within the same joint or animal), and the use of "empty defect" controls. The groups also debated the value of nonoperated controls (e.g., no operation on the opposite leg) versus simulations of clinical standard of care.

The groups examined the advantages and disadvantages of running internal controls. If carefully performed with minimal influence or interaction, treatments could be contrasted among multiple locations in an individual joint or after contralateral surgeries in paired limbs (including the use of sham operations). These controls can avoid statistically underpowered observations that commonly occur when interanimal differences exceed intraanimal differences for specific evaluation measures. Such interanimal, biological variance can be a significant barrier that masks our ability to identify a successful TE construct and then to publish the results.

A treatment might also be contrasted against whatever is appropriate for the specific question being addressed. For example, the comparison might be to a "blank" or empty defect control (no treatment) to demonstrate the natural healing ability in the model of interest. As noted above, this approach could be used to demonstrate that the TE solution does better than no treatment, especially if this blank control does not heal on its own. However, this control would be incomplete on its own, since available treatments are expected to be better than the blank control.

Participants also questioned if a tissue-engineered repair should be compared to a nonoperated, normal tissue. "Normal" is certainly an "ideal" standard, but few TE solutions achieve this goal and normal may not be necessary for clinical success. Normal, within a functional loading range, might be more achievable, however, especially in the early stage of development. If normal was the only control and goal of the experiment, one might judge a TE treatment to have failed, especially since few TE solutions achieve normal properties under abnormal conditions. Over time, this target can hopefully be approached (where required), and for this reason, we have included some of the key features, target parameters, and evaluation measures (with a few references) in Table 2 for the interested reader (AC,[21–26] ACL,[27] rotator cuff,[28–30] bone,[31] IVD,[32–39] TMJ,[40–44] and meniscus[45–48]).

Instead, treatments could be validated against a "simulation" of the current clinical standard of care for that condition, if that option was available and could be tested in the animal model of choice. This comparison would probably be required at some point, since the purpose of developing a new TE construct is to improve on the "existing" clinical options (both in terms of clinical efficacy and cost).

Participants eventually recommended that investigators use multiple controls and seek to show positive effects of the treatment relative to normal and simulations of standard of care. The choice of control(s) will depend on the specific purpose of the experiment and the sensitivity of the

TABLE 2. NORMAL CHARACTERISTICS OF CANDIDATE TISSUES CLASSIFIED BY SOME POTENTIAL "KEY STRUCTURAL AND FUNCTIONAL CONSIDERATIONS" FOR TE REPLACEMENTS, WITH A FEW SELECTED REFERENCES TO THESE FEATURES

MSK and craniofacial tissues with TE potential	*Normal targets—imaging, gross appearance, and some key characteristics*	*Normal histology; cell types, matrix organization*	*Normal tissue functions and biomechanical properties*	*Normal biochemistry (markers of normal)*	*Key references to normal structures and functions*
Cartilage	Thin, uniform thickness (3–6 mm), white, avascular, aneural, low friction	Chondrocytes (no cloning), zonal, matrix highly ordered, dense proteoglycan staining, surface intact	Nearly frictionless, firm viscoelastic, low permeability, fracture resistant	Collagen II, aggrecan, matrix metalloproteinases	Cohen *et al.*,[21] Faber *et al.*,[22] Hasler *et al.*,[23] Mankin *et al.*,[24] Mow and Hayes,[25] and Treppo *et al.*[26]
ACL	Organized collagen fascicles, low signal on T2 imaging, vascular, innervated, strong in tension, TE construct stiffness?	Fibroblasts, collagen in parallel bundles making fascicles with vessels and nerves running along the fascicles, crimp, synovial layer covering ligament, highly specific ligament insertion site	Very strong in tension Toe region in stress–strain curve to allow normal motion Equivalent tangent stiffness to peak *in vivo* forces plus safety factor	Collagen I, collagen I/III ratio, matrix metalloproteinases, decorin, proteoglycans	Murray and Spector[27]
Rotator cuff	Organized collagen fascicles, low signal on T2 imaging, vascular, innervated, strong in tension	Fibroblasts, collagen in parallel bundles making fascicles with vessels and nerves running along the fascicles, crimp, synovial layer covering tendon, highly specific tendon insertion site	Very strong in tension Very small toe region in stress–strain curve to allow efficient transfer of muscle force to bone Equivalent tangent stiffness to peak *in vivo* forces plus safety factor	Collagen I, collagen I/III ratio, matrix metalloproteinases, decorin, proteoglycans	Blevins *et al.*,[28] Clark and Harryman,[29] and Soslowsky *et al.*[30]
Bone	High radiodensity Integrated with adjacent bone	Osteoblasts, osteocytes, and osteoclasts Woven bone initially but remodeled into highly organized lamellar bone	Very strong in compression High fracture toughness and fatigue resistance	Collagen I, hydroxyapatite mineral	Taylor *et al.*[31]

	Vascularized and remodeling				
IVD	Normal disc height by radiography	Fibroblast-like in annulus fibrosus, chondrocytic in inner annulus and nucleus pulposus, notochordal cells in young human, chondrocytic cells in adult	Pliant, viscoelastic, stiff in compression (approximately 4 MPa)	Opposing gradients of collagen I (outer annulus) and collagen II (nucleus)	Adams *et al.*,[32] Ferguson and Steffen,[33] Guerin and Elliott,[34] Johannessen and Elliott,[35] Nerurkar *et al.*,[36] Roberts *et al.*,[37] Schnake *et al.*,[38] and Setton and Chen[39]
	MRI normal signal on T2 imaging, no herniation		Compressive strength to exceed ADL estimates (approximately three to five times body weight)	Aggrecan gradient from outer annulus to nucleus	
	Fibrous annular rings, gelatinous nucleus in younger individuals, crabmeat like in older individuals		Flexible in bending	Aggrecan and collagen II in endplate	
	Hyaline cartilage endplate across entire disc in young, extending to inner annulus in adult		Exhibiting a "neutral zone"	Low cytokine levels	
				Low lactate levels	
TMJ	Disc is fibrocartilage and/or fibrous tissue; articular condyle is fibrocartilage; age variation; CT and MR used in diagnosis; bilaterally linked and must function in unison	Disc is mostly type I collagen, although type II collagen can be found; both disc and articular condyle consist of large and small proteoglycans, including aggrecan, versican, decorin, bigalycan, etc.; age variation	Withstands tensile, compressive, and shear forces; fibrocartilage's compressive properties between fibrous tissue and hyaline cartilage; regional differences in mechanical properties	Type I and type II collagens; regional differences in the distribution of proteoglycans; adaptation with functional demands in matrix composition	Alhadlaq and Mao,[40] Allen and Athanasiou,[41] Hu *et al.*,[42] and Mao *et al.*[43,44]
Meniscus	Intact circumferential collagen fibrils and attachments	Meniscus cells viable in entire tissue	Act like normal meniscus the loads on AC in that specific compartment	Types I and II collagen	Hauger *et al.*,[45] Kambic and McDevitt,[46] McDevitt and Webber,[47] and Upton *et al.*[48]
	Simulate the normal collagen/PG distribution	Spatial organization of collagen-circumferential and radial	Similar tensile and compression properties	Type VI collagen	
	No extrusion or tears	PG matrix Vascular outer rim		Aggrecan PGs Matrix genes	

MRI, magnetic resonance imaging; PG, proteoglycan.

evaluation measures being used. Showing positive effects of a treatment, especially without a suitable clinical standard of care, might still be useful in pursuing a treatment option.

Evaluation parameters and values in preclinical models for TE constructs—issues leading to summary and recommendations

With these considerations in mind, specific evaluation parameters in preclinical models were identified for each tissue (AC,[49,50] ACL,[7,51–54] rotator cuff,[28–30,55,56] bone,[10,57–62] IVD,[12,32,33,38,63–70] TMJ,[14–17,40–44] and meniscus[18–20,45–48,71–76]), and then specific parameter values were chosen that were considered to be successful relative to a specific standard (Table 3). The group determined that an extensive list of criteria must be considered when assessing the potential "success" of any TE construct. The group focused more on the clinical and research areas of interest rather than the late-stage development and marketing issues such as the ability to pass regulatory requirements, ensure quality, etc., introduced at the beginning of the conference.

Some participants voiced concern that by expressing "common evaluation issues," we would overlook specific criteria that are unique to individual tissues. Therefore, these "generic" evaluation suggestions are presented only as a summary of what the group felt should be "minimum expectations" and recommendations for those considering TE research. Evaluation criteria common to all tissues were identified as follows. These are divided into three sections: must have, should have, and nice to have, as follows.

"Must have" criteria: (1) Be able to be implanted and retained under appropriate early loading conditions. (2) Meet or exceed current "best" treatment for that tissue in the model of interest according to one or more quantitative measures. These measurement tools could include implant integrity, imaging, structure, mechanics, or biochemistry over time. Specific examples might include imaging and noninvasive assessments (ideally quantitative); joint function (inflammation, pain, etc.), since it assesses more than the tissue itself; tissue mechanics if possible (acutely, locally, and over a reasonable time period after surgery); individual tissue assessment (gross histology, etc.) as well as assessment of other tissues in or around the joint; geometry; other relevant time-related properties like durability, longevity, and recovery; biological measures like cellularity, viability, organization, vascularity, and matrix composition; and molecular measures to understand mechanisms leading to iterative and relevant improvements in repair outcome. (3) Be viable (cellular) after implantation (cell-based therapy). (4) Be safe (no signs of adverse reaction *in vivo*). And (5) be functionally integrated into surrounding tissues and/or be replaced by functional host tissue.

"Should have" criteria: (1) Be evaluated by more than one validated quantitative outcome measure; (2) aspire to achieve normal tissue properties by as many measures as possible.

"Nice to have" criteria: Promote improved endogenous repair or ingrowth of surrounding injured or degenerated host tissues. This criterion would enhance fixation and/or longevity of the replacement.

Based on this list and on tissue-specific needs, evaluation parameters were then identified for each tissue and values were known (Table 3).

For AC, the primary clinical problem is repair of focal defects and cartilage resurfacing as a treatment for OA. The current standard of care for focal defects is microfracture, and the current standard of care for OA is treatment of symptoms, osteotomy, or joint replacement, depending on stage of disease. At animal sacrifice, TE constructs for both repair of focal defects and cartilage resurfacing as a treatment for OA should be evaluated by noninvasive imaging, gross examination, biochemistry, histology, histochemistry, and mechanics. Noninvasive imaging could include plain film radiography with characterization of radiographic features of OA, including narrowing of the cartilage space, marginal osteophytes, subchondral sclerosis, and breaking of the tibial spines. Imaging could also include magnetic resonance imaging (MRI) techniques designed specifically for cartilage evaluation. Function of the animal should also be evaluated using validated outcome instruments, which would ideally include indices of pain and motor function. Parameters from these measurements should be assembled into one of the available composite scoring systems (e.g., Outerbridge or India Ink staining for gross score, O'Driscoll for histology, and International Cartilage Repair Society (ICRS) for composite appearance) and should be found to improve over values for those in knees undergoing the current standard of treatment for the target condition.

For the ACL, the primary clinical problem is treatment after traumatic rupture. The current standard of care after ACL rupture (when surgery is indicated) is removal of the ligament and replacement or reconstruction with autologous patellar tendon or hamstring tendons, or with allograft tissues. New methods for treating ACL rupture using TE techniques should be evaluated using functional methods and mechanical assessments, as well as biologic measures that indicate continuation of function over time. Evaluations should be carried out in a large animal model, such as goat, pig, sheep, or dog (rabbit and smaller models not recommended). Observations should be recorded at 1–3 months for biologic and histologic changes and between 3 and 12 months for biomechanical properties or development of AC changes. Biologic parameters include gross inspection parameters (cartilage, synovium, effusion, and India ink staining of cartilage), as well as microscopic evaluations of the bone–ligament interface; presence of inflammatory cells; vascularization; histology of the ACL tissue, graft material, and joint cartilage; and the appearance of the ACL on noninvasive imaging. Functional evaluations include measurements of anteroposterior (AP) laxity of the knee, the stiffness and maximum load of the ACL construct, the condition of the AC and overall joint function measures, including joint range of motion, gait abnormalities, and activity monitoring. The target values for these outcome measures should compare favorably with the current gold standard of treatment (ACL reconstruction with autograft tendon). The mechanical properties should have 100% of the stiffness of the normal ACL in low load regions (up to 20% of the intact ACL maximum load) in addition to stiffness and strength similar to ACL reconstruction. The joint function measures should also have values similar to knees undergoing ACL reconstruction in terms of range of motion, effusion, AC changes, gait abnormalities, and activity changes.

For the rotator cuff, the primary clinical problem is tendon tears that are unresponsive to nonsurgical treatment. The current standard of care for these injuries is suture repair of

TABLE 3. PRECLINICAL MODELS, MEASURES, AND VALUES

Tissue type	*Preclinical model options*	*Models that are not recommended (if any)*	*Assessment times based on condition and/or model(s)*	*Proposed evaluation parameters*	*Target values—specify controls (%N:%C)*	*References*
Cartilage	Focal defect (into bone or partial, depending on target condition) or larger defect in a medium-sized animal model (e.g.,sheepanddog)	Immature animals	Depends on question(s)	Joint function (surrogate of pain)	Should exceed "treatment controls"—e.g., C×110%, where C = microfracture for focal defects, or appropriate treatment for target stage for OA resurfacing	Lee *et al.*[49] and Troken *et al.*[50]
		Models that cannot assess joint function	More than one time point	Cartilage integrity and composition scores	Should not just exceed "blank controls"	
			At least months (to understand processes)	OA scores		
ACL	Central defect	Animal size—rabbit or smaller not recommended	1–3 months for biological and histologic changes	AP knee laxity	Similar to laxity for ACL autograft reconstruction	Spindler *et al.*,[7] Butler *et al.*,[51] Hunt *et al.*,[52] Rasmussen *et al.*,[53] and Schwartz *et al.*[54]
	Complete transection	Goat, sheep, dog, and pig are acceptable	3–12 months for biomechanical and joint changes	Stiffness and strength (max. load) of ACL construct	100% of stiffness up to 20–30% of maximum force for normal ACL; similar to stiffness and strength of ACL autograft reconstruction	
	Delayed repair			Condition of AC	Similar AC condition and joint function to ACL reconstruction	
Rotator cuff	Complete tear	Animal size—rabbit or smaller not recommended	3–12 months	Overall joint function Recurrence of tear	Rate similar to suture repair	Blevins *et al.*,[28] Clark and Harryman,[29] Soslowsky *et al.*,[30] Derwin *et al.*,[55] and Glaser *et al.*[56]

(*continued*)

TABLE 3. (CONTINUED)

Tissue type	*Preclinical model options*	*Models that are not recommended (if any)*	*Assessment times based on condition and/or model(s)*	*Proposed evaluation parameters*	*Target values—specify controls (%N:%C)*	*References*
		Animals where cuff tear is not intrasynovial (unless capsular defect made as well)		Muscle strength and histology	Appearance and function similar to repair	
				Strength of tendon	30% of intact or similar to suture repair	
Bone	Large segmental defects	Immature animals	1–6 months for bone bridging	Bone bridging by CT	Rapid return to full and symmetrical weight bearing	Kneser *et al.*,[10] Bruder and Fox,[57] Cancedda *et al.*,[58] Einhorn,[59] Guldberg *et al.*,[60] Laurencin *et al.*,[61] and Liebschner[62]
	Nonhealing craniofacial and long bone defects	Noncritically sized defects	3–6 months for biomechanical properties	Biology (revascularization and remodeling by histology)	Restoration of full-intact bone strength and work to failure	
	Spine fusion	Large (dog, sheep, and goat) animal models to test therapeutic angiogenesis strategies		Integration strength by biomechanical testing	Accelerated repair compared to current standards	
	Fracture nonunion Compromised models (irradiated, aged, immunodeficient)					
IVD	No ideal model	Stab models made with large wounds through the annulus	Depends on question(s)	Disc height	>90% of normal height	Garfin,[12] Adams *et al.*,[32] Ferguson and Steffen,[33] Schnake *et al.*,[38] An and Masuda,[63] An *et al.*,[64] Anderson *et al.*,[65] Lotz,[66] Lotz and Kim,[67] Lotz and Ulrich,[68] O'Halloran and Pandit,[69] and Paesold *et al.*[70]
	Large animal preferred to mimic nutritional, surgical constraints	Animals with notochordal cells predominant in nucleus pulposus	More than one time point	MRI	Normal T2-weighted image on MRI	

			At least months (to understand processes)	ECM production	Normal kinematics of spine	
				Cytokine levels	Normal ECM and cytokine composition	
				Delamination	Normal compressive strength and pressure–volume relationship	
				Motion segment testing	No nerves or vessels in nucleus pulposus	
				Compressive strength		
				Pressure–volume testing		
				Histologic assessment of nucleus pulposus		
TMJ	Effective small and large animal models of disease to be established such as OA		Multiple time points	Joint function including range of motion, bite forces; tissue quality	Should restore function over time; range of motion and mastication need to be restored over time	Fricton,[14] Kapila,[15] Okeson,[16] Sindelar and Herring,[17] Alhadlaq and Mao,[40] Allen and Athanasiou,[41] Hu *et al.*,[42] and Mao *et al.*[43,44]
Meniscus	Repair	Not rodents	Repair: 3–6 months	All: (1) Protection against OA compartment; (2) avoid extrusion	All: (1) no tears or "loose body" formation; (2) delay in time by 30–50% onset OA	Lozano *et al.*,[18] Matava,[19] Ryzewicz *et al.*,[20] Hauger *et al.*,[45] Kambic and McDevitt,[46] McDevitt and Webber,[47] Upton *et al.*,[48] Arnoczky *et al.*,[71] Cook *et al.*,[72,73] Peretti *et al.*,[74] Valiyaveettil *et al.*,[75] and Webber *et al.*[76]
	Scaffold Transplantation	Maybe rabbit Recommended: dog, goat/sheep, pig	Scaffolds: 6–12 months Transplantation: 12 months	Repair/scaffold: (1) integration with normal; (2) repair site strength; (3) scaffold–meniscus interface strength		

AP, anteroposterior; ECM, extracellular matrix.

the failed ends of the tendon. Repair using a TE construct in an animal model should be evaluated by both functional and biologic measures. The animal model should be larger than a rabbit to assure similar requirements of tissue healing to the human case. The animal model should also have an intraarticular location of the torn tendon, either by the naturally occurring anatomy or by creating a capsular defect so that the tear is exposed to synovial fluid during the healing process. Outcomes should be evaluated at 3–12 months for recurrence of tear, muscle strength, and histologic changes, as well as repair strength. Functional measures include activity monitoring and altered joint motions relative to the normal shoulder, as well as mechanical assessments of *in vivo* and *in vitro* joint laxity versus time as well as stiffness and failure loads from load–displacement tests in the laboratory. Biologic measures encompass gross inspection (size of defect or gap between tendon and repair site on the bone and degree of muscle contraction), histology (presence of inflammatory cells, vascularization, histology of repair, and insertions into bone and muscle), as well as appearance of the tendon and muscle on noninvasive imaging. The healing musculotendinous unit should be carefully evaluated at times up to 3 months and possibly at 6 and 12 months postsurgery as well. The target values for these outcome measures should compare favorably with the current gold standard of treatment (rotator cuff suture repair). The maximum load of the repairs should be at least 30% of the intact cuff tendon, or similar to suture repair values. The joint function measures should also have values similar to shoulders undergoing suture repair in terms of range of motion, effusion, AC changes, gait abnormalities for quadrupeds, and activity changes.

For bone, the main clinical problems are large segmental defects, nonhealing craniofacial bone defects, bone–soft tissue interfaces, spine fusion, and fracture nonunions. The current standard of care is autograft or allograft, although the use of BMPs is increasing rapidly. Restoration of full mechanical properties is a realistic goal for bone repair, so bone TE constructs should be compared to normal intact bone as well as allograft and collagen sponge/BMP standards. Construct integration should be evaluated as a function of time by morphology (CT or micro-CT), biology (revascularization by histology, osteoclast/osteoblast remodeling, and physiologic Ca/P ratios to lamellar bone by x-ray photoelectron spectroscopy/Fourier transform infrared spectroscopy (XPS/FTIR), and mechanics (torsion testing and correlation of three-dimensional bone volume/distribution with integration strength).

For IVD, the main clinical problem is painful disc degeneration. This is typically attributed to unstable spinal biomechanics or abnormal disc biochemistry. The goal of clinical treatment is pain-free motion. There is no current gold standard of care. Treatments include physical therapy, local anesthetic injection, and surgery as a last resort (typically spinal arthrodesis, although total disc replacement is gaining in popularity). The TE goal should be restoration of the disc's physical and biochemical properties, with both fusion and the "normal" disc as suitable comparison standards in a large animal model. At animal sacrifice, the group recommended that tissues should be evaluated for structural integrity from MRI (normal T2-weighted image with at least 90% of normal disc height as compared to adjacent levels and absence of adjacent segmental degeneration), biochemistry (ECM molecular ratios and cytokine levels restored to normal, inhibition of innervation and vascularization into the nucleus pulposus), and biomechanics (adequate initial fixation strength under functional loads, *in vitro* strength and concentric range of motion of the motion segment, and restoration of normal pressure–volume relationships).

For the TMJ, the primary clinical problems are pain, clicking and opening deviation, degenerative joint disease, OA and rheumatoid arthritis, and ankylosis. The current standards of care are conservative treatment, pain management, intraarticular injections, and surgical replacement with metallic implants and tissue grafts that are condition specific. Clinical outcome of current treatments is not well documented, leading to difficulty in predicting a successful prognosis. There are few valid animal models of TMJ arthritis. Some of the mechanical, structural, and biochemical properties of the TMJ, including the disc, ligaments, and condyle, have been documented but are nonetheless incomplete. Outcome measures should include functional assessment (e.g., range of motion, chewing capacity, and bite force) and, at animal sacrifice, the tissue should be evaluated by structure/morphology (biological fixation and integration, biochemistry, histology, mechanical properties, and imaging).

For the meniscus, the primary clinical problems are direct repair of the tissue in the avascular zone and replacement of irreparably damaged meniscus after partial meniscectomy. The rationale for performing these procedures is that loss of meniscus function leads to premature OA. A TE meniscus construct for either repair or replacement in an animal should be evaluated by structure/morphology measures (imaging, integration with suitable tissue, and histology), biochemistry, and mechanics (contact pressure and extrusion under compression). The articular surfaces in the compartment where the TE meniscus is inserted must be evaluated by histologic, biochemical, and mechanical assessments because the primary goal of inserting a TE meniscus is to prevent arthritis.

In Vitro Models of TE—Rationale and Evaluation

In vitro TE studies can be pursued once the clinical problem has been carefully defined and the preclinical model, measures, and values have been identified. While these models are not intended to simulate the *in vivo* situation (and thus direct extrapolations should be avoided), they do offer certain advantages. (1) They can be especially useful if the effects of certain treatments on *in vitro* response measures directly correlate with repair outcomes after surgery.[77] Treatment effects can then be rapidly screened *in vitro* to identify and even optimize promising cell, matrix, or stimulus methods to ultimately pursue at surgery. (2) These models are also beneficial from a scientific and ethical standpoint by minimizing preclinical surgery and reducing time and cost of development. (3) Investigators can also perform studies to define mechanisms of action (e.g., to study cell behavior with and without matrices or the action of specific growth factors and cytokines on cell phenotype). (4) Others may seek to test different strategies of construct enhancement or augmentation at surgery (e.g., by crosslinking biomaterials to enhance construct stiffness while also preserving cell phenotype).

This meeting was not intended to identify all *in vitro* TE evaluation issues for MSK and craniofacial applications. How-

ever, the concept of preengineering or preconditioning a TE construct before surgery remains attractive in accelerating the development process toward preclinical and clinical design goals. Better understanding the relationship between the state of the engineered construct before surgery and the final repair outcome remains an important goal.

Institutional Tools, Priority Programs, and Partnerships

In addition to addressing these research needs, conference participants recognized that academic, government, and industry barriers are slowing the effective and efficient evaluation of TE constructs. For example, multidisciplinary teams typically evaluate the complex, interactive factors noted above. However, most universities do not fully promote and reward the individual talents in "multidisciplinary" teams. In a similar way, funding mechanisms and funding programs at granting agencies are only beginning to be created that encourage teams of researchers to pursue these difficult translational studies. Industrial partners must also be engaged early in the process to facilitate and ensure "practical" development toward a clinical solution.

In the final plenary session, delegates were asked to identify possible models and partnerships as well as funding mechanisms that could enhance the rate of investigation and development. (1) Models and partnerships: Participants suggested that TE evaluation centers or networks be created as well as multiple principal investigator programs in TE. They also recommended that leaders in TE seek to form University–Corporate and Federal–Corporate (i.e., public–private) partnerships in TE. The FDA should also be engaged as a partner. The group suggested the formation of a Clinician–Scientist program in TE to encourage physicians to participate early in the development process and a Translational Scientist program for researchers to more fully appreciate the end product of the TE process. Several organizations are examining these possibilities at this time. (2) Funding mechanisms: TE research has usually relied on government, foundation, and private funding and this should continue. However, longer-term, high-risk funding programs from agencies like NIH (e.g., extended R-21 grants) would be most useful during the early TE development phase. Tissue engineers should also pursue corporate and venture capital funding, particularly when developing solutions for specific problems that must be addressed in a targeted research and development program. For TE to be optimally developed, funding must be available at the critical, albeit early stage research activities, and tissue engineers must better appreciate the challenges of delivering the final product to the surgeon.

All are encouraged to seriously consider these programs and funding strategies in the short term if TE is to match the potential that many claimed it would have when the field was just beginning. Only then can truly novel methods be taken from the "benchtop to the bedside."

Acknowledgments

The organizers wish to thank the following organizations for support of this conference: National Institutes of Health (R13AR54721-1; DB, PI) (National Institute of Arthritis and Musculoskeletal and Skin Diseases [NIAMS], National Institute of Biomedical Imaging and Bioengineering [NIBIB], and National Institute of Dental and Craniofacial Research [NIDCR]); the Orthopaedic Research and Education Foundation; the Orthopaedic Research Society; Bose Corporation; Flexcell International Corporation; LifeCell Corporation; Johnson & Johnson Regenerative Therapeutics; Smith & Nephew; Stryker Orthopedics Corporation; and Synthasome, Inc. We wish to also acknowledge Kathleen Derwin, Ph.D., Assistant Staff Scientist in the Department of Biomedical Engineering at the Cleveland Clinic, who edited the rotator cuff portion of this paper and provided relevant literature.

References

1. Fung, Y.C. NSF Workshop. From Skalak, R., and Fox, C.F. (eds). Tissue Engineering. New York: Alan R. Liss, Inc., 1988.
2. Aroen, A., Loken, S., Heir, S., Alvik, E., Ekeland, A., Granlund, O.G., and Engebretsen, L. Articular cartilage lesions in 993 consecutive knee arthroscopies. Am J Sports Med **32**, 211–215, 2004.
3. Arthritis Foundation. Disease center. http://www.arthritis.org/conditions/DiseaseCenter/oa.asp, 2004.
4. American Academy of Orthopaedic Surgeons. Osteoarthritis. American Academy of Orthopaedic Surgeons Fact Sheet, http://orthoinfo.aaos.org/fact/thr_report.cfm?Thread_ID=365&topcategory=Arthritis, 2004.
5. American College of Rheumatology. Osteoarthritis. http://www.rheumatology.org/public/factsheets/oa.asp?aud=pat, 2004.
6. Myer, G.D., Ford, K.R., and Hewett, T.E. Rationale and clinical techniques for anterior cruciate ligament injury prevention among female athletes. J Athl Train **39**, 352–364, 2004. http://www.ncbi.nlm.nih.gov/entrez/query.fcgi?cmd=Retrieve&db=PubMed&dopt=Citation&list_uids=15592608.
7. Spindler, K.P., Kuhn, J.E., Freedman, K.B., Matthews, C.E., Dittus, R.S., and Harrell, F.E., Jr. Anterior cruciate ligament reconstruction autograft choice: bone-tendon-bone versus hamstring. Does it really matter? A systematic review. Am J Sports Med **32**, 1986–1995, 2004.
8. Von Porat, A., Roos, E.M., and Roos, H. High prevalence of osteoarthritis 14 years after an anterior cruciate ligament tear in male soccer players: a study of radiographic and patient relevant outcomes. Br J Sports Med **38**, 263,2004. http://www.ncbi.nlm.nih.gov/entrez/query.fcgi?cmd=Retrieve&db=PubMed&dopt=Citation&list_uids=15155422.
9. Galatz, L.M., Ball, C.M., Teefey, S.A., Middleton, W.D., and Yamaguchi, K. The outcome and repair integrity of completely arthroscopically repaired large and massive rotator cuff tears. J Bone Joint Surg Am **86-A**, 219–224, 2004. http://www.ncbi.nlm.nih.gov/entrez/query.fcgi?cmd=Retrieve&db=PubMed&dopt=Citation&list_uids=14960664.
10. Kneser, U., Schaefer, D.J., Polykandriotis, E., and Horch, R.E. Tissue engineering of bone: the reconstructive surgeon's point of view. J Cell Mol Med **10(1)**, 7–19, 2006.
11. Swiontkowski, M.F., Aro, H.T., Donell, S., Esterhai, J.L., Goulet, J., Jones, A., Kregor, P.J., Nordsletten, L., Paiement, G., and Patel, A. Recombinant human bone morphogenetic protein-2 in open tibial fractures. A subgroup analysis of data combined from two prospective randomized studies. J Bone Joint Surg Am **88(6)**, 1258–1265, 2006.
12. Garfin, S. Spine. In: Fitzgerald, R.H., Kaufer, H., and Malkani, A.L., eds. Orthopaedics, section 8. St. Louis: Mosby, Inc., 2002, pp. 1125–1220.

13. Johannessen, W., Auerbach, J.D., Wheaton, A.J., Kurji, A., Borthakur, A., Reddy, R., and Elliott, D.M. Assessment of human disc degeneration and proteoglycan content using T1rho-weighted magnetic resonance imaging. Spine **31(11)**, 1253–1257, 2006.
14. Fricton, J. Current evidence providing clarity in management of temporomandibular disorders: summary of a systematic review of randomized clinical trials for intra-oral appliances and occlusal therapies. J Evid Based Dent Pract **6**, 48–52, 2006.
15. Kapila, S. Does the relaxin, estrogen and matrix metalloproteinase axis contribute to degradation of TMJ fibrocartilage? J Musculoskelet Neuronal Interact **3**, 401–405, 2003.
16. Okeson, J.P. Joint intracapsular disorders: diagnostic and nonsurgical management considerations. Dent Clin North Am **51**, 85–103, 2007.
17. Sindelar, B.J., and Herring, S.W. Soft tissue mechanics of the temporomandibular joint. Cells Tissues Organs **180**, 36–43, 2005.
18. Lozano, J., Ma, C.B., and Cannon, W.D. All-inside meniscus repair: a systematic review. Clin Orthop Related Res **455**, 134–141, 2007.
19. Matava, M.J. Meniscal allograft transplantation: a systematic review. Clin Orthop Related Res **455**, 142–157, 2007.
20. Ryzewicz, M., Peterson, B., Siparsky, P.N., and Bartz, R.L. The diagnosis of meniscus tears: the role of MRI and clinical examination. Clin Orthop Related Res **455**, 123–133, 2007.
21. Cohen, Z.A., McCarthy, D.M., Kwak, S.D., Legrand, P., Fogarosi, F., Ciaccio, E.J., and Ateshian, G.A. Knee cartilage topography, thickness, and contact areas from MRI: *in-vitro* calibration and *in-vivo* measurements. Osteoarthr Cartil **7**, 95–109, 1999.
22. Faber, S.C., Eckstein, F., Lukasz, S., Mühlbauer, R., Hohe, J., Englmeier, K.-H., and Reiser, M. Gender differences in knee joint cartilage thickness, volume and articular surface areas: assessment with quantitative three-dimensional MR imaging. Skeletal Radiol **30**, 144–150, 2001.
23. Hasler, E.M., Herzog, W., Wu, J.Z., Müller, W., and Wyss, U. Articular cartilage biomechanics: theoretical models, material properties, and biosynthetic response. Crit Rev Biomed Eng **27(6)**, 415–488, 1999.
24. Mankin, H.J., Grodzinsky, A.J., and Buckwalter, J.A. Articular cartilage and osteoarthritis. In: Orthopaedic Basic Science, chapter 9. Rosemont, IL: American Academy of Orthopaedic Surgeons, 2007, pp. 161–174.
25. Mow, V.C., and Hayes, W.C. Basic Orthopaedic Biomechanics. Lippincott-Raven, Philadelphia, PA, 1997.
26. Treppo, S., Koepp, H., Quan, E.C., Cole, A.A., Kuettner, K.E., and Grodzinsky, A.J. Comparison of biomechanical and biochemical properties of cartilage from human knee and ankle pairs. J Orthop Res **18**, 739–748, 2000.
27. Murray, M.M., and Spector, M. Fibroblast distribution in the anteromedial bundle of the human anterior cruciate ligament: the presence of alpha-smooth muscle actin-positive cells. J Orthop Res **17**, 18–27, 1999.
28. Blevins, F.T., Djurasovic, M., Flatow, E.L., and Vogel, K.G. Biology of the rotator cuff tendon [Review]. Orthop Clin North Am **28(1)**, 1–16, 1997.
29. Clark, J.M., and Harryman, D.T. Tendons, ligaments and capsule of the rotator cuff. Gross and microscopic anatomy. J Bone Joint Surg Am **74**, 713–725, 1992.
30. Soslowsky, L.J., Carpenter, J.E., Bucchieri, J.S., and Flatow, E.L. Biomechanics of the rotator cuff [Review]. Orthop Clin North Am **28(1)**, 17–30, 1997.
31. Taylor, D., Hazenberg, J.G., and Lee, T.C. Living with cracks: damage and repair in human bone. Nat Mater **6(4)**, 263–268, 2007.
32. Adams, M.A., Bogduk, N., Burton, K., and Dolan, P. The Biomechanics of Back Pain. Edinburgh: Churchill Livingstone Press, 2002.
33. Ferguson, S.J., and Steffen, T. Biomechanics of the aging spine. Eur Spine J **12 Suppl 2**, S97–S103, 2003.
34. Guerin, H.L., and Elliott, D.M. Quantifying the contributions of structure to annulus fibrosus mechanical function using a nonlinear, anisotropic, hyperelastic model. J Orthop Res **25(4)**, 508–516, 2007.
35. Johannessen, W., and Elliott, D.M. Effects of degeneration on the biphasic material properties of human nucleus pulposus in confined compression. Spine **30(24)**, E724–E729, 2005.
36. Nerurkar, N.L., Elliott, D.M., and Mauck, R.L. Mechanics of oriented electrospun nanofibrous scaffolds for annulus fibrosus tissue engineering. J Orthop Res **25**, 1018–1028, 2007.
37. Roberts, S., Evans, H., Trivedi, J., and Menage, J. Histology and pathology of the human intervertebral disc. J Bone Joint Surg Am **88 Suppl 2**, 10–14, 2006.
38. Schnake, K.J., Putzier, M., Haas, N.P., and Kandziora, F. Mechanical concepts for disc regeneration. Eur Spine J **15 Suppl 3**, S354–S360, 2006.
39. Setton, L.A., and Chen, J. Mechanobiology of the intervertebral disc and relevance to disc degeneration. J Bone Joint Surg Am **88 Suppl 2**, 52–57, 2006.
40. Alhadlaq, A., and Mao, J.J. Tissue-engineered osteochondral constructs in the shape of an articular condyle. J Bone Joint Surg Am **87(5)**, 936–944, 2005.
41. Allen, K.D., and Athanasiou, K.A. Tissue engineering of the TMJ disc: a review. Tissue Eng **12(5)**, 1183–1196, 2006.
42. Hu, K., Radhakrishnan, P., Patel, R.V., and Mao, J.J. Regional structural and viscoelastic properties of fibrocartilage upon dynamic nanoindentation of the articular condyle. J Struct Biol **136(1)**, 46–52, 2001.
43. Mao, J.J., Rahemtulla, F., and Scott, P.G. Proteoglycan expression in the rat temporomandibular joint in response to unilateral bite raise. J Dent Res **77(7)**, 1520–1528, 1998.
44. Mao, J.J., Giannobile, W.V., Helms, J.A., Hollister, S.J., Krebsbach, P.H., Longaker, M.T., and Shi, S. Craniofacial tissue engineering by stem cells. J Dent Res **85(11)**, 966–979, 2006.
45. Hauger, O., Frank, L.R., Boutin, R.D., Lektrakui, N., Chung, C.B., Haghighi, P., and Resnick, D. Characterization of the "red zone" of knee meniscus: MR imaging and histologic correlation. Radiology **217(1)**, 193–200, 2000.
46. Kambic, H.E., and McDevitt, C.A. Spatial organization of types I and II collagen in the canine meniscus. J Orthop Res **23(1)**, 142–149, 2005.
47. McDevitt, C.A., and Webber, R.J. The ultrastructure and biochemistry of meniscal cartilage. Clin Orthop Relat Res **252**, 8–18, 1990.
48. Upton, M.L., Chen, J., and Setton, L.A. Region-specific constitutive gene expression in the adult porcine meniscus. J Orthop Res **24(7)**, 1562–1570, 2006.
49. Lee, C.R., Grodzinsky, A.J., Hsu, H.-P., Martin, S.D., and Spector, M. Effects of harvest and selected cartilage repair procedures on the physical and biochemical properties of articular cartilage in the canine knee. J Orthop Res **18**, 790–795, 2000.
50. Troken, A.J., Mao, J.J., Marion, N.W., Wan, L.Q., and Mow, V.C. Properties of cartilage and menisci. In: Encyclopedia of Medical Devices and Instrumentation. Hoboken, N.J.: John Wiley and Sons, **55**:63–80, 2007.

51. Butler, D.L., Grood, E.S., Noyes, F.R., Olmstead, M.L., Hohn, R.B., Arnoczky, S.P., and Siegel, M.G. Mechanical properties of primate vascularized vs. nonvascularized patellar tendon grafts: changes over time. J Orthop Res **7**, 68–79, 1989.
52. Hunt, P., Scheffler, S.U., Unterhauser, F.N., and Weiler, A. A model of soft-tissue graft anterior cruciate ligament reconstruction in sheep. Arch Orthop Trauma Surg **125**, 238–248, 2005. http://www.ncbi.nlm.nih.gov/entrez/query.fcgi?cmd=Retrieve&db=PubMed&dopt=Citation&list_uids=15024579.
53. Rasmussen, T.J., Feder, S.M., Butler, D.L., and Noyes, F.R. The effects of 4 Mrad gamma irradiation sterilization on the initial structural properties of ACL and PCL patellar tendon allografts. Arthroscopy **10(2)**, 188–197, 1994.
54. Schwartz, H.E., Matava, M.J., Proch, F.S., Butler, C.A., Ratcliffe, A., Levy, M., and Butler, D.L. The effect of gamma irradiation on anterior cruciate ligament allograft biomechanical and biochemical properties in the caprine model at time zero and at 6 months after surgery. Am J Sports Med **34**, 1747–1755, 2006. http://www.ncbi.nlm.nih.gov/entrez/query.fcgi?cmd=Retrieve&db=PubMed&dopt=Citation&list_uids=16735581.
55. Derwin, K.A., Baker, A.R., Codsi, M.J., and Iannotti, J.P. Assessment of the canine model of rotator cuff injury and repair. J Shoulder Elbow Surg **16(5)**, 140S–148S, 2007.
56. Glaser, D.L., Sher, J.S., Ricchetti, E.T., Williams, G.R., and Soslowsky, L.J. Anatomy, biomechanics and pathophysiology of rotator cuff disease. In: Iannotti and Williams, eds. Disorder of the Shoulder, second edition. Philadelphia: Lippincott Williams and Wilkins, 2007, pp. 3–38.
57. Bruder, S.P., and Fox, B.S. Tissue engineering of bone. Clin Orthop Relat Res **367S**, S68–S83, 1999.
58. Cancedda, R., Giannoni, P., and Mastrogiacomo, M. A tissue engineering approach to bone repair in large animal models and in clinical practice. Biomaterials, 2007 [E-pub ahead of print].
59. Einhorn, T.A. Clinically applied models of bone regeneration in tissue engineering research. Clin Orthop **367 Suppl**, S59–S67, 1999.
60. Guldberg, R.E., Peister, A., Boerckel, J., Dosier, C., Dupont, K., Johnson, M., Lin, A., Oest, M., and O'Keefe, R. Translational approaches for engineering bone repair. In: Mao, J., Vunjak-Novakovic, G., Mikos, A., and Atala, A., eds. Translational Approaches in Tissue Engineering and Regenerative Medicine. Artech House, chapter 7, pp. 1257–144, 2008.
61. Laurencin, C., Khan, Y., and El-Amin, S.F. Bone graft substitutes. Expert Rev Med Devices **3(1)**, 49–57, 2006.
62. Liebschner, M.A. Biomechanical considerations of animal models used in tissue engineering of bone. Biomaterials **25(9)**, 1697–1714, 2004.
63. An, H.S., and Masuda, K. Relevance of *in vitro* and *in vivo* models for intervertebral disc degeneration. J Bone Joint Surg Am **88 Suppl 2**, 88–94, 2006.
64. An, H.S., Thonar, E.J., and Masuda, K. Biological repair of intervertebral disc. Spine **28(15 Suppl)**, S86–S92, 2003.
65. Anderson, D.G., Albert, T.J., Fraser, J.K., Risbud, M., Wuisman, P., Meisel, H.J., Tannoury, C., Shapiro, I., and Vaccaro, A.R. Cellular therapy for disc degeneration. Spine **30(17 Suppl)**, S14–S19, 2005.
66. Lotz, J.C. Animal models of intervertebral disc degeneration: lessons learned. Spine **29(23)**, 2742–2750, 2004.
67. Lotz, J.C., and Kim, A.J. Disc regeneration: why, when, and how. Neurosurg Clin N Am **16(4)**, 657–663, vii, 2005.
68. Lotz, J.C., and Ulrich, J.A. Innervation, inflammation, and hypermobility may characterize pathologic disc degeneration: review of animal model data. J Bone Joint Surg Am **88 Suppl 2**, 76–82, 2006.
69. O'Halloran, D.M., and Pandit, A.S. Tissue-engineering approach to regenerating the intervertebral disc. Tissue Eng **13(8)**, 1927–1954, 2007.
70. Paesold, G., Nerlich, A.G., and Boos, N. Biological treatment strategies for disc degeneration: potentials and shortcomings. Eur Spine J **16(4)**, 447–468, 2007.
71. Arnoczky, S.P., Warren, R.F., and Spivak, J.M. Meniscal repair using an exogenous fibrin clot. An experimental study in dogs. J Bone Joint Surg Am **70(8)**, 1209–1217, 1988.
72. Cook, J.L., Cushner, F.D., and Scuderi, G.R. Minimal-incision total knee arthroplasty. J Knee Surg **19(1)**, 45–51, 2006.
73. Cook, J.L., Fox, D.B., Malaviya, P., Tomlinson, J.L., Kuroki, K., Cook, C.R., and Kladakis, S. Long-term outcome for large meniscal defects treated with small intestinal submucosa in a dog model. Am J Sports Med **34(1)**, 32–42, 2006.
74. Peretti, G.M., Gill, T.J., Xu, J.W., Randolph, M.A., Morse, K.R., and Zaleske, D.J. Cell-based therapy for meniscal repair: a large animal study. Am J Sports Med **32(1)**, 146–158, 2004.
75. Valiyaveettil, M., Mort, J.S., and McDevitt, C.A. The concentration, gene expression, and spatial distribution of aggrecan in canine articular cartilage, meniscus, ACL and PCL: a new molecular distinction between hyaline cartilage and fibrocartilage in the knee joint. Connect Tissue Res **46(2)**, 83–91, 2005.
76. Webber, R.J., York, L., Vanderschilden, J.L., and Hough, A.J. An organ culture model for assaying wound repair of the fibrocartilaginous knee joint meniscus. Am Orthop Soc Sports Med **17**, 393–400, 1989.
77. Butler, D.L., Juncosa-Melvin, N., Boivin, G., Galloway, M.T., Shearn, J.T., Gooch, C., and Awad, H. Functional tissue engineering for tendon repair: a multidisciplinary strategy using mesenchymal stem cells, bioscaffolds and mechanical stimulation (Kappa Delta Paper). J Orthop Res **26(1)**, 1–9, 2008.

Address reprint requests to:
David L. Butler, Ph.D.
Department of Biomedical Engineering
University of Cincinnati
840 Engineering Research Center
2901 Woodside Drive
Cincinnati, OH 45221-0048

E-mail: david.butler@uc.edu

Received: November 18, 2007
Accepted: June 26, 2008

Appendix

Report coauthors including conference organizers and participants

Conference Organizers

David L. Butler, Ph.D., Professor, Department of Biomedical Engineering, University of Cincinnati, Cincinnati, OH; E-mail: david.butler@uc.edu.

Jack L. Lewis, Ph.D., Professor, Department of Orthopaedic Surgery, University of Minnesota, Minneapolis, MN; E-mail: lewis001@umn.edu.

Cyril B. Frank, M.D., Professor, Division of Orthopaedic Surgery, Department of Surgery, University of Calgary, Calgary, Alberta, Canada; E-mail: cfrank@ucalgary.ca.

Conference Participants

Albert J. Banes, Ph.D., Professor, Joint Department of Biomedical Engineering, University of North Carolina, Raleigh, NC; President, Flexcell International Corp.; E-mail: albert_banes@med.unc.edu.

Arnold I. Caplan, Ph.D., Professor, Department of Biology, Case Western Reserve University, Cleveland, OH; E-mail: arnold.caplan@case.edu.

Patrick G. De Deyne, M.PT., Ph.D., Principal Engineer, Preclinical Biology, Johnson & Johnson Regenerative Therapeutics, Raynham, MA; E-mail: pdedeyne@rtxus.jnj.com.

Mary-Ann Dowling, Ph.D., Endoscopy Project Leader, Smith & Nephew Research Centre, York, United Kingdom; E-mail: Mary-Ann.Dowling@Smith-Nephew.com.

Braden C. Fleming, Ph.D., Associate Professor, Department of Orthopaedic Surgery, Brown University, Providence, RI; E-mail: Braden_Fleming@brown.edu.

Julie Glowacki, Ph.D., Professor, Departments of Orthopedic Surgery and Oral & Maxillofacial Surgery, Harvard Schools of Medicine and Dental Medicine, Boston, MA; E-mail: jglowacki@rics.bwh.harvard.edu.

Robert E. Guldberg, Ph.D., Professor, George W. Woodruff School of Mechanical Engineering, Georgia Institute of Technology, Atlanta, GA; E-mail: robert.guldberg@me.gatech.edu.

Brian Johnstone, Ph.D., Professor, Department of Orthopaedics and Rehabilitation, Oregon Health and Science University, Portland, OR; E-mail: johnstob@ohsu.edu.

David L. Kaplan, Ph.D., Professor, Department of Biomedical Engineering, Tufts University, Medford, MA; E-mail: David.Kaplan@tufts.edu.

Marc E. Levenston, Ph.D., Associate Professor, Department of Mechanical Engineering, Stanford University, Stanford, CA; E-mail: levenston@stanford.edu.

Jeffrey C. Lotz, Ph.D., Professor, Department of Orthopaedic Surgery, University of California, San Francisco, San Francisco, CA; E-mail: lotzj@orthosurg.ucsf.edu.

Ed Yiling Lu, Ph.D., Principal Scientist, Johnson & Johnson Regenerative Therapeutics, Raynham, MA; E-mail: elu1@rtxus.jnj.com.

Nadya Lumelsky, Ph.D., Director, Tissue Engineering and Dental and Craniofacial Regenerative Medicine Research Program; National Institute of Dental and Craniofacial Research, Bethesda, MD; E-mail: nadyal@nidcr.nih.gov.

Jeremy J. Mao, D.D.S., Ph.D., Professor and Director, Tissue Engineering and Regenerative Medicine Laboratory (TERML), Columbia University, New York, NY; E-mail: jmao@columbia.edu.

Robert L. Mauck, Ph.D., Assistant Professor, Department of Orthopaedic Surgery, University of Pennsylvania, Philadelphia, PA; E-mail: lemauck@mail.med.upenn.edu.

Cahir A. McDevitt, Ph.D., Professor, Department of Biomedical Engineering, Cleveland Clinic Foundation, Cleveland, OH; E-mail: mcdevitt@bme.ri.ccf.org.

Lito C. Mejia, M.S., Director of Product & Market Development, Bose Corporation, Eden Prairie, MN; E-mail: Lito_Mejia@bose.com.

Martha Murray, M.D., Assistant Professor, Department of Orthopaedic Surgery, Harvard Medical School, Boston, MA; E-mail: martha.murray@childrens.harvard.edu.

Anthony Ratcliffe, Ph.D., President and CEO, Synthasome, Inc., San Diego, CA; E-mail: anthonyratcliffe@synthasome.com.

Kurt P. Spindler, M.D., The Kenneth D. Schermerhorn Professor and Vice Chairman, Orthopaedics and Rehabilitation, Vanderbilt Orthopaedic Institute, Nashville, TN; E-mail: kurt.spindler@vanderbilt.edu.

Scott Tashman, Ph.D., Associate Professor, Department of Orthopaedic Surgery, University of Pittsburgh, PA; E-mail: tashman@upmc.edu.

Christopher T. Wagner, Ph.D., Director of Research, LifeCell Corporation, Branchburg, NJ; E-mail: cwagner@lifecell.com.

Elijah M. Weisberg, M.S.E., Program Analyst, National Institute of Arthritis and Musculoskeletal Diseases, Bethesda, MD; E-mail: weisberge@mail.nih.gov.

Chrysanthi (Sandy) Williams, Ph.D., Product Manager, Biomaterials and Tissue Engineering, Bose Corporation, Eden Prairie, MN; E-mail: Sandy_Williams@bose.com.

Renwen Zhang, M.D., Ph.D., Manager, Orthobiologics Group, Stryker Orthopaedics, Mahwah, NJ; E-mail: renwen.zhang@stryker.com.